VILNIUS UNIVERSITY

Vytautas PETKEVIČIUS

Investigation of pyridine-ring-attacking oxygenases

DOCTORAL DISSERTATION

Natural sciences, Biochemistry N 004

VILNIUS 2019

This dissertation was written between 2014 and 2018 at the Institute of Biochemistry, Life Sciences Center of Vilnius University. The research was supported by the European Social Fund (grant no: DOTSUT-34(09.3.3-LMT-K712-01-0058/LSS-600000-58)], and EU Horizon 2020 project INMARE: Industrial Applications of Marine Enzymes (BG-2014-2634486).

Academic supervisor:

Prof. Dr. Rolandas Meškys (Vilnius University, Natural sciences, Biochemistry – N 004).

Dissertation Defence Panel:

Chairman – **Assoc. Prof. Dr. Eglė Lastauskienė** (Vilnius university, Natural sciences, Biology – N 010);

Members:

Prof. Habil. Dr. Eugenijus Butkus (Vilnius University, Natural sciences, Chemistry – N 003);

Dr. Mantas Mališauskas (Merck Group, Natural sciences, Biochemistry – N 004);

Prof. Dr. Daumantas Matulis (Vilnius University, Natural sciences, Biochemistry – N 004)

Prof. Dr. Saulius Serva (Vilnius University, Natural sciences, Biochemistry – N 004);

The dissertation shall be defended at a public meeting of the dissertation defence panel at 10 AM on 27th of September, 2019 at the Life Science Center of Vilnius University, Auditorium R101.

Address: Saulėtekio av. 7, LT-10257, Vilnius, Lithuania.

The text of this dissertation can be accessed at the Library of Vilnius University as well as on the website of Vilnius University: www.vu.lt/lt/naujienos/ivykiu-kalendorius

VILNIAUS UNIVERSITETAS

Vytautas PETKEVIČIUS

Piridino žiedą atakuojančių oksigenazių tyrimas

DAKTARO DISERTACIJA

Gamtos mokslai, Biochemija N 004

VILNIUS 2019

Disertacija rengta 2014 – 2018 metais Vilniaus universiteto, Gyvybės mokslų centro, Biochemijos institute. Mokslinius tyrimus rėmė Europos socialinis fondas, dotacija – DOTSUT-34(09.3.3-LMT-K712-01-0058/LSS-600000-58)] ir Europos sąjungos programa Horizontas 2020, projektas INMARE (BG-2014-2634486).

Mokslinis vadovas:

prof. dr. Rolandas Meškys (Vilniaus universitetas, gamtos mokslai, biochemija – N 004).

Gynimo taryba:

Pirmininkė – **doc. dr. Eglė Lastauskienė** (Vilniaus universitetas, gamtos mokslai, biologija – N 010);

Nariai:

prof. habil. dr. Eugenijus Butkus (Vilniaus universitetas, gamtos mokslai, chemija – N 003);

dr. Mantas Mališauskas (Merck Group, gamtos mokslai, biochemija – N 004);

prof. dr. Daumantas Matulis (Vilniaus universitetas, gamtos mokslai, biochemija – N 004)

prof. dr. Saulius Serva (Vilniaus universitetas, gamtos mokslai, biochemija – N 004);

Disertacija ginama viešame Gynimo tarybos posėdyje 2019 m. rugsėjo mėn. 27 d. 10 val. Vilniaus universiteto Gyvybės mokslų centre, R101 auditorijoje.

Adresas: Saulėtekio al. 7, LT-10527, Vilnius, Lietuva.

Disertaciją galima peržiūrėti Vilniaus universiteto bibliotekoje VU interneto svetainėje adresu: https://www.vu.lt/naujienos/ivykiu-kalendorius

TABLE OF CONTENTS

LAYOUT OF THE THESIS6
ABBREVIATIONS7
INTRODUCTION9
RESULTS AND DISCUSSION
Burkholderia sp. MAK1 strain – a versatile biocatalyst for oxyfunctionalization of pyridine derivatives
Indetification of 2-hydroxypyridine catabolic genes in <i>Burkholderia</i> sp. MAK1
Exploring soluble diiron monooxygenases as novel biocatalysts for oxidation of <i>N</i> -heteroaromatic compounds
Altering substrate specificity of PML
FUTURE DIRECTIONS
CONCLUSIONS
SUMMARY/SANTRAUKA30
REPORTS
CURRICULUM VITAE
REFERENCES
COPIES OF PUBLICATIONS41
ACKNOWLEDGMENT
NOTES 98

LAYOUT OF THE THESIS

The introduction of the thesis details the goal, main tasks and significance of the study. The result and discussion section was divided into four parts on the basis of publications (listed below) prepared during my PhD studies. Each part is a short overview of a relevant publication. The sequence of publications was arranged chronologically in order to keep a continuous storyline. Additional parts include: a list of abbreviations, conclusions, summary, references, copies of the publications and acknowledgement.

List of publications:

<u>Publication I.</u> Stankevičiūtė J, Vaitekūnas J, **Petkevičius V**, Gasparavičiūtė R, Tauraitė D, Meškys R. Oxyfunctionalization of pyridine derivatives using whole cells of *Burkholderia* sp. MAK1. *Sci. Rep.* 2016, 6:39129.

<u>Publication II.</u> **Petkevičius V**, Vaitekūnas J, Stankevičiūtė J, Gasparavičiūtė R, Meškys R. Catabolism of 2-hydroxypyridine by *Burkholderia* sp. strain MAK1: a 2-hydroxypyridine 5-monooxygenase encoded by *hpdABCDE* catalyzes the first step of biodegradation. *Appl. Environ. Microbiol.* 2018, 84, e00387-18.

<u>Publication III.</u> **Petkevičius V**, Vaitekūnas J, Tauraitė D, Stankevičiūtė J, Šarlauskas J, Čėnas N, Meškys R. A biocatalytic synthesis of heteroaromatic *N*-oxides by whole cells of *Escherichia coli* expressing the multicomponent, soluble di-iron monooxygenase (SDIMO) PmlABCDEF. *Adv. Synth. Catal.* 2019, 361, 2456-2465.

<u>Publication IV.</u> **Petkevičius V**, Vaitekūnas J, Vaitkus D, Čėnas N, Meškys R. Tailoring a soluble diiron monooxygenase for synthesis of aromatic *N*-oxides. *Catalysts*. 2019, 9(4), e356.

ABBREVIATIONS

25DHP – 2,5-dihydroxypyridine

2HP – 2-hydroxypyridine

ArN–OX – aromatic *N*-oxides

DCM – dichloromethane

hpd – 2-hydroxypyridine degradation cluster

HPLC-MS – high pressure liquid chromatography-mass spectroscopy

m-CPBA – *meta*-chloroperoxybenzoic acid

MSA – multi-sequence alignment

NMR – nuclear magnetic resonance

PML – phenol monooxygenase like protein

SDIMO – soluble diiron monooxygenase

THP – 2,3,6-trihydroxypyridine

INTRODUCTION

Pyridine ring is perhaps the most recognizable structural motif among all of the natural N-heterocycles. It is a constituent of coenzymes and vitamins (nicotinamide, pyridoxal phosphate, niacin), and is found in various alkaloids such as, nicotine, mimosine, or trigonelline (Kaiser et, 1996). In addition, synthetic pyridines are extensively used in industrial chemistry. precursors for the synthesis important of numerous pharmaceuticals, dyes, pesticides and even explosives (Mfuh and Larionov, 2015). Pyridine by itself is an indispensable solvent and reagent in many chemical processes. Pyridines are produced by the chemical industry as part of coal and shale oil production, pharmaceutical manufacture and agricultural activities (Padoley et al., 2007). Due to their heterocyclic nature, these compounds are easily transported through soil and contaminate groundwater (Kuhn and Suflita, 1989). In general, pyridine and its derivatives are toxic and are considered hazardous pollutants (Richards and Shieh, 1986).

Surprisingly, for many bacteria those harmful compounds serve as the sole source of carbon and energy. Currently, a number of species from *Pseudomonas, Ochrobactrum, Arthrobacter, Rhodococcus, Achromobacter, Nocardia, Alcaligenes* and *Burkholderia* genera are known to utilize pyridine derivatives (Vaitekūnas et al., 2015; Zhang et al., 2019). Biodegradation pathways of compounds such as nicotine or nicotinic acid are well studied (Jiménez et al., 2008; Tang et al., 2012; Yu et al., 2015). Meanwhile the microbial degradation of alkyl-, cyano-, halogenated and, especially, hydroxypyridines is barely investigated. The proposed degradation pathways for hydroxypyridines are mostly based on indirect evidence rather than genetic or enzymatic data (Fetzner, 1998). Only a limited number of genes and/or enzymes have been identified (Vaitekūnas et al., 2015), while the key steps in the biodegradation of hydroxypyridines remain obscure.

Usually, the first step in the aerobic biodegradation of xenobiotics and, apparently, of pyridine derivatives as well, is substrate hydroxylation (Fuchs et al., 2011). However, little is known about specific monooxygenases and dioxygenases involved in the assimilation of 2-hydroxypyridine (Fetzner, 1998; Yao et al., 2013). It has been shown that one of the degradation pathways leads to the accumulation of 2,3,6-trihydroxypyridine (Gupta and Shukla, 1975), an intermediate

frequently encountered in bacteria utilizing various pyridine derivatives (Kaiser et al., 1996; Fetzner, 1998). This trihydroxylic metabolite blue (4,5,4',5'-tetrahydroxy-3,3'spontaneously forms pigment a diazadiphenoquinone-2,2') which serves as a distinguishable phenotypic determinant of the catabolism of 2-hydroxypyridine (Kolenbrander and Weinberger, 1977). Nevertheless, a number of reports describing bacteria consuming 2-hydroxypyridine without the formation of a blue pigment (Cain et al., 1974) may be found in the literature, though the proposed 2-hydroxypyridine oxidation to 2,5-dihydroxypyridine has been supported by neither genetic nor enzymatic data. The microbial degradation of pyridine has also been the subject of hot dispute since major steps of the proposed catabolic pathways have not been elaborated (Khasaeva et al., 2011). There monooxygenase-catalysed pyridine pyridine-1-oxide as a possible initiation step in the degradation of pyridine (Sun et al., 2014). However, N-oxidation reactions are uncommon in nature and there are only a few records about bacteria or enzymes capable of catalyzing this type of transformation (Ullrich et al., 2008; Mitsukura et al., 2013; Zhao et al., 2016).

From the chemical point of view, hydroxylation of pyridine derivatives is a challenging task. Due to the inductive effect of nitrogen, π electrons are shifted towards this atom, leaving the rest of the ring itself electron-deficient, and impassive for electrophilic substitution (Clayden et al., 2012). Therefore, the most common hydroxylation techniques that are based on electrophilic oxidizers and that serve well for benzene derivatives, are not suitable for pyridines (Eicher et al., 2013). On the other hand, a hydroxyl group can be introduced applying nucleophilic substitution, condensation and cyclization reactions (Hill, 2010). Nevertheless, typical methods feature harsh reaction conditions and usually are non-selective. The reactivity of pyridine ring vastly increases when various electron-donating substituents are present, thus N-heterocycles regularly undergo N-oxidation before the actual synthesis process takes place (Clayden et al., 2012; Eicher et al., 2013). Aromatic N-oxides are reactive towards both electrophilic and nucleophilic substitution while the modification itself is easily removable (Clayden et al., 2012; Eicher et al., 2013). There are a lot of chemical methods to produce N-oxides (Larionov et al., 2014; Rozen et al., 2014) though most of them feature poor selectivity and employ hazardous oxidizers, hence, safer alternatives are required.

Nowadays, modern chemical synthesis faces more strict environmental regulations and, as a result, shifts toward so-called green chemistry, where biocatalytic methods play a key role (Badenhorst and Bornscheuer, 2018). Hence, the need for the new biocatalysts increases tremendously. Unexplored degradation pathways of pyridine derivatives likely hide unique enzymes with the potential for biotechnological applications. Keeping all that in mind, **the aim of this work** – to investigate pyridine-ring-attacking oxygenases, and to explore their application in the biocatalysis of *N*-heteroaromatic compounds.

In order to achieve this aim, four **main tasks** were outlined:

- 1) to investigate the biocatalytic potential of 2-hydroxypyridine-degrading strain *Burkholderia* sp. MAK1;
- 2) to determine *Burkholderia* sp. MAK1 genes that code for catabolic enzymes responsible for 2-hydroxypyridine degradation;
- 3) to explore the biocatalytic capabilities of the unstudied oxygenases acting on *N*-heteroaromatic derivatives;
- 4) to investigate options for improvement of isolated biocatalysts *via* directed evolution.

Scientific novelty of the dissertation

Burkholderia sp. MAK1 strain was previously isolated from soil contaminated with various organic compounds. Its distinguishable feature was the ability to use 2-hydroxypyridine (2HP) as the sole source of carbon and energy. Since pyridines are an uncommon substrate for Burkholderia, the corresponding biocatalysts for pyridine derivatives are unknown. Nevertheless, it was demonstrated that Burkholderia sp. MAK1cells pregrown in the presence of 2HP were able to hydroxylate C-5 position of a wide range of 2-amino- and 2-hydroxypyridines bearing methyl-, cyano-, halogens and other substituents. On the other hand, pyridine, pirazine and their alkylated derivatives were converted to N-oxides. As a result, Burkholderia sp. MAK1 whole cells emerged as a unique biocatalyst for oxyfunctionalization of pyridine derivatives.

Isolation of the 2HP-degradation-deficient mutant *Burkholderia* sp. MAK1 Δ P5, led to the identification of 2HP catabolism genes – the real culprit behind biocatalytic capabilities of *Burkholderia* sp. MAK1. For the

first time, the genes responsible for 2HP catabolism, during which the formation of a blue pigment is not observed, have been identified. The 2-hydroxypyridine biodegradation (hpd) gene cluster is a 13-kb-long DNA fragment containing 12 open reading frames. The oxygenase-type of reactions were attributed both to hpdF-encoded 2.5-dihydroxypyridine (25DHP) 5.6-dioxygenase multicomponent 2-hydroxypyridine and 5-monooxygenase, encoded by *hpdABCDE* gene cluster. The latter belongs to the family SDIMO comprised of soluble diiron monooxygenases. Since enzymes of this family have never been related to the biodegradation of N-heteroaromatic compounds, HpdABCDE monooxygenase stands out as an illustrious enzyme. Whole-cell transformations employing *Burkholderia* sp. MAK1ΔP5 strain were used to investigate the enzymatic activity of HpdABCDE. HPLC-MS analysis of the reaction end products provided evidence of HpdABCDE-catalysed 2HP conversion to 25DHP. Such enigmatic reaction has never been demonstrated at the enzymatic level to date. Overall, these findings allowed for proposing a new 2HP degradation pathway in bacteria.

The discovery of HpdABCDE hinted that other SDIMOs may catalyse oxidation of *N*-heteroaromatics as well. Screening of the metagenomic library of various oxygenases allowed the identifiction of a new SDIMO enzyme capable of *N*-oxidation of pyridine derivatives. The sequence analysis revealed a gene cluster consisting of six open reading frames belonging to SDIMO group of phenol monooxygenases and it was designated as *pmlABCDEF* (**p**henol **m**onooxygenase **l**ike protein). PmlABCDEF possesses an extraordinary substrate scope for *N*-aromatic compounds, which are converted to corresponding mono-*N*-oxides. Current biocatalytic synthesis of aromatic *N*-oxides is defined by a handful of limited approaches. In this context, the application of SDIMO enzyme allowed the introduction of PmlABCDEF-catalysed synthesis as a mild, regio- as well as chemoselective, efficient, and scalable method for the preparation of specific *N*-oxides.

Since no SDIMO enzyme was shown to possess an *N*-oxidation capability so far, no improvements for this type of reaction *via* a directed evolution were possible. The potential hotspots for mutagenesis were deduced from the multi-sequence alignment of characterized SDIMOs and by analysing the structural model of PmlABCDEF catalytic subunit. Subsequently, six amino acids (I106, A113, G109, F181, F200 and F209) situated near the active center were chosen for mutagenesis. New enzyme

variants were selected applying a chromogenic screening method based on the formation of indigo-like pigments, as a result, total of 19 different mutants were selected. The A113G variant possessed the most distinguishable *N*-oxidation capacity relative to wild type enzyme. The A113G mutant exhibited reshaped regioselectivity as well as the ability to produce dioxides and specific mono-*N*-oxides. Tailoring PmlABCDEF monooxygenase is a promising precedent exploiting further opportunities for biooxidation of *N*-heteroaromatic compounds by the SDIMO enzymes.

RESULTS AND DISCUSSION

Burkholderia sp. MAK1 strain – a versatile biocatalyst for oxyfunctionalization of pyridine derivatives

Various pyridine derivatives are widely used as starting material in diverse chemical syntheses and play an essential role as a scaffold in design of herbicides, pesticides, and drugs (Balzarini et al., 2005). The regioselective hydroxylation of pyridine ring by chemical reagents is quite a complicated transformation (Clayden et al., 2012), thus preparation of those compounds employing enzymes or whole cells is an attractive and environmentally friendly strategy to obtain the desired products (Turner et al., 2018). Successful applications such as biocatalytic synthesis of 2,5-dihydroxypyridine utilizing 6-hydroxynicotinic acid 3-monooxygenase, production of 6-hydroxynicotinic acid employing whole cells of *Serratia marcescens* IF012648 and biotransformation of 3-cyanopyridine to 3-cyano-6-hydroxypyridine with *Comamonas testosteroni* MCI2848 whole cells (industrialized process, Mitsubishi Chemicals) prompted the search for novel biocatalysts (Hurh et al., 1994; Yasuda et al., 1995; Nakano et al., 1999).

In this study, 2HP-degrading Burkholderia sp. MAK1 was investigated for its oxyfunctionalization capabilities. It was assumed that enzymes from the 2HP catabolic pathway could also transform structurally derivatives. Indeed. various 2-aminopyridine 2-hydroxypyridines were converted into products whose molecular mass increased by 16 Da. Moreover, the maxima of UV spectra of those compounds shifted into a range of longer wavelengths by ~ 20-30 nm. Altogether, that was a clear indication of pyridine ring hydroxylation. In order to determine the regiospecificity of hydroxylation, the end products of conversions were isolated and submitted for ¹H and ¹³C NMR analysis, which revealed that halogenated 2-aminopyridines were hydroxylated at C-5 position (Publication I, Table 1). In the case of 2-hydroxpyridines, the outcome appeared to be the same - hydroxylation at C-5 (Publication I, Table 2). However, most of 2-hydroxypyridines as substrates were not sufficiently explored as only the consumption of a substrate was registered (Publication I, Figure 2 and 3, Panels a). Most likely, the emerging hydroxylation products were metabolized to opened-ring derivatives by

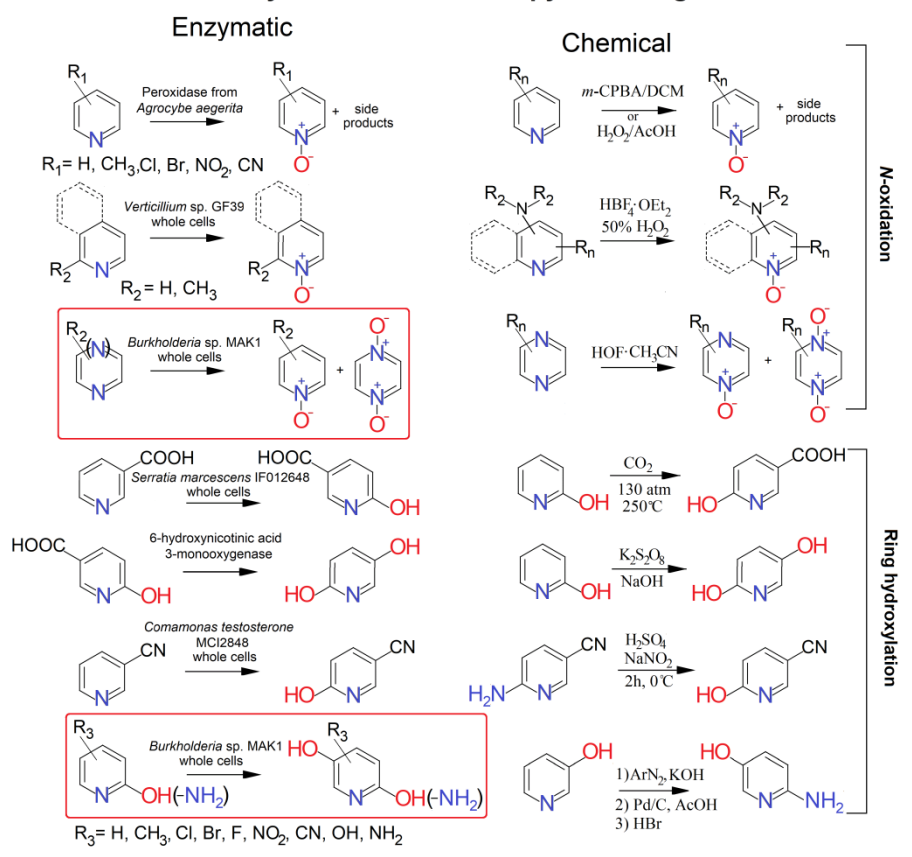
other enzymes of 2HP degradation pathway. After screening more than 100 of *N*-heteroaromatic derivatives, some distinct patterns of product formation have emerged. Apparently, the preferred substrates for *Burkholderia* sp. MAK1 were 2-aminopyridine derivatives bearing hydroxy-, methoxy-, cyano-, amino- and halogen moieties at C-3, C-4 or/and C-6 positions (Publication I, Figure 4). Additionally, 2-hydroxypyridines comprised another large group of *Burkholderia* sp. MAK1 substrates. Preferable substrates were compounds with hydroxy-, methoxy-, cyano-, amino- and halogen substituents at C-3 and C-6 positions while most of the moieties at C-4 position seemed undesirable (Publication I, Figures 2 and 3). *Burkholderia* sp. MAK1 was also able to hydroxylate *N*-alkylpyridin-2-one derivatives (Publication I, Table 2). The specific features of substrates unrecognised by *Burkholderia* sp. MAK1 included two *ortho*-substituents, carboxylic acids and complex compounds possessing more than one-ring structure.

Pyridine, pyrazine and their alkylated derivatives also fell into the substrate space of Burkholderia sp. MAK1. HPLC-MS analysis of the end products indicated the increase of molecular mass by 16 Da, as was with 2-amino- and 2-hydroxypyridines. UV spectra of conversion products shifted into a range of shorter wavelengths by ~ 10-20 nm suggesting a different type of oxidation. The properties of pyridine conversion product were compared with those of all possible hydroxypyridine derivatives. The retention time, UV spectrum and ionisation profile matched those of analytical standard of pyridine-1-oxide. Various methylpyridines were also transformed to corresponding *N*-oxides with the exception 2,6-dimethylpyridine and 2,4,6-trimethylpyridine as they possess two o-substituents with respect to nitrogen, and this possibly hinders the attack (Publication I, Figure 5). Interestingly, conversion of pyrazine resulted in the formation of two products with molecular masses that were 16 Da and 32 Da higher than that of the parent compound. Those products were isolated separately, and NMR analysis identified them as pyrazine-1-oxide and pyrazine-1,4-dioxide.

Overall, *Burkholderia* sp. MAK1 stands out as a functional biocatalyst for pyridine ring oxyfunctionalization. Compounds bearing polar group (-OH or -NH₂) at C-2 position are hydroxylated regioselectively at C-5 position. Unsubstituted pyridine and pyrazine as well as their methylated derivatives are converted to corresponding *N*-oxides, making *Burkholderia*

sp. MAK1 a promising alternative for the preparation of various pyridine-5-ols and pyridine-N-oxides (Scheme 1).

Oxyfunctionalization of pyridine ring



Scheme 1. Different approaches in oxyfunctionalization of compounds containing pyridine ring. Enzymatic methods are presented on the left, while relevant transformations by chemical reagents are shown on the right. Reactions catalysed by *Burkholderia* sp. MAK1 whole cells are given in red squares.

Identification of 2-hydroxypyridine catabolic genes in *Burkholderia* sp. MAK1

Since biotransformation capabilities of *Burkholderia* sp. MAK1 were linked to 2HP catabolism, the identification of 2HP catabolic genes was carried out. There are several proposed pathways of 2HP degradation in

nature (Publication II, Figure 1). The most studied degradation pathways for 2HP involve the formation of 2,3,6-trihydroxypyridine (THP) as intermediate (Stanislauskiene et al., 2012; Vaitekūnas et al., 2015). THP autooxidizes spontaneously to form a blue pigment (also known as nicotine blue), which is a distinct phenotypic feature (Kolenbrander and Weinberger, 1977). However, a 2HP degradation pathway was reported, without the accumulation of a blue pigment (Cain et al., 1974). This pathway is less studied and only indirect evidence suggests the degradation through the formation of 25DHP, though the putative 2HP 5-monooxygenase has never been identified. Notably, *Burkholderia* sp. strain MAK1 assimilates 2HP without the formation of a blue pigment and transforms substituted 2-hydroxypyridines to corresponding pyridine-5-ols. All the findings point to the unexplored 2HP degradation pathway potentially encompassing unique genes and enzymes.

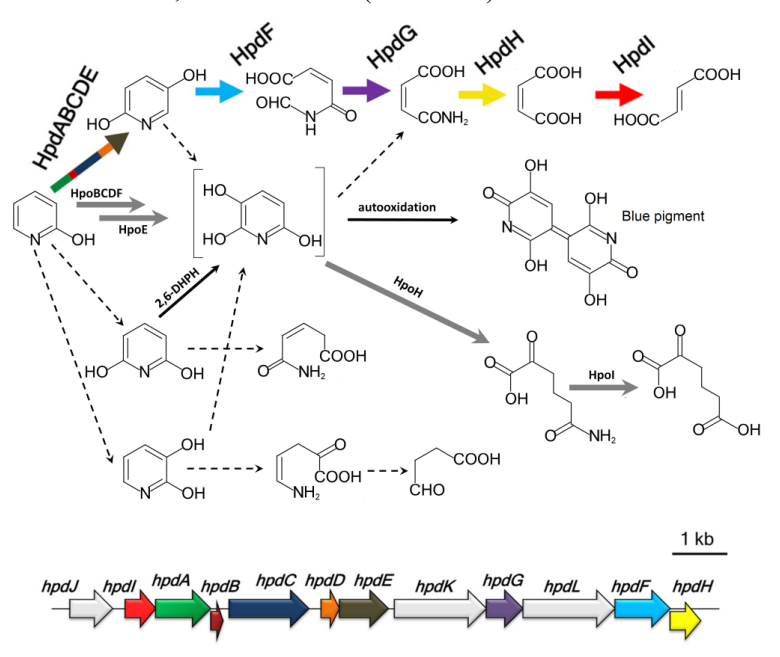
To identify 2HP catabolic genes in *Burkholderia* sp. MAK1, a random mutagenesis with plasposon pTnMod-OKm¹ (Dennis and Zylstra, 1998) was used. This system incorporates kanamycin resistant cassette into host's genome; a distortion of 2HP assimilation genes should yield kanamycin resistant *Burkholderia* sp. MAK1 mutant with a lost capacity for 2HP degradation. To identify such a mutant, the chromogenic screening was used based on indigo pigment formation. Indole oxidation to this blue pigment was only present in 2HP-induced bacteria, thus it was linked to the activity of enzymes from the 2HP degradation pathway. In this manner, the proper mutant with no capacity to synthesize indigo dye and to degrade 2HP was isolated and designated *Burkholderia* sp. MAK1ΔP5 (Publication II, Figure 2).

After sequencing kanamycin resistance cassette-flanking regions, the gene cluster (designated *hpd*) responsible for the degradation of 2HP in *Burkholderia* sp. MAK1 was identified. The *hpd* gene cluster is a 13-kb-long DNA fragment containing 12 open reading frames (Publication II, Table 1). Four genes (*hpdF*, *hpdG*, *hpdH*, and *hpdI*) show high sequence similarity to those encoding the catabolism of 25DHP (25DHP 5,6-dioxygenase, *N*-formylmaleamate deformylase, maleamate amidase, and maleate isomerase). The enzymes responsible for the degradation of 25DHP are found in nicotine- and nicotinate-degrading bacteria (Jiménez et al., 2008; Tang et al., 2012; Yu et al., 2015), though never been documented in 2HP degradation. The presence of aforementioned genes was a strong indication that, in *Burkholderia* sp. MAK1, 2HP is catabolized via the formation of

25DHP and that 2HP is being directly hydroxylated to form 25DHP. Three genes (hpdJ, hpdL, and hpdK) from the hpd locus appear to be indirectly involved in the biodegradation of 2HP and have been associated with transcription regulation, protein folding, and transport. The most intriguing was a five-gene cluster hpdABCDE (hpdA, hpdB, hpdC, hpdD, and hpdE) aparently coding for the hypothetical 2HP 5-monooxygenase. It was similar to the genes of soluble diiron monooxygenase (SDIMO) family. SDIMOs multicomponent enzymatic systems usually found xenobiotic-degrading microorganisms, where they often catalyze the first steps of phenol, toluene, xylene, methane, izoprene, etc., degradation (Leahy et al., 2003; Notomista et al., 2003). However, HpdABCDE seems to be a unique enzyme, as it shares only little sequence similarity with characterized homologous proteins, and encompases a different gene architecutre relative to other SDIMOs (Publication II, Figure 4). Notably, no SDIMO enzymes directly involved in the biodegradation of pyridine and its derivatives have been reported thus far.

A further investigation was focused on proving the 2HP hydroxylation to 25DHP, presumably catalyzed by HpdABCDE, and the following ring opening of 25DHP potentially driven by HpdF. The overexpression of HpdF was successfully achieved in E. coli BL21 (DE3) cells. The whole cells as well as free-cell extract harbored 25DHP dioxygenase activity, which was inspected by monitoring reaction progress with UV-Vis spectrophotometer and HPLC-MS (Publication II, Figure 7). However, the biosynthesis of HpdABCDE monooxygenase was more difficult. Numerous cloning strategies were attempted and various protein expression techniques were tested, none of which resulted in the enzymatic activity of recombinant HpdABCDE in E. coli. Instead, Burkholderia sp. MAK1ΔP5 cells were considered as an alternative host for HpdABCDE expression. For this purpose a broad-host-range arabinose-inducible expression vector, pBAD-MCS-1, was created (Publication II, Figure 6, panel A). A plasmid pBAD-MCS-1 possessed a framework of pBBR1MCS plasmid vector (Kovach et al., 1995) along with P_{BAD} promoter, araC regulator and terminator sequences instead of native P_{lac} promoter elements. Next, hpdABCDE gene cluster was cloned into pBAD-MCS-1 vector, which was transferred to Burkholderia sp. MAK1ΔP5. These cells were grown in the presence of arabinose for recombinant protein biosynthesis (Publication II, Figure 6, panel B), and were used in the bioconversion experiments. Whole cells conversion of 2HP was inspected by recording UV spectra at fixed time intervals. The time-dependent decline of 2HP absorbance at 290 nm and the formation of a new compound with an absorbance peak at 320 nm were observed (Publication II, Figure 7). HPLC-MS analysis revealed that a new UV spectrum belonged to the compound whose molecular mass was 16 Da higher than that of 2HP, a clear indication of monooxyganase activity. To evaluate the regioselectivity of the hydroxylation, a chromatogram of the conversion product was compared with that of dihydroxypyridine standards. The properties (retention time and absorbance spectrum) of the conversion product were found to exactly match 25DHP (Publication II, Figure 8). As a result, 2HP conversion to 25DHP catalyzed by HpdABCDE monooxygenase was confirmed.

This study unraveled one of the most puzzling microbial 2HP degradation pathways as gene cluster *hpd*, containing all the necessary genes for 2HP assimilation, was identified (Scheme 2).



Scheme 2. Proposed and elucidated pathways of aerobic 2HP biodegradation in bacteria. Colored arrows present genes and enzymes of *Burkhoderia* sp. MAK1 (a degradation pathway via 25DHP). Solid grey arrows represent enzymes of *Rhodococcus* sp. PY11 (a pathway via THP; Vaitekūnas et al., 2015). Solid black arrows depict other known catalysts (2,6-DHPH – 2,6-dihydroxypyridine 3-hydroxylase from *Arthrobacter nicotinovorans*). Dashed arrows indicate putative transformations.

The elusive 2-hydroxypyridine 5-monooxygenase proved to be HpdABCDE, an enzyme of SDIMO family. Next step in the biodegradation was proven to be dioxygenolysis of 25DHP catalyzed by HpdF. After the ring opening, the degradation process possibly proceeds via the so-called maleamate pathway since all genes associated with this pathway have homologues in the *hpd* cluster.

Exploring soluble diiron monooxygenases as novel biocatalysts for oxidation of *N*-heteroaromatic compounds

Although HpdABCDE possessed exceptional biocatalytic capabilities for pyridine derivatives, its usage was limited by the current expression system. While *Burkhoderia* sp. MAK1 strain was a troublesome biocatalyst because of its poor productivity and growth features, attempts to express this monooxygenase in different E. coli strains or in hosts related to Burkholderia genus (Pseudomonas, Cupriavidus, Caballeronia) failed to produce an active enzyme. However, the discovery of HpdABCDE revealed that particular SDIMOs are able to catalyse oxidation of pyridine derivatives. Since especially desirable would be those functional in E. coli, DNA sequences of our laboratory collection of various oxygenases obtained from metagenomes were explored to search for an occurrence of SDIMOs. Seven clones were selected and initial experiments indicated that one clone (designated p577A) was capable of pyridine oxidation. After a plasmid was fully sequenced, a 4.5 kb gene cluster containing six open reading frames was identified. It showed high sequence homology with SDIMO group of phenol monooxygenases, and the closest BLAST hit (~80% overall a.a. sequence identity) was butylphenol monooxygenase from Pseudomonas The gene cluster was designated *pmlABCDEF* (phenol monooxygenase like protein) and cloned into pET-28b plasmid (Publication III, Table 3) for further studies.

Whole cells of *E. coli* bearing PmlABCDEF monooxygenase (from here on – PML monooxygenase) were used in the bioconversion experiments. As was the case with HpdABCDE monooxygenase, PML-catalysed pyridine oxidation product was identified as pyridine-1-oxide whereas methylpyridines and pyrazines were converted to corresponding *N*-oxides. However, unlike in HpdABCDE catalysed

reactions, most of 2-amino- and 2-hydroxypyridines were either poor substrates for PML or remained unaffected at all. Moreover, HPLC-MS and UV-Vis data suggested that 2-amino- and 2-hydroxypyridines undergo N-oxidation rather than ring hydroxylation. These initial results revealed PML as a potential biocatalyst for the synthesis of aromatic N-oxides (ArN-OX) exclusively. These compounds are extensively studied as promising anticancer, antibacterial, antihypertensive, antiparasitic, anti-HIV, anti-inflammatory, herbicidal, neuroprotective, precognitive, and auxiliary agents (Mfuh and Larionov, 2015). They are also used as protecting groups, oxidants, ligands, propellants, and explosives (Balzarini et al., 2005). Currently, the synthesis of ArN-OX is based on chemical methods (Sloboda-Rozner et al., 2004; Kokatha et al., 2011; Veerakumar et al., 2012; Larionov et al., 2014, Rozen et al., 2014), of which most are both unspecific and employ hazardous materials. There are only a few reports on biocatalytic synthesis for ArN-OX that all possess very limited applications (Ullrich et al., 2008; Mitsukura et al., 2013; Zhao et al., 2016), thus a new productive method is much needed.

The elucidation of PML substrate scope was achieved by testing 98 N-aromatic compounds, 70 of which were shown to be converted to some extent into products whose molecular mass increased by 16 Da (Publication III, Table 1). The derivatives of pyridine comprised a significant part of the examined compounds. Pyridines harbouring small aliphatic groups (methyl-, ethyl-) were fully converted by PML. Other favourable substrates for PML included those bearing hydroxymethyl, methoxy, chloro and cyano moieties, most of which were substrates for HpdABCDE as well. However, PML-catalysed conversions featured tenfold higher productivity than transformations with Burkholderia sp. MAK1 whole cells. PML also showed great preference for diazine compounds as pyrazine, pyrimidine, pyridazine and their derivatives were converted by various degrees into corresponding mono-N-oxides. A number of two-ring heterocycles also fell into the range of PML substrates. Unsubstituted compounds like quinoline, isoquinoline, quinoxaline, 1,5-naphtyridine, and quinazoline were transformed at high conversion yields. Their derivatives with one alicyclic ring or a methyl group also showed good reactivity. Two-ring substrates were not accepted by Burkholderia sp. MAK1. From all known biocatalysts, only Verticillium sp. GF39 cells (Mitsukura et al., 2013) were shown to utilize two-ring heterocycles. PML also catalysed N-oxidation of larger and more complex such as 4-(4-nitrobenzyl)pyridine, 4-(pyridin-4-ylsulfanyl) substrates,

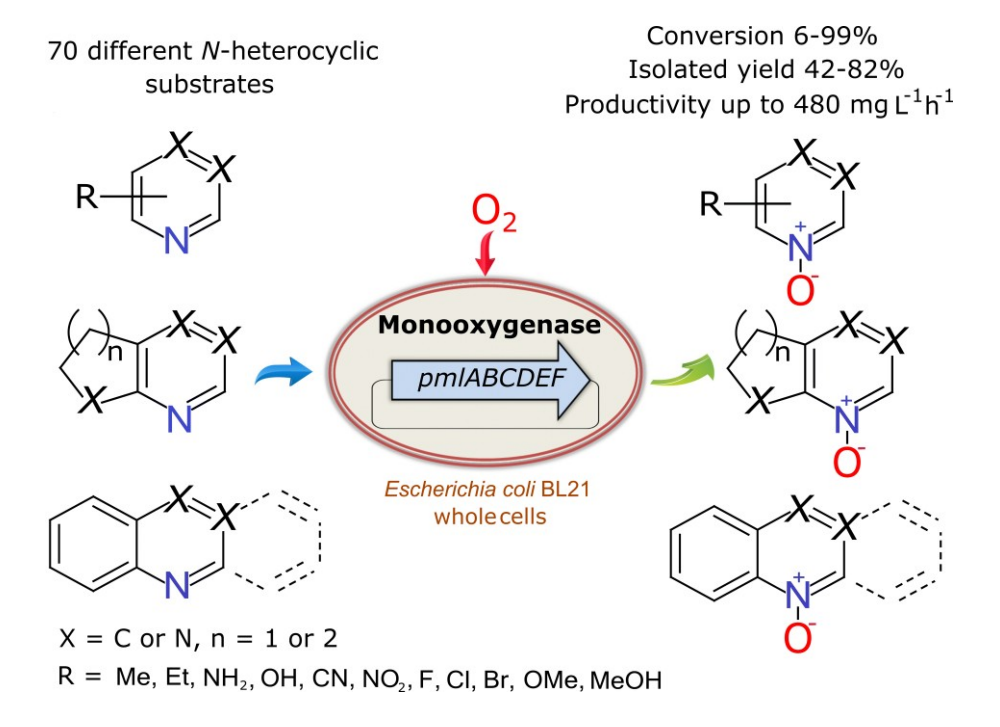
pyridine, 3-(pyrrol-1-yl)pyridine, 4-(pyridin-4-yl)pyridine, 4-(1,3-oxazol-5-yl)pyridine, and 2-phenylpyridine. Three-ring heterocycles (acridine, phenazine, norharmane, 4,7-phenantroline) were substrates for PML as well, though only minor amounts of possible *N*-oxides were detected. From the reported biocatalysts, only *Lysobacter antibioticus* (Zhao et al., 2016) catalysed the *N*-oxidation of three-ring *N*-heterocycles (phenazine).

For the preparative-scale synthesis of N-oxides, 14 compounds (Publication III, Table 2) were selected. All of these N-heterocycles reflected the elucidated substrate range of PML, and some were difficult to synthesize by conventional methods. The chemical synthesis of mono-N-oxides from pyrazine derivatives is challenging, as dioxides may form as well (Kokatha et al., 2011; Veerakumar et al., 2012; Rozen et al., 2014). Usually, the side reactions are avoided by adding an equimolar amount of the oxidizing agent and conducting the reaction at low temperatures. However, in the case of PML, only monoxides were produced from 2,6-dimethylpyrazine, quinoxaline, and 5,6,7,8-tetrahydroquinoxaline, using PML as catalyst. Moreover, this method proved to be suitable for regioselective synthesis. Direct oxidation of 2,6-dimethylpyrazine and quinazoline by conventional chemical methods (m-CPBA, H₂O₂) would produce mixtures of different mono-N-oxides (Klein and Berkowitz, 1959; Kobayashi et al., 1974; Dickschat et al., 2005). However, PML driven catalysis yielded only single products, namely 3,5-dimethylpyrazine-1-oxide and quinazoline-3-oxide, respectively. For compounds containing reactive substituents, exposure to typical oxidizing agents may modify the substituent as well (Rozen et al., 2014). PML-catalysed approach also was shown to be chemoselective, as 2-hydroxymethylpyridine was converted to single product (2-hydroxymethylpyridine-1-oxide) without the traces ofpossible pyridine-2-carbaldehyde or pyridine-2-carboxylic acid. Additionally, 4-(pyridin-4-ylsulfanyl) pyridine was transformed to the corresponding mono-N-oxide, avoiding the formation of a sulfoxide. Finally, oxidation of 4-(1,3-oxazol-5-yl)pyridine resulted in N-oxidation of the pyridine ring, while the attack on a substituent oxazole ring was not observed.

This *E. coli* biocatalytic system was put to the test when the synthesis of pyrazine-1-oxide on a multi-gram scale in 1 L bioreactor was performed. Compared with the conversion in flasks, this technique increased the productivity tenfold, from 40.0 mg L⁻¹h⁻¹ to 480 mg L⁻¹h⁻¹. As a result, gram-scale synthesis of pyrazine-1-oxide was reached in a few hours. Hence, PML-catalysed *N*-oxidation in bioreactor should increase the productivity in

the case of other substrates as well, and this could be an attractive 'green' method in addition to existing chemical approaches.

PML proved to be an exceptional biocatalyst for ArN–OX synthesis. It offered broad substrate specificity, favourable productivity, and an adaptable synthesis platform (Scheme 3), thus surpassing the scale of previous studies. The method described here also featured regio- and chemoselectivity, and as such has an advantage over typical synthesis of ArN–OX by chemical oxidizers. In fact, 4-(pyridin-4-ylsulfanyl)pyridine-1-oxide and 4-(1,3-oxazol-5-yl)pyridine-1-oxide have not been previously prepared either by biocatalytic or chemical approaches. Moreover, further improvements of the biocatalyst are possible *via* a directed evolution of the PmlABCDEF oxygenase.



Scheme 3. *N*-oxidation capabilities of *Escherichia coli* whole cells bearing PML monooxygenase.

Altering substrate specificity of PML

Over the last decades, SDIMO enzymes have emerged as a new class of oxidizing biocatalysts. Desirable catalytic features include broad substrate scope, favourable kinetics, possible stereo,- regio, and chemoselectivities (Notomista et al., 2011). Also, SDIMOs were improved *via* a directed evolution which resulted in the production of new enzymes with altered or unnatural catalytic properties (Chan Kwo Chion et al., 2005; Sönmez et al., 2014; Carlin et al., 2015). The extensive studies on SDIMO engineering also revealed potential hotspots for mutagenesis (Nichol et al., 2015). However, PML as well as HpdABCDE from *Burkholderia* sp. MAK1 have been studied for their oxidation capabilities on *N*-heteroaromatic compounds, something that was never shown for SDIMOs. The investigation of mutations that affect *N*-oxidation would contribute to both the field of SDIMO engineering and the biocatalysis in general.

The impact of mutagenesis on the PML-catalysed reactions was investigated. The possible hotspots for mutagenesis were deduced from the multi-sequence alignment (MSA) of characterized SDIMOs (Publication IV, Figure 1) and the structural model of PML (Publication IV, Figure 2). First, the goal was to engineer PML which would prefer bulkier and more complex substrates. Three phenylalanine residues (F181, F200, F209) situated near the diiron center in the 3D model were chosen, since previous reports indicated that amino acids in these positions have potential to change substrate specificity (Chan Kwo Chion et al., 2005; Notomista et al., 2009; Sönmez et al., 2014). Thus, F181, F200, and F209 underwent site-directed mutagenesis to alanine, with the expectation that enlarged active centre cavity would produce desirable mutants. Both single mutants (F181A, F200A, F209A) and double mutants (F181A/F200A, F181A/F209A, F200A/F209A) were obtained. However, only F200A and F209A variants showed N-oxidation capabilities, as the rest of mutants lost enzymatic activity completely. F200A and F209A mutants were tested towards a number of larger substrates (acridine, phenazine, 4,7-phenantroline, norharmane), nevertheless they did not possess enhanced N-oxidation capacity with bulkier substrates. Actually, these variants seemed to retain a substrate scope of the parental enzyme with some loss in efficiency of conversion (Publication IV, Table 1).

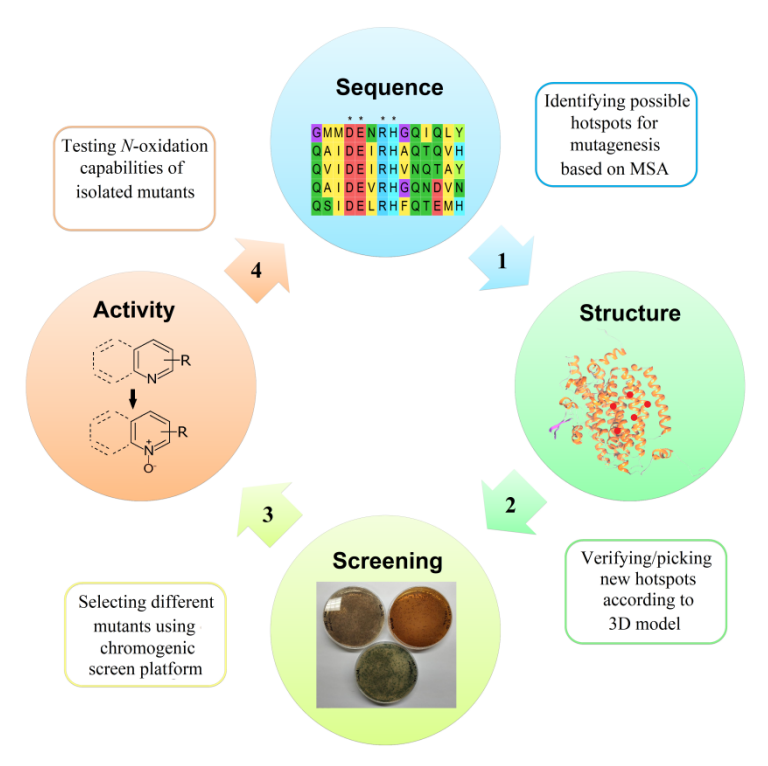
Afterwards, other important amino acids surrounding the active centre were targeted. The selected hotspots were cross-checked with the literature, to assure their significance in substrate specificity. As a result, three residues in PML, namely I106, A113, and G109, were selected for saturation mutagenesis. I106 corresponds to the so-called substrate gate (Borodina et al., 2007) that permits the substrate to enter the active site; usually its component is an aliphatic hydrophobic amino acid. Other important hotspot in PML is A113 that is conserved in almost all analysed sequences of well-studied SDIMOs. This site was shown to be decisive in substrate orientation and binding (Tao et al., 2004; Carlin et al., 2015). Another hotspot features great variability among characterized SDIMOs, nevertheless modifications at this site were reported to strongly affect catalytic properties (Vardar and Wood, 2004; Fishman et al., 2005). The corresponding amino acid in PML monooxygenase is G109.

To select potentially improved/changed enzymes from the library of mutants, a convenient method was required. It has been already demonstrated (with HpdABCDE from Burkholderia sp. MAK1) that SDIMOs catalyse the transformation of indole to indigo pigment. Actually, enzymatic oxidation of indole results in a variety of pigments (indigo, indirubin, isoindigo) and colourful hydroxyindole derivatives (isatin, 6hydroxyindole, 7-hydroxyindole) (McClay et al., 2005). It was demonstrated that in certain SDIMOs, indole oxidation specificity could be altered by mutagenesis (McClay et al., 2005; Rui et al., 2005). The latter enabled the selection of distinct mutants on the base of diverse colour development. Thus, it was assumed that PML mutants with an altered oxidation regiospecificity of indole transformation may possess different N-oxidation patterns as well. A total of 19 differently coloured colonies were selected (Publication IV, Figure 3). Sequencing revealed that four new variants (I106A, I106C, I106E, I106N) from I106 library were produced, three (A113G, A113F, A113V) from A113 library and six (G109T, G109H, G109L, G109K, G109M, G109Q) from G109 library.

The catalytic properties of the isolated mutants were then investigated. The substrate scope was reduced to a number of compounds including various diazines and triazines to investigate the possibility of multiple *N*-oxidation, asymmetric compounds for potential regioselectivity shift, and some bulky derivatives that were barely oxidized by the wild type PML. From all tested mutants, the A113G variant exhibited the most distinctive catalytic properties (Publication IV, Figure 4). The A113G

variant transformed quinoxaline to a mixture of two products. One compound (molecular mass increased by 16 Da) was previously identified as quinoxaline-1-oxide (Publication III, Table 2). The other product (molecular mass increased by 32 Da) was separated and purified during this work. NMR as UV spectra of the compound matched those of quinoxaline-1,4-dioxide; di-N-oxides were not characteristic for the parental PML. A similar outcome was observed for 2,5-dimethylpyrazine, which was converted to a mixture of 2,5-dimethylpyrazine-1-oxide and compound 2,5-dimethylpyrazine-1,4-dioxide. Moreover, A113G exhibited a substantial increase in the conversion efficiency for 2,3,5-trimethylpyrazine. The mutant was able to utilize almost completely (92% conversion) the latter compound, while conversion by the wild type enzyme barely reached 6%. The most distinct feature of the mutant A113G was the changed regioselectivity of N-oxidation. Quinazoline was oxidized to the compound with different retention time and UV spectra than quinazoline-3-oxide, a product produced by the parental PML. After isolation and NMR analysis, the product was confirmed as quinazoline-1-oxide, demonstrating a shift of oxygen attack from N3 to N1 position.

It appears that for PML, the molecular volume at the active site was a decisive factor determining the substrate specificity and enzymatic activity towards *N*-heteraromatic compounds. It is likely that large substituents (mutant A113F) supposedly occluded the hydrophobic pocket and as a result, the catalysis was severely obstructed. However, drastic attempts to expand the hydrophobic pocket (F181, F200 and F209 substituted to alanine) did not yield desirable modifications either. On the other hand, alanine-to-glycine substitution in the position 113 produced only minimal extra space, nevertheless it was crucial in accepting substrates not used by the wild type enzyme. Also, A113G mutation was shown to influence substrate binding and orientation, as quinazoline oxidation shifted from N3 to N1 position, compared with the parental enzyme. Overall, the introduced chromogenic screening method has been shown to be effective, and may be applied for future studies (Scheme 4).



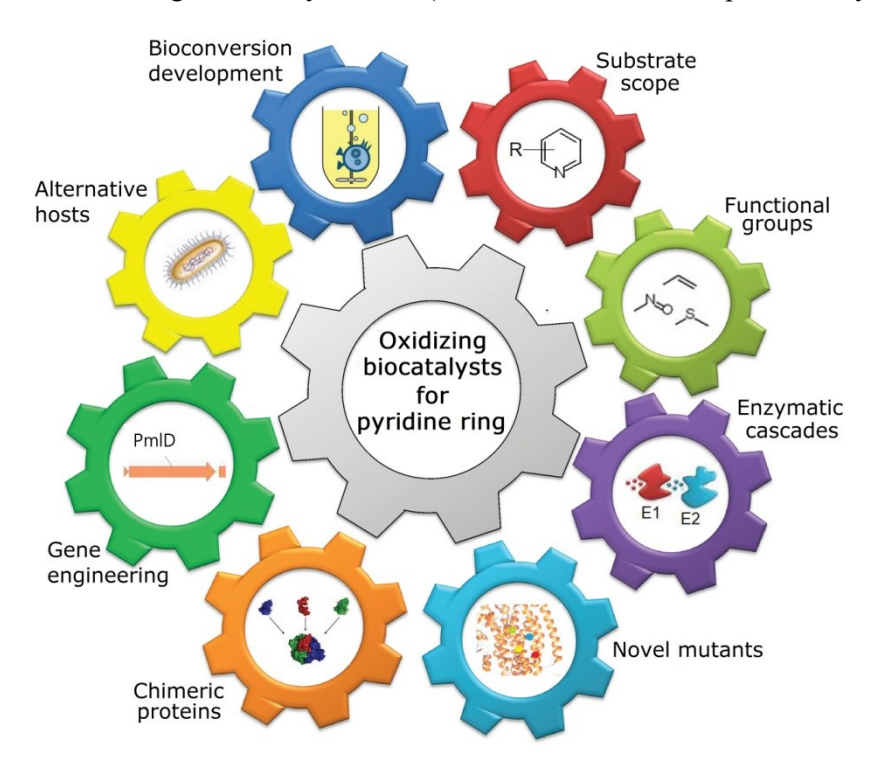
Scheme 4. SDIMO-based protein engineering strategy to obtain biocatalysts featuring altered *N*-oxidation capacity.

Although only several notable substitutions affecting *N*-oxidation have been identified so far, targeted SDIMO engineering is a promising platform for designing novel biocatalysts for oxyfunctionalization of *N*-heteroaromatic compounds.

FUTURE DIRECTIONS

The results presented in this study provide guidelines for future research (Scheme 5). The substrate scope of the studied biocatalyst is far from being complete. The future studies should focus on issues of regio- and chemoselectivity as well as the production of compounds of interest. On the other hand, substrates bearing functional groups that have not been investigated thus far, yet susceptible for oxidation, may serve as precursors for novel biocatalytic applications. Pyridinols and aromatic *N*-oxides are often used as intermediates in the chemical synthesis, thus oxygenase-driven

oxyfunctionalization of N-heterocycles could be used as a first step in semi-enzymatic or enzymatic cascade reactions. Pyridine ring biocatalysts also have a room for improvement via evolution in vitro. Although the side-directed as well as saturation mutagenesis produced a collection of new enzymes, they do not reflect the possible variety. A more complex engineering is also feasible. PML could be used as a scaffold for the construction of chimeric enzymes exhibiting novel properties (e. g. fusion of HpdABCDE catalytic centre with the elements of PML to build pyridinol-producing biocatalyst functional in E. coli). Further possible modifications include the reduction of the enzymatic system to a minimum number of subunits necessary for the catalytic activity, or a fusion of these proteins into a single polypeptide. If successful, such approaches would not only gain biotechnological value, but would also receive fundamental importance. Finally, PML bioconversion parameters as well as up-scale synthesis have the capacity for additional improvements (aqueous biphasic systems, different hosts as new producents, aeration flow, continuous substrate feeding or batch system, etc.) in order to increase the productivity.



Scheme 5. Possible applications of pyridine-ring-attacking oxygenases.

CONCLUSIONS

- 1) *Burkholderia* sp. MAK1 whole cells are a novel biocatalyst for the oxyfunctionalization of pyridine derivatives. It produces a variety of 2-hydroxy- and 2-aminopyridin-5-ols, and catalyses the formation of specific *N*-oxides from methylpyridines and methylpyrazines.
- 2) 13 kb long *hpd* gene cluster encodes genes required for the degradation of 2-hydroxypyridine in *Burkholderia* sp. MAK1.
- 3) *Burkholderia* sp. MAK1 assimilates 2-hydroxypyridine through the formation of 2,5-hydroxypyridine. This transformation is catalysed by a new type of soluble diiron monooxygenase HpdABCDE.
- 4) Whole cells of *Escherichia coli* bearing soluble diiron monooxygenase PML represent a productive, scalable, regio- and chemoselective enzyme-based toolkit for the synthesis of aromatic *N*-oxides.
- 5) Protein engineering of PML monooxygenase, together with chromogenic screening platform, is a promising new toolbox for designing unique SDIMO enzymes for biooxidation of *N*-heteroaromatic compounds.

SUMMARY/SANTRAUKA

Piridino dariniai vra tiek plačiai gamtoje aptinkamos medžiagos (piridoksalio fosfatas, nikotinas, nikotinamidas), tiek svarbūs pirmtakai vaistu, dažu ir net sprogmenu cheminėje sintezėje. Šiuo metu žinoma gana didelė įvairovė mikroorganizmų, gebančių panaudoti piridino junginius kaip vienintelius anglies ir energijos šaltinius. Daugelio piridinu skaidyme kaip tarpiniai metabolitai susidaro hidroksipiridinai. Manoma, kad tokiu junginiu susidarymą dažniausiai katalizuoja įvarios piridino žiedą atakuoti gebančios oksigenazės. Tokie fermentai yra mažai ištirti, žinomi tik keli pavyzdžiai. Cheminiais reagentais ivesti hidroksigrupe i piridino žieda nėra lengva užduotis. Dažnai reikalingos griežtos reakcijos salvgos, naudojami toksiški ir pavojingi reagentai, neišvengiama nespecifinių produktų susidarymo, kartais sintezė vykdoma per keletą etapų. Šiuolaikinė cheminė sintezė vis daugiau remiasi biokataliziniais metodais, o pastariesiems būtini naujomis savybėmis pasižymintys fermentai. Iki šiol neištirti piridino darinių skaidymo keliai yra potencialus unikalių fermentų šaltinis. Visai tai ir suformulavo šio darbo tikslą – tirti piridino žiedą atakuojančias oksigenazes ir jų taikymą N-heteroaromatinių junginių biokatalizėje.

Igyvendinti išsikeltam tikslui suformuluoti keturi uždaviniai.

- Ištirti 2-hidroksipiridiną skaidančio *Burkholderia* sp. MAK1. kamieno biokatalizines savybes.
- 2) Nustatyti genus, koduojančius 2-hidroksipiridino skaidymo fermentus, *Burkholderia* sp. MAK1 kamiene.
- 3) Ištirti ir įvertinti naujų piridino žiedą atakuojančių oksigenazių biokatalizines savybes.
- 4) Ištirti naujų oksigenazių tobulinimo galimybes pasitelkiant baltymų evoliuciją *in vitro*.

Šio darbo tyrimų objektas – *Burkholderia* sp. MAK1 kamienas 2-hidroksipiridiną (2HP) vartojančios kaip vienintelį anglies ir energijos šaltinį. Buvo pademontruota, kad 2HP indukuotos *Burkholderia* sp. MAK1 ląstelės yra unikalus biokatalizatorius. Jos katalizavo įvairių 2-amino- ir 2-hidroksipiridinų hidroksilinimą susidarant atitinkamiems piridin-5-oliams. Tuo tarpu piridinas, pirazinas ir jų metilinti dariniai buvo tranformuojami į *N*-oksidus. Buvo iškelta hipotezė, kad šiuos virsmus katalizuoja fermentai dalyvaujantys 2HP skaidyme. Katabolizmo genai buvo nustatyti sukūrus ir

atrinkus mutanta Burkholderia sp. MAK1\DeltaP5, kuris negalėjo skaidyti 2HP. Genu sankaupa hpd vra 13 kb ilgio DNR rajonas, koduojantis 12 genu. Trvs genai (hpdG, hpdH, hpdI) priklauso maleamo rūgšties skaidymo keliui – dažnai pasitaikančiam piridinų metabolizme. Fermentai koduojami hpdJ, hpdL ir hpdK genu siejami su transkripcijos reguliacija, baltymu sulankstymu ir transportu. Buvo nustatytos ir potencialios oksigenazės dalyvaujančios 2HP skaidyme. HpdF yra 2,5-dihidroksipiridino (25DHP) 5,6-dioksigenazė, kurios aktyvumas stebėtas biosintetinant ši fermenta E. coli bakterijose. Galimas 2HP virtimas i 25DHP buvo priskirtas daugiakomponentei monooksigenazei tirpiai geležies (SDIMO) HpdABCDE. Fermentinis aktyvumas parodytas sukūrus monooksigenazės raiškos sistemą *Burkholderia* sp. MAK1ΔP5 kamiene. Taip pirmą kartą buvo SDIMO pademonstruota, kad grupės fermentai gali dalyvauti N-heteroaromatiniu junginiu skaidyme. Tuo pačiu tai leido pasiūlyti nauja 2HP skaidymo kelia gamtoje.

HpdABCDE monooksigezės atradimas leido daryti prielaida, kad tarp SDIMO grupės fermentų galima atrasti naujų piridino žiedą atakuojančių monooksigenaziu. Šiu fermentu paieška vykdyta bioinformatiniais irankiais tiriant ankstesnių tyrimų metu sukurtą laboratorijos oksigenazių kolekciją iš metagenominių bibliotekų. Pirminiai eksperimentai parodė, kad vienas klonas (p577A) gebėjo katalizuoti piridino oksidacija iki N-oksido. Atlikus sekoskaita paaiškėjo, kad tai SDIMO grupės fermentas, koduojamas šešiu genu sankaupos, pavadinots pmlABCDEF. Perkėlus genus i baltymui biosinetezei skirtą plazmidini vektorių pET-28b, pavyko gauti gausią tirpaus fermento PmlABCDEF (PML) raišką E. coli BL21 ląstelėse. PML pasižymėjo plačiu substratiniu aktyvumu, iš 98 tirtu įvariu N-heterocikliniu junginių 70 buvo konvertuojami į produktus, kurių molekulinė masė padidėjo 16 Da. Tolimesnei analizei buvo pasirinkta 14 junginių, kurių produktai išgryninti ir atliktos ¹H BMR ir ¹³C BMR analizės. Paaiškėjo, kad PML katalizuoja N-heterociklinių junginių oksidaciją iki specifinių mono-Noksidy ir pasižymėjo tam tikru regio- ir chemoselektyvumu. Atlikus pirazino-1-oksido sinteze 1L fermentatoriuje buvo pademonstruotas šio biokatalizinio metodo potencialas – gramų eilės produktyvumas pasiektas per kelias valandas. PML katalizuojama N-oksidų sintezė – naujas SDIMO fermentų biotechnologinis panaudojimas.

Piridinų ir kitų *N*-heteroaromatinių junginių biooksidacija toliau buvo tiriama atliekant PML monooksigenazės evoliuciją *in vitro*. Potencialios aminorūgštys mutagenezei buvo parinktos lyginant PML seką su SDIMO

pavyzdžiais iš literatūros, taip pat pagal tretinės struktūros modeli. Tokiu būdu mutagenezei buvo parinktos šešios aminorūgštys (I106, A113, G109, F181, F200 ir F209) supančios aktyvųjį fermento centrą. PML mutantai buvo atrenkami pritaikius spalvinį, indolo oksidcija pagrįstą, metodą. Iš viso taip buvo atrinkti 19 skirtingo spalvinio profilio mutantu, kurie toliau buvo tiriami pagal gebėjima oksiduoti N-heteroaromatinius junginius. Daugiausiai naujų katalizinių savybių, lyginant su laukinio tipo PML, igavo A113G mutantas. Jis katalizavo dioksidu (chinoksalino-1,4-dioksido, 2,5-dimetilpirazino-1,4-dioksido) ir tam tikru monoksidu (2.3.5-trimetilpirazino-1-oksidas) susidarymą – laukinio tipo fermentas šių virsmų nekatalizavo. A113G mutantas taip pat pasižymėjo pakitusiu regioselektyvumu chinazolinui. Galutinis konversijos produktas buvo chinazolino-1-oksidas. kai laukinio tipo **PML** produkavo chinazolino-3-oksida. Tokiu būdu pavyko parodyti, kad SDIMO fermentu pagrindu galima kurti naujus biokatalizatorius N-heteroaromatinių junginių biooksidacijai.

Išvados:

- 1) *Burkholderia* sp. MAK1 ląstelės yra naujo tipo biokatalizatorius piridino darinių biooksidacijai. Jos katalizuoja įvairių 2-hidroksi- ir 2-aminopiridin-5-olių sintezę, o iš metil- piridinų ir pirazinų produkuoja atitinkamus *N*-oksidus.
- 2) 13 kb ilgio *hpd* genų sankaupa koduoja genus, reikalingus 2-hidroksipiridino skaidymui *Burkholderia* sp. MAK1 kamiene.
- 3) *Burkholderia* sp. MAK1 kamienas 2-hidroksipiridiną skaido susidarant 2,5-dihidroksipiridinui. Šią reakciją katalizuoja naujo tipo tirpi geležies monooksigenazė HpdABCDE.
- 4) *Escherichia coli* ląstelės gaminančios tirpią geležies monooksigenazę PML yra naujas, švelniomis sąlygomis veikiantis, produktyvus, regio- ir chemoselektyvus biokatalizatorius aromatinių *N*-oksidų sintezei.
- 5) Fermentų kūrimas tirpios geležies monoksigenazės PML pagrindu, panaudojant indolo oksidacija grįstą atrankos sistemą, yra naujas metodas kurti unikalių biokatalizinių savybių fermentus *N*-heteroaromatinių junginių sintezei.

REPORTS

- Biocat 2014, Hamburg, Germany. Poster: "2-Hydroxypyridine degradation in *Rhodococcus* sp. PY11". Authors: Stankevičiūtė J., Vaitekūnas J., Gasparavičiūtė R., **Petkevičius V**., Tauraitė D., Meškys R.
- 2) FEBS-EMBO 2014, Paris, France. Poster: "Whole cell regioselective hydroxylation of *N*-heteroaromatic compounds using *Burkholderia* sp. MAK1. Authors: Stankevičiūtė J., Vaitekūnas J., Gasparavičiūtė R., **Petkevičius V**., Tauraitė D., Urbonavičius J., Meškys R.
- 3) XIVth International Conference of the Lithuanian Biochemical Society 2016, Druskininkai, Lithuania, June 28-30, 2016. Poster: "Transposon mutagenesis of the 2-hydroxypyridine degrading *Burkholderia* sp. MAK1 reveals genes of the 2-hydroxypyridine monooxygenase". Authors: **Petkevičius V**., Vaitekūnas J., Stankevičiūtė J., Gasparavičiūtė R., Meškys R.
- 4) XIVth International Conference of the Lithuanian Biochemical Society 2016, Druskininkai, Lithuania, June 28-30, 2016. Poster: "Direct screening of alcohol dehydrogenases in metagenomic libraries." Authors: Gasparavičiūtė R., Stankevičiūtė J., **Petkevičius** V., Vaitekūnas J., Časaitė V., Meškienė R., Meškys R.
- 5) Biocat2018, Hammburg, Germany, August 26-30, 2018. Poster: "Catabolism of 2-hydroxypyridine by *Burkholderia* sp. MAK1: a five-gene cluster encoded 2-hydroxypyridine 5-monooxygenase HpdABCDE catalyses the first step of biodegradation". Authors: **Petkevičius V**., Vaitekūnas J., Stankevičiūtė J., Gasparavičiūtė R., Meškys R.

CURRICULUM VITAE

Name, Last name	Vytautas Petkevičius
Education/Competence:	
1996 - 2008	Birštonas gymnasium.
2008 - 2012	Vilnius University, Faculty of Chemistry and Geosciences. Bachelor's degree in biochemistry.
2012 - 2014	Vilnius University, Institute of Biosciences. Master's degree in biochemistry.
2014 - 2018	PhD studies. Vilnius University, Life Sciences Center, Institute of Biochemistry.
Record of employment:	
2014 07 - 2016 12	Specialist, Vilnius University, Institute of Biochemistry.
2016 10 - 2016 12 2017 10 - 2017 12 2018 10 - 2018 12	Lecturer (gene engineering), Vilnius University, Institute of Biosciences.
2017 02 - 2017 07	Lecturer (biochemistry for ERASMUS students), Vilnius University, Institute of Biosciences.
2017 10 - 2017 12 2018 10 - 2018 12	Lecturer (bioorganic chemistry), Vilnius University, Institute of Biosciences.
2017 02 - 2017 12 2018 10 - present	Research assistant, Vilnius University, Institute of Biochemistry.

Participation in projects:

European Social Fund according to the activity "Improvement of researchers' qualification by implementing world-class R&D projects" of measure no. 09.3.3-LMT-K-712 [grant no. DOTSUT-34(09.3.3-LMT-K712-01-0058/LSS-600000-58)].

EU Horizon 2020 project INMARE: Industrial Applications of Marine Enzymes (BG-2014-2634486).

Other activities:

Lectures for high school students (National student academy, Lithuanian centre of non-formal youth education).

REFERENCES

- 1. Badenhorst CPS, Bornscheuer UT. Getting momentum: From biocatalysis to advanced synthetic biology. *Trends. Biochem. Sci.* **2018**, *43*, 180–98.
- 2. Balzarini J, Stevens M, De Clercq E, Schols D, Pannecouque C. Pyridine *N*-oxide derivatives: unusual anti-HIV compounds with multiple mechanisms of antiviral action. *J. Antimicrob. Chemother.* **2005**, 55, 135–8.
- 3. Borodina E, Nichol T, Dumont MG, Smith TJ, Murrell JC. Mutagenesis of the "leucine gate" to explore the basis of catalytic versatility in soluble methane monooxygenase. *Appl. Environ. Microbiol.* **2007**, *73*, 6460-7.
- 4. Cain RB, Houghton C, Wright KA. Microbial metabolism of the pyridine ring. Metabolism of 2- and 3-hydroxypyridines by the maleamate pathway in *Achromobacter* sp. *Biochem. J.* **1974**, *140*, 293–300.
- 5. Carlin DA, Bertolani SJ, Siegel, JB. Biocatalytic conversion of ethylene to ethylene oxide using an engineered toluene monooxygenase. *Chem. Commun.* **2015**, *51*, 2283–5.
- 6. Chan Kwo Chion CK, Askew SE, Leak DJ. Cloning, expression, and site-directed mutagenesis of the propene monooxygenase genes from *Mycobacterium* sp. strain M156. *Appl. Environ. Microbiol.* **2005**, *71*, 1909-14.
- Clayden J, Greeves N, Warren SG. Aromatic heterocycles 1: Reactions. In Organic Chemistry, 2nd ed.; Oxford University Press: New York, NY, USA, 2012; pp. 730–731.
- 8. Dennis JJ, Zylstra GJ. Plasposons: modular self-cloning minitransposon derivatives for rapid genetic analysis of Gram-negative bacterial genomes. *Appl Environ Microbiol*. 1998, 64, 2710 –5.
- 9. Dickschat JS, Reichenbach H, Wagner-Döbler I, Schulz S. Novel Pyrazines from the Myxobacterium *Chondromyces crocatus* and Marine Bacteria. *Eur. J. Org. Chem.* **2005**, 2005, 4141–53.
- 10. Eicher T, Hauptmann S, Speicher A. 6.14 Pyridine. In The Chemistry of Heterocycles: Structures, Reactions, Synthesis, and Applications, 3rd ed.; WILEY: Hoboken, New Jersey, USA, **2013**; pp. 345–81.

- 11. Fetzner S. Bacterial degradation of pyridine, indole, quinoline, and their derivatives under different redox conditions. *Appl Microbiol. Biotechnol.* **1998**, *49*, 237–50.
- 12. Fishman A, Tao Y, Rui L, Wood TK. Controlling the regiospecific oxidation of aromatics via active site engineering of toluene paramonooxygenase of *Ralstonia pickettii* PKO1. *J. Biol. Chem.* **2005**, *280*, 506–14.
- 13. Fuchs G, Boll M, Heider J. Microbial degradation of aromatic compounds—from one strategy to four. *Nat. Rev. Microbiol.* **2011**, *9*, 803–16.
- 14. Gupta RC, Shukla OP. Microbial metabolism of 2-hydroxypyridine. *Indian. J. Biochem. Biophys.* **1975**, *12*, 296 –8.
- 15. Hurh B, Yamane T, Nagasawa T. Purification and characterization of nicotinic acid dehydrogenase from *Pseudomonas fluorescens* TN5. *J. Ferment. Bioeng.* **1994**, *78*, 19–26.
- 16. Jimenez JI, Canales A, Jimenez-Barbero J, Ginalski K, Rychlewski L, Garcia JL. Deciphering the genetic determinants for aerobic nicotinic acid degradation: the nic cluster from *Pseudomonas putida* KT2440. *Proc Natl Acad Sci U S A.* 2008, 105, 11329-34.
- 17. Kaiser JP, Feng Y, Bollag JM. Microbial metabolism of pyridine, quinoline, acridine, and their derivatives under aerobic and an aerobic conditions. *Microbiol. Rev.* **1996**, *60*, 483–98.
- 18. Khasaeva F, Vasilyuk N, Terentyev P, Troshina M, Lebedev A. A novel soil bacterial strain degrading pyridines. *Environ. Chem. Lett.* **2011**, *9*, 439–45.
- 19. Klein B, Berkowitz J. Pyrazines. I. Pyrazine-*N*-oxides. Preparation and Spectral Characteristics. *J. Am. Chem. Soc.* **1959**, *81*, 5160–6.
- Kobayashi Y, Kumadaki I, Sam H, Sekine Y, Hara T. Studies on the Reaction of Heterocyclic Compounds. XII. N-Oxidation of Diazabenzene and Diazanaphthalene. Chem. Phann. Bull. 1974, 2, 2097.
- 21. Kokatha HP, Thomson PF, Bae S, Doddi VR, Lakshman MK. Reduction of Amine *N*-Oxides by Diboron Reagents *J. Org. Chem.* **2011**, *76*, 7842–8.
- 22. Kolenbrander PE, Weinberger M. 2-Hydroxypyridine metabolism and pigment formation in three *Arthrobacter* species. *J. Bacteriol.* **1977**, *132*, 51–9.

- 23. Kovach ME, Elzer PH, Hill DS, Robertson GT, Farris MA, Roop RM, Jr, Peterson KM. Four new derivatives of the broad-host-range cloning vector pBBR1MCS, carrying different antibiotic-resistance cassettes. *Gene.* **1995**, *166*, 175–6.
- 24. Kuhn EP, Suflita JM. Microbial degradation of nitrogen, oxygen and sulfur heterocyclic compounds under anaerobic conditions: studies with aquifer samples. *Environ. Toxicol. Chem.* **1989**, *8*, 1149 –58.
- 25. Larionov OV, Stephens D, Mfuh AM, Arman HD, Naumova AS, Chavez G, Skenderi B. Insights into the mechanistic and synthetic aspects of the Mo/P-catalyzed oxidation of *N*-heterocycles. *Org. Biomol. Chem.* **2014**, *12*, 3026–36.
- 26. Leahy JG, Batchelor PJ, Morcomb SM. Evolution of the soluble diiron monooxygenases. *FEMS Microbiol. Rev.* **2003**, *27*, 449-79.
- 27. McClay K, Boss C, Keresztes I, Steffan RJ. Mutations of toluene-4-monooxygenase that alter regiospecificity of indole oxidation and lead to production of novel indigoid pigments. *Appl. Environ. Microbiol.* **2005**, *71*, 5476-83.
- 28. Mfuh AM, Larionov OV. Heterocyclic *N*-Oxides An Emerging Class of Therapeutic Agents. *Curr. Med. Chem.* **2015**, *22*, 2819–57.
- 29. Mitsukura K, Hayashi M, Yoshida T, Nagasawa T. Oxidation of aromatic *N*-heterocyclic compounds to *N*-oxides by *Verticillium* sp. GF39 cells. *J. Biosci. Bioeng.* **2013**, *115*, 651–3.
- 30. Nakano H, Wieser M, Hurh B, Kawai T, Yoshida T, Yamane T, Nagasawa T. Purification, characterization, and gene cloning of 6-hydroxynicotinate 3-monooxygenasefrom *Pseudomonas fluorescens* TN5. *Eur. J. Biochem.* **1999**, *260*,120-6.
- 31. Nichol T, Murrell JC, Smith TJ. Controlling the Activities of the Diiron Centre in Bacterial Monooxygenases: Lessons from Mutagenesis and Biodiversity. *Eur. J. Inorg. Chem.* **2015**, *2015*, 3419–31.
- 32. Notomista E, Cafaro V, Bozza G, Di Donato A. Molecular determinants of the regioselectivity of toluene/o-xylene monooxygenase from *Pseudomonas* sp. strain OX1. *Appl. Environ. Microbiol.* **2009**, 75, 823–36.
- 33. Notomista E, Lahm A, Di Donato A, Tramontano A. Evolution of bacterial and archaeal multicomponent monooxygenases. *J. Mol. Evol.* **2003**, *56*, 435–45.

- 34. Notomista E, Scognamiglio R, Troncone L, Donadio G, Pezzella A, Di Donato A. Tuning the specificity of the recombinant multicomponent toluene o-xylene monooxygenase from *Pseudomonas* sp. strain OX1 for the biosynthesis of tyrosol from 2-phenylethanol. *Appl. Environ. Microbiol.* **2011**, 77, 5428–37.
- 35. Padoley KV, Mudliar SN, Pandey RA. Heterocyclic nitrogenous pollutants in the environment and their treatment options--an overview. *Bioresour. Technol.* **2008**, *99*, 4029–43.
- 36. Richards DJ, Shieh WK. Biological fate of organic priority pollutants in the aquatic environment. *Water. Res.* **1986**, *20*, 1077–90.
- 37. Rozen S. HOF·CH₃CN: probably the best oxygen transfer agent organic chemistry has to offer. *Acc. Chem. Res.* **2014**, *47*, 2378–89.
- 38. Rui L, Reardon KF, Wood TK. Protein engineering of toluene orthomonooxygenase of *Burkholderia cepacia* G4 for regiospecific hydroxylation of indole to form various indigoid compounds. *Appl. Microbiol. Biotechnol.* **2005**, *66*, 422–9.
- 39. Sloboda-Rozner D, Witte P, Alsters P, Neumann R. Aqueous Biphasic Oxidation: A Water-Soluble Polyoxometalate Catalyst for Selective Oxidation of Various Functional Groups with Hydrogen Peroxide. *Adv. Synth. Catal.* **2004**, *346*, 339–45.
- 40. Sönmez B, Yanık-Yıldırım KC,Wood TK, Vardar-Schara G. The role of substrate binding pocket residues phenylalanine 176 and phenylalanine 196 on *Pseudomonas* sp. OX1 toluene o-xylene monooxygenase activity and regiospecificity. *Biotechnol. Bioeng.* **2014**, *111*, 1506–12.
- 41. Stanislauskiene R, Gasparaviciute R, Vaitekunas J, Meskiene R, Rutkiene R, Casaite V, Meskys R. Construction of *Escherichia coli-Arthrobacter-Rhodococcus* shuttle vectors based on a cryptic plasmid from *Arthrobacter rhombi* and investigation of their application for functional screening. *FEMS. Microbiol. Lett.* **2012**, *327*, 78–86.
- 42. Tang H, Yao Y, Wang L, Yu H, Ren Y, Wu G, et al. Genomic analysis of *Pseudomonas putida*: genes in a genome island are crucial for nicotine degradation. *Sci. Rep.* **2012**, *2*, 377–85.
- 43. Tao Y, Fishman A, Bentley WE, Wood TK. Altering toluene 4-monooxygenase by active-site engineering for the synthesis of 3-methoxycatechol, methoxyhydroquinone, and methylhydroquinone. *J. Bacteriol.* **2004**, *186*, 4705–13.

- 44. Turner NJ, Kumar R. Editorial overview: Biocatalysis and biotransformation: The golden age of biocatalysis. *Curr. Opin. Chem. Biol.* **2018**, *43*, A1–A3.
- 45. Ullrich R, Dolge C, Kluge M, Hofrichter M. Pyridine as novel substrate for regioselective oxygenation with aromatic peroxygenase from *Agrocybe aegerita*. *FEBS Lett.* **2008**, *582*, 4100–6.
- 46. Vaitekunas J, Gasparaviciute R, Rutkiene R, Tauraite D, Meskys R. A 2-Hydroxypyridine Catabolism Pathway in *Rhodococcus rhodochrous* Strain PY11. *Appl. Environ. Microbiol.* **2015**, *82*, 1264–73.
- 47. Vardar G, Wood TK. Protein engineering of toluene-o-xylene monooxygenase from *Pseudomonas stutzeri* OX1 for synthesizing 4-methylresorcinol, methylhydroquinone, and pyrogallol. *Appl. Environ. Microbiol.* **2004**, *70*, 3253–62.
- 48. Veerakumar P, Balakumar S, Velayudham M, Lu KL, Rajagopal S. Ru/Al₂O₃ catalyzed *N*-oxidation of tertiary amines by using H₂O₂. *Catal. Sci. Technol.* **2012**, *2*, 1140–5.
- 49. Yao Y, Tang H, Ren H, Yu H, Wang L, Zhang W, et al. Iron(II)-dependent dioxygenase and *N*-formylamide deformylase catalyze the reactions from 5-hydroxy-2-pyridone to maleamate. *Sci. Rep.* **2013**, *3*, 3235.
- 50. Yasuda M, Sakamoto T, Sashida R, Ueda M, Morimoto Y, Nagasawa T. Microbial hydroxylation of 3-cyanopyridine to 3-cyano-6-hydroxypyridine. *Biosci. Biotech. Biochem.* 1995, 59, 572–5.
- 51. Yu H, Tang H, Zhu X, Li Y, Xu P. Molecular mechanism of nicotine degradation by a newly isolated strain, *Ochrobactrum* sp. strain SJY1. *Appl. Environ. Microbiol.* **2015**, *81*, 272–81.
- 52. Zhang Y, Ji J, Xu S, Wang H, Shen B, He J, Qiu J, Chen Q. Biodegradation of Picolinic Acid by *Rhodococcus* sp. PA18. *Appl. Sci.* **2019**, *9*, 1006.
- 53. Zhao Y, Qian G, Ye Y, Wright S, Chen H, Shen Y, Liu F, Du L. Heterocyclic Aromatic *N*-Oxidation in the Biosynthesis of Phenazine Antibiotics from *Lysobacter antibioticus*. *Org. Lett.* **2016**, *18*, 2495–8.

COPIES OF PUBLICATIONS

Publication I

Stankevičiūtė J, Vaitekūnas J, **Petkevičius V**, Gasparavičiūtė R, Tauraitė D, Meškys R. Oxyfunctionalization of pyridine derivatives using whole cells of *Burkholderia* sp. MAK1. *Sci. Rep.* 2016, 6:39129



Open Oxyfunctionalization of pyridine derivatives using whole cells of Burkholderia sp. MAK1

Received: 18 August 2016 Accepted: 17 November 2016 Published: 16 December 2016 Jonita Stankevičiūtė, Justas Vaitekūnas, Vytautas Petkevičius, Renata Gasparavičiūtė, Daiva Tauraitė & Rolandas Meškys

Pyridinols and pyridinamines are important intermediates with many applications in chemical industry. The pyridine derivatives are in great demand as synthons for pharmaceutical products Moreover, pyridines are used either as biologically active substances or as building blocks for polymers with unique physical properties. Application of enzymes or whole cells is an attractive strategy for preparation of hydroxylated pyridines since the methods for chemical synthesis of pyridinols particularly aminopyridinols, are usually limited or inefficient. Burkholderia sp. MAK1 (DSM102049), capable of using pyridin-2-ol as the sole carbon and energy source, was isolated from soil. Whole cells of Burkholderia sp. MAK1 were confirmed to possess a good ability to convert different pyridin-2-amines and pyridin-2-ones into their 5-lydroxy derivatives. Moreover, several methylpyridines as well as methylated pyrazines were converted to appropriate N-oxides. In conclusion, regioselective oxyfunctionalization of pyridine derivatives using whole cells of Burkholderia sp. MAK1 is a promising method for the preparation of various pyridin-5-ols and pyridin-N-oxides.

The pyridine ring is found in various man-made compounds, such as dyes, industrial solvents, herbicides, pesticides as well as in many natural metabolites. Among the N-heterocyclic rings, pyridin-2-ol has considerable ticides as well as in many natural metabolites. Among the N-heterocyclic rings, pyridin-2-ol has considerable chemical and pharmacological importance. Due to a peptidomimetric functionality of III-pyridin-2-one tautomer, it plays an essential role as a scaffold in drug design¹⁻². Pharmacophores containing 1H-pyridin-2-ones are found in various therapeutic agents, including reverse transcriptase inhibitors², antibiotics and antifungals⁴⁻⁶, anti-allergic drugs² and analgesics². Moreover, 1H-pyridin-2-ones are promising compounds for the preparation of modified nucleotides and oligonucleotides³⁻¹!

A powel class of subpendic antioxidates (-aminopyridin-3-ols age more effective than many other

of modified nucleotides and oligonucleotides⁸⁻¹¹. A novel class of phenolic antioxidants, 6-aminopyridin-3-ols, are more effective than many other phenolic-class compounds reported to date¹². Pyridin-2-amines serve as a starting material for production of fused heterocycles, including imidazo-derivatives that possess significant biological activities similar to those of antiviral and immunosuppressive agents¹³⁻¹⁵. Moreover, 3-amino-imidazol [12-alpyridines were identified as a novel class of Mycobacterium tuberculosis glutamine synthetase inhibitors¹⁶, and 6-aminopyridin-3-ol was applied for the amthetic of para artificities¹⁷. for the synthesis of new antibiotics¹⁷.

Preparation of some 5-hydroxy-2-pyridones is achievable by both organo-chemical and biocatalytic approaches¹⁸, whereas no satisfactory synthetic methods leading to 6-aminopyridin-3-ols have been described thus far. In addition, only a few synthetic methods to aminopyridinol structures may be found in literature to date^{12,19,20}. Recently, a chemical synthesis of pyridine-3,5-diol derivatives from renewable carbohydrates has been demonstrated21

Oxyfunctionalization of chemical compounds by using enzymes or whole cells is an attractive strategy to obtain the desired products²²⁻³¹. The degradation of N-heterocyclic compounds, especially with regard to the production of metabolic intermediates, has received considerable attention in biotechnology as the starting process for the synthesis of fine and commodity chemicals, e.g., pyridine-2,5-diol (an intermediate for production of 5-aminolevulinic acid), 6-hydroxynicotinic acid and other pyridine derivatives²⁵⁻²⁸. Recently, the hydroxylation of the pyridine ring has been achieved using tetramethylpyrazine-degrading bacteria. It has been also shown that pyridine N-oxides can be prepared using microbial cells and enzymes; however, this has been accomplished

Department of Molecular Microbiology and Biotechnology, Institute of Biochemistry, the Life Sciences Centre, Vilnius University, Sauletekio al. 7, LT-10257 Vilnius, Lithuania. Correspondence and requests for materials should be addressed to J.S. (email: jonita.stankeviciute@bchi.vu.lt)

SCIENTIFIC REPORTS | 6:39129 | DOI: 10.1038/srep39129

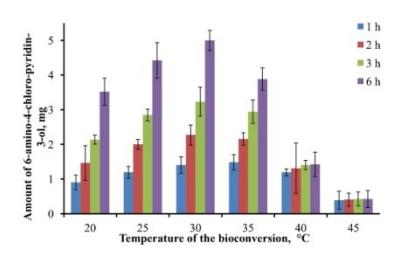


Figure 1. The dependence of the rate of 6-amino-4-chloro-pyridin-3-ol biosynthesis on temperature. 2-hydroxypyridine-induced *Burkholderia* sp. MAK1 cells were used as biocatalyst. The values represent the average of three independent experiments ±standard deviation.

using Methylococcus capsulatus monooxygenase²⁹, Agrocybe aegerita peroxygenase³⁰, and Verticillium sp. GF39 cells³¹ only.

Several bacteria belonging to the genera Arthrobacter, Achromobacter, Rhodococcus, and Nocardia are able to grow on pyridin-2-0l³²⁻³⁵. The first common steps in the microbial metabolism of pyridin-2-0l involve the hydroxylation of the ring yielding di- or trihydroxypyridine intermediates ^{22,35,36} that are promising synthons for the preparation of substituted pyridines.

the preparation of substituted pyridines.

In this study, the oxyfunctionalization of the pyridine ring by whole bacterial cells was investigated. The pyridin-2-ol-degrading Burkholderia sp. MAKI was found to be an efficient biocatalyst for the hydroxylation of various pyridin-2-ols and pyridin-2-amines. Moreover, Burkholderia sp. MAKI was capable of oxidising several N-heterocyclic ring systems to corresponding N-oxides.

Results and Discussion

Isolation of pyridin-2-ol-degrading bacteria. The gram-negative bacterial isolate MAK1, capable of using pyridin-2-ol as a sole carbon and energy source, was isolated from soil. The 165 rRNA gene sequence of MAK1 showed similarity to that of bacteria belonging to Burkholderia sordidicola. Based on the results of 165 rRNA gene sequence analysis (Supplementary information Fig. S-1) and biochemical characterization (Supplementary information Table S-1) the strain MAK1 was identified as Burkholderia sp. MAK1.

(supplementary innormation Labors-1) the strain Marki was Ineminied as *Burkhouerlus Sp. MAKL*.

In bacteria, pyridin-2-ol may be catabolized by two different pathways. The first pathway proceeds via formation of pyridine-2,3,6-triol, which spontaneously oxidises and dimerises to a blue pigment, 4,5,4°,5° eterahydroxy-3,3°-diazadiphenoquinone-(2,2°)^{2,2,3,5,7}. The other known catabolic pathway proceeds via formation of pyridine-2,5-diol, maleamic acid, maleic acid, and furnaric acid³³.

on pyraume-2,9-cno, material cacis, material action, and rumaric action.

In the case of Burkholderia sp. MAK1 described here, pyridin-2-ol was catabolized without the formation of a blue pigment. Assuming that pyridin-2,5-diol is an intermediate in pyridin-2-ol catabolic pathway, the activity of pyridin-2,5-diol 5,6-dioxygenase detected in the pyridin-2-ol-induced cells of Burkholderia sp. MAK1 suggested that this strain possesses an inducible pyridin-2-ol 5-monooxygenase.

Selection of pyridine derivatives as substrates for hydroxylation with Burkholderia sp. As we found out that Burkholderia sp. MAK1 consumes pyridine-2-ol via pyridine-2-5-diol by supposedly pyridine-2-ol inducible pyridin-2-ol 5-monoxygenase we wanted to test whether Burkholderia sp. MAK1 is capable of hydroxylating other pyridine derivatives. In this study, more than 100 of pyridine, pyrimidine, and pyrazine derivatives were screened for the hydroxylation using Burkholderia sp. MAK1 as a whole-cell biocatalyst (supplementary information Table S-2). The pyridin-2-ol-induced Burkholderia sp. MAK1 as delived with a potential substrate as described in the Methods section. The progress of the reaction was followed by HPLC-MS. The efficiency of conversion of several compounds by whole cells of Burkholderia sp. MAK1 is presented as Supplementary information Table S-3.

It is worth mentioning that induction of Burkholderia sp. MAK1 hydroxylation activity was observed only

It is worth mentioning that induction of Burkholderia sp. MAK1 hydroxylation activity was observed only in the presence of pyridin-2-ol. Several other tested compounds (pyridine, pyridine-2,5-diol, pyridin-2-amine) were not able to trigger the induction. Also no hydroxylation occurred when cells were cultivated with other sole carbon source (glucose or succinate) instead of pyridin-2-ol.

Optimization of cultivation and reaction conditions. Burkholderia sp. MAK1 grew poorly in rich nutrient medium, but the growth was observed in mineral medium (EFA or Koser) with pyridin-2-ol as a sole carbon source. The growth reached its peak after 40 h of incubation in EFA medium (OD₆₀=0.4). The optimal temperature for cultivation of Burkholderia sp. MAK1 appeared to be 30 °C. At higher tested temperature (37 °C), Burkholderia sp. MAK1 cells were not able to grow. Although bacterial growth was observed at 25 °C; it was rather slow compared to 30 °C. The effect of temperature on Burkholderia sp. MAK1-mediated synthesis of hydroxytaded pyridine derivatives was also investigated (Fig. 1). For this experiment 4-chloropyridin-2-amine was selected due

43

Substrate		Product				
Name	[M+H]+	[M+H]+	NMR	Name/Possible outcome	Conversion %	
Pyridin-2-amine	95	111	-	Hydroxylated at the 5-position	99	
3-Fluoropyridin-2-amine	113	129	0.70	Hydroxylated at the 5-position	43	
3-Bromopyridin-2-amine	173 and 175	189 and 191	-	Hydroxylated at the 5-position	48	
3-Chloropyridin-2-amine	129	145	+	6-amino-5-chloro-pyridin-3-ol	88	
Pyridin-2,6-diamine	110	214	-	Hydroxylation followed by dimerization	88	
4-Bromopyridin-2-amine	173 and 175	189 and 191	-	Hydroxylated at the 5-position	48	
4-Fluoropyridin-2-amine	113	129	+	6-amino-4-fluoro-pyridin-3-ol	70	
4-Chloropyridin-2-amine	129	145	+	6-amino-4-chloro-pyridin-3-ol	96	
4-methyl-pyridin-2-amine	109	125	+	6-Amino-4-methyl-pyridin-3-ol	74	
6-Bromopyridin-2-amine	173 and 175	189 and 191	-	Hydroxylated at the 5-position	53	
6-Chloropyridin-2-amine	129	145	+	6-amino-2-chloropyridin-3-ol	89	

Table 1. The bioconversion features of substituted pyridine-2-amines for which reactions products were detectable. For the NMR analysis approximately 10 mg of purified bioconversion product was used.

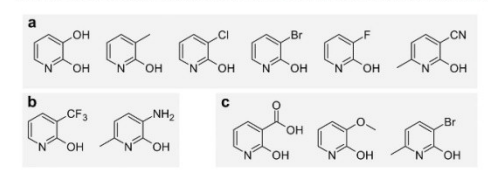


Figure 2. The 2-hydroxypyridines substituted at the third position, which were used as potential *Burkholderia* sp. MAK1 substrates. (a) Substrate consumption occurs, no products detected, (b) substrate consumed, product detected, (c) no reaction observed. The 2-hydroxypyridine induced cells were suspended in 10 mM potassium phosphate buffer, pH 7.2, supplemented with 15 mM glucose and 0.25 mM of corresponding substrate. Reactions were carried out at 30 °C. The progress of each reaction was observed by HPLC-MS.

to its great conversion percentage and definite product (Table 1). During the first hour of the experiment, the bioconversion of 4-chloropyridin-2-amine was most rapid at 30°C and 35°C with 6-amino-4-chloro-pyridin-3-ol production rate of 7 mg (g biomass)-1 h-1 and 7-4 mg (g biomass)-1 h-1, respectively. Higher temperatures (40–45°C) were found to be unfavorable for the synthesis, probably because of the inactivation of the biocatalyst. The conversion reached near completion (–97%) after six hours at 30°C .

Biotransformation of various pyridin-2-ols by Burkholderia sp. MAK1 cells. The study of N-alkylpyridine transformation revealed that 1-methyl-, 1-ethyl- and 1-propylpyridin-2-ol were transformed to the final dihydroxy products by Burkholderia sp. MAK1 cells. In the chromatogram of 1-ethylpyridin-2-ol bioconversion, two dominant peaks A and B were detected (Supplementary information Fig. S-II) corresponding to the newly formed compound and the residual substrate, respectively. The absorption maximum of the product, compared with that of the substrate, shifted to longer wavelengths (-30 mm), which is characteristic of compounds with additional hydroxy group. Also, the mass of the molecular ion of the product was 16 Da higher than that of the head of the control of the product was 16 Da higher than the compounds with additional hydroxy group. Also, the mass of the molecular ion of the product was 16 Da higher than that of the parent compounds, supporting the hydroxylation of 1-ethylpyridin-2-ol. Similar results were obtained with 1-methyl- and 1-propylpyridin-2-ol. In all cases, the formation of a single product was observed indicating the position-specific hydroxylation. Moreover, the apparent equivalence with pyridin-2-ol transformation suggested that 1-alkylpyridin-2-ols represented that 1-alkylpyridin-2-ols remained unchanged, which is most likely due to its bulkiness. In summary, pyridin-2-ols containing small 1-alkyl substituent are hydroxylated regioselectively, but further pyridine ring opening reaction does not occur. Thus, Burkholderia sp. MAK1 is capable of producing 1-alkylpyridin-2-ol-s substituted at position 3 (Fig. 2). HPIC-MS analysis revealed that compounds containing hydroxyl, methyl, bromo, chloro, or fluoro functional groups were completely catabolized by Burkholderia sp. MAK1 cells since no significant peaks corresponding to any hydroxylated products were detected. The latter suggests that the hydroxylated metabolites were likely further metabolized to aliphatic products. However, 3-(trifluoromethyl)pyridin-2-ol was slowly converted into a detectable new compound whose molecular mass was 16 Da higher than that of the substrate. Burkholderia sp. MAK1 is were not able to hydroxylated pyridin-2-ol scontaining carboxyl or methylory groups at position 3.

is MAKI cells were not able to hydroxylate pyridin-2-ols containing carboxyl or methoxy groups at position 3. Pyridin-2-ols carrying substituents at positions 3 and 6 were also examined. The pyridin-2-ol-induced cells were able to metabolize 2-hydroxy-6-methyl-pyridin-2-atomitrile: substrate concentration decreased over time, and no new products were detectable by HPLC-MS. After incubation of Burkholderia sp. MAKI with

44

Figure 3. 2-Hydroxypyridine derivatives substituted at the fourth, the sixth or both the fourth and the sixth positions, which were used as potential substrates for regioselective oxidation by *Burkholderia* sp. MAKI. (a) Substrate consumption occurs; (b) no reaction observed. The 2-hydroxypyridine induced cells were suspended in 10 mM potassium phosphate buffer, pH 7.2, supplemented with 15 mM glucose and 0.25 mM of corresponding substrate. Reactions were carried out at 30 °C. The progress of each reaction was observed by HPLC-MS.

Substrate	Product		Conversion	
Name	[M+H]+	[M+H]+	Possible outcome	%
1-Methylpyridin-2-one	110	126	Hydroxylated at the 5-position	20
1-Ethylpyridin-2(1H)-one	124	140	Hydroxylated at the 5-position	17
1-Propylpyridin-2(1 <i>H</i>)-one	138	154	Hydroxylated at the 5-position	Traces of product
3-(Trifluoromethyl) pyridin-2-ol	164	178 [M+H]	Hydroxylated at the 5-position	46
3-amino-6-methyl-pyridin-2-ol	125	279	Hydroxylation followed by dimerization	88
Pyridine-2,6-diol	112	-	Hydroxylation followed by dimerization (blue pigment)	-

Table 2. The bioconversion features of substituted pyridine-2-ols for which reactions products were detectable

3-amino-6-methyl-pyridin-2-ol, a new compound with a molecular mass of 278 Da accumulated in the reaction mixture. Since the molecular mass of the expected 3-amino-6-methyl-pyridin-2-ol-hydroxylation prod-uct is 140 Da, it is likely that the oxidation of the substrate is followed by the spontaneous dimerization. When Burkholderia ps. MAK1 cells were incubated with 3-bromo-6-methyl-pyridin-2-ol, neither hydroxylation, nor any other transformation occurred suggesting that 3-bromo functional group disrupted the proper orientation of the substrate.

Pyridin-2-ols substituted at positions 4 and/or 6 were also used as substrates in this study (Fig. 3). Pyridine-2,4-diol was completely oxidized by *Burkholderia* sp. MAK1 cells after 20 hours of incubation. However, the inter-mediate product accumulating in the reaction mixture was detected by HPLC-MS and its absorption special

mediate product accumulating in the reaction mixture was detected by HPLC-MS and its absorption spectra as well as molecular mass ([M+H]"=128.05, [M+H_2O+H]"=146.10, [2M+H]"=125.05) were consistent with those of hydroxylated pyridine-2.4-diol (Supplementary information Fig. S-III). Using 4-cyano, 4-chloro, 4-bromo, or 4-trifluomethyl substituted pyridin-2-ols, hydroxylation of the pyridine ring did not occur suggesting that the nature of a substituent at position 4 is important for the hydroxylation process. Pyridine-2.6-diol was transformed by Burkholderia sp. MAK1 to a blue pigment. Previously, Holmes with colleagues described dimerization of pyridine-2.3-6-triol, which led to the formation of a blue pigments'. Following this observation, the hydroxylation of the symmetric pyridine-2.6-diol by Burkholderia sp. MAK1 cells likely occurred at position 3 of the pyridine ring and the resulting pyridine-2.5-e-triol synonaeously dimerized to a blue compound. Moreover, if the sixth position of pyridin-2-ol was occupied by a small and uncharged functional group, the pyridine ring cleavage probably followed the hydroxylation event. Summarizing experiments with substituted pyridin-2-ol we can make the statement that most of the substrates were consumed without detectable products. Although we were unable to provide any data about structures of the detectible product there were strong evidences suggesting regioselective hydroxylation at 5-position (Table 2).

Screening of pyridin-2-amines as potential substrates for regioselective hydroxylation by *Burkholderia* sp. MAK1 cells. The ability of *Burkholderia* sp. MAK1 to transform various pyridin-2-ols encouraged us to study pyridin-2-amines as another group of potential substrates. During the initial experiments, the cells were incubated with pyridin-2-amine for 20 hours. HPLC-MS analysis revealed that pyridin-2-amine

SCIENTIFIC REPORTS | 6:39129 | DOI: 10.1038/srep39129

Figure 4. The 2-aminopyridines, which were tested as potential substrates for conversion by 2-hydroxypyridine-induced whole cells of Burkholderia sp. MAK1. (a) The 2-aminopyridine derivatives substituted at the third position; (b) the regioselective hydroxylation of 2-aminopyridines substituted at the fourth position ($X = CH_b$, C, E); (c) the 2-aminopyridines substituted at the sixth position.

was completely consumed, and the new peak in the chromatogram belonged to the expected product. The molecular mass of the product, which was 16 Da higher than that of pyridin-2-amine, confirmed the notion that hydroxylation of the substrate occurred. The UV-Vis spectrum of the product was compared with spectra of commercially available reference standards (pyridin-2-amine hydroxylated at position 3, 4, or 6), yet none of these spectra matched that of the product (Supplementary information Fig. S-IV). From this we presume that in the case of Burkholderia sp. MAK1, pyridin-2-amine undergoes hydroxylation at position 5. Next, pyraxin-2-amine, a homolog of gryidin-2-amine containing two nitrogen atoms in the aromatic ring,

Next, pyrazin-2-amine, a homolog of pyridin-2-amine containing two nitrogen atoms in the aromatic ring, was chosen as a substrate for the bioconversion. HPLC-MS analysis showed that the molecular mass of the biotransformation product was 16 Da higher than that of pyrazin-2-amine, suggesting that Burkholderia p. MAKI cells are also capable of pyrazin-2-amine hydroxylation.

Pyridin-2-amines with methyl, nitro, chloro, bromo, or fluoro substituent at position 3 (Fig. 4a) were all trans-

Pyridin-2-amines with methyl, nitro, chloro, bromo, or fluoros substituent at position 3 (Fig. 4a) were all transformed by Burkholderia ps. MAK1. Moreover, the pyridin-2-ol-induced cells were also capable of hydroxylating ethyl-2-aminopyridine-3-carboxylate, a compound with a bulky functional group at the 3-position. The conversion product of 3-chloropyridin-2-amine was purified as described in the Materials and Methods section, and its structure was analysed by 'H NMR, "C NMR, and HPLC-MS analyses. The molecular mass of the product (145 Da) corresponded to that of 6-amino-5-chloro-pyridin-3-ol. The compound showed four peaks in the 1H NMR spectrum (DMSO-d₀, ppm): 8 – 5.51 (s. 2 H. NH₂), 7.11 (d. J = 2.6 Hz, 1H, CH), 7.56 (d. J = 2.6 Hz, 1H, CH), 9.24 (brs, 1H, OH), and five peaks in the 13C NMR spectrum (DMSO-d₀, ppm): 8 – 113.58, 125.21, 133.73, 146.21, 149.46), identifying the product as 6-amino-5-chloro-pyridin-3-ol. The production yield of 6-amino-5-chloro-pyridin-3-ol. 3 49%.

146.21, 149.46), identifying the product as 6-amino-5-chloro-pyridin-3-ol. The production yield of 6-amino-5-chloro-pyridin-3-ol was 34%.

Both pyridine-2,3-diamine and 2-aminopyridin-3-ol were transformed into colored compounds, with a molecular mass of 213 Da (yellow-brown) and 214 Da (yellow-green), respectively. The retention time, UV-Vis spectra, and ionisation profile of the oxidation product of 2-aminopyridin-3-ol matched those of the analytical standard (2-amino-3H-dipyrido)3,2-b:2/3-'e][1,4]oxazine-3-one) suggesting that Burkholderia sp. MAK1 catalyzes the oxidative dimerization of 2-aminopyridin-3-ol. Also, although another analytical standard, pyridine-2,3-diamine derivative, is commercially unavailable, our results indicate, that MAK1 catalyzes dimerization of by ridine-2,3-diamine as well. These dimers are potential anticancer and antimicrobial drugs?

pyramic-22-diamine derivarie, is commercially unavailable, our Testian Brucker, Inta WANT Claralyzes uniterization of pyridine-23-diamine as well. These dimers are potential anticancer and antimicrobial drugs. Next, the ability of Burkholderia sp. MAKI cells to transform pyridin-2-amines substituted at position 4 was investigated. Compounds with methyl, chloro, bromo, or fluoro substituents were hydroxylated. In all cases, the molecular mass of reaction products, as estimated by HPLC-MS, was 16 Da higher than that of parent compounds indicating that oxidation of substrates had occurred.

indicating that oxidation of substrates had occurred.

In the case of 4-methyl-pyridin-2-amine, 4-chloro-pyridin-2-amine, and 4-fluoro-pyridin-2-amine, the bioransformation catalyzed by the pyridin-2-ol-induced *Burkholderia* sp. MAK1 cells resulted in the formation of a single product. The products of all three reactions were purified by a reverse phase chromatography (C18 cartridges, water/methanol mixture, 10:0 — 10:5), and their structures were analysed by 'H NMR and 'PC NMR. 6-Amino-4-methyl-pyridin-3-ol (H NMR (DMSO-d₀, pmp): 8 = 2.18 (s. 3.H, CH), 6.1 (d.) = 6.6. 2.3 Hz, 1H, CH), 6.70 (s. 2H, NH₂), 7.87 (d.) = 6.6 Hz, 1H, CH), ¹³C NMR (DMSO-d₀, ppm):

SCIENTIFIC REPORTS | 6:39129 | DOI: 10.1038/srep39129

 $\delta = 20.52,\,109.39,\,113.72,\,136.73,\,138.00,\,150.61),\,6$ -amino-4-chloro-pyridin-3-ol ('H NMR (DMSO-d_6-ppm): $\delta = 6.66$ (dd, $J = 7.0,\,2$ Hz, J = 1.000, $\delta = 1.000$, $\delta =$ 4-chloropyrimidin-2-amine, pyrimidine-2,4-diamine, and 2-aminopyrimidin-4-ol were also hydroxylated by the pyridin-2-ol-induced *Burkholderia* sp.MAK1 cells. According to the ¹H NMR and ¹³C NMR analyses, the purified product of 2-aminopyrimidin-4-ol conversion was 2-aminopyrimidine-4,5-diol, and the conversion yield was 18%. To our knowledge, biocatalytical production of 6-amino-4-methyl-pyridin-3-ol has never been described previously. Moreover, there is no available information concerning the synthesis of 6-amino-4-chloro-pyridin-3-ol or 6-amino-4-fluoro-pyridin-3-ol. By analogy to aminophenols, the new compounds described in this study

have great potential as materials for the production of dyes, drugs, pesticides, and etc. 40.

The compounds substituted at position 6 (Fig. 4c) were also transformed by Burkholderia sp. MAK1. HPLC-MS analysis showed that pyridine-2,6-diamine was consumed; however, no new compounds were detected. Nevertheless, in the case of pyridine-2,6-diamine, the reaction mixture turned brown suggesting that after oxidation, further transformations (e. g. polymerisation) occurred. The compounds with 6-chloro or 6-bromo substituents were converted to the corresponding hydroxylated products. The product of oxidation of 6-chloropyridin-2-amine, 6-amino-2-chloropyridin-3-ol, was purified and identified by 1 H NMR (DMSO-d $_{\Theta}$ ppm): δ= 5.90 (s, 2H, NH₂), 6.38 (d, J = 7.8 Hz, 1H, CH), 6.84 (d, J = 7.8 Hz, 1H, CH), 9.79 (brs 1H, OH). While 6-fluoropyridin-2-amine conversion was very slow, the transformation of 6-methoxypyridin-2-amine did not

occur at all. The conversion of 6-aminopyridin-2-ol led to several compounds suggesting that the substrate is hydroxylated at position 3 and/or 5, so that a mixture of several products in varying proportions results. Unlike the aforementioned pyridin-2-ols, the products of hydroxylation of 6-substituted pyridin-2-amines were not metabolised further suggesting that Burkholderia sp. MAKI may be applied for the regioselective synthesis of 6-substituted 2-aminopyridinols (Table 1).

Oxyfunctionalization of pyridine, pyrazine and their derivatives using whole-cell biocatalyst. The study on pyridin-2-amine and pyridin-2-ol bioconversion by *Burkholderia* sp. MAKI cells showed that the pyridin-2-ol-inducible pyridin-2-ol 5-monooxygenase has broad substrate specificity and strict regiospecificity since it catalyzes hydroxylation at position 5 on the aromatic ring. With very few exceptions, microbation 5 on the aromatic ring. With very few exceptions, microbation 5 on the aromatic ring. hydroxylation of pyridine-2-amines has been scarcely studied. One such exception is the study on the biotrans-formation of 4-methyl-3-nitro-pyridin-2-amine using whole-cells of fungus Cunninghamella elegans ATCC 26269. During this biotransformation, a mixture of three products, 6-amino-4-methyl-3-nitropyridin-3-0, 2-amino-4-hydroxymethyl-3-nitropyridine, and 2-amino-4-methyl-3-nitropyridine-1-oxide was obtained suggesting that both aromatic and aliphatic positions as well as the heterocyclic nitrogen atom undergo oxida-tion⁴¹. In the case of *Burkholderia* sp. MAK1 cells, oxidation of the heterocyclic nitrogen atom was not observed when pyridin-2-ols were used as substrates. To determine if these bacteria were capable of producing N-oxides, various pyridine and pyrazine compounds without amino or hydroxy group at position 2 were tested as sub-strates for pyridin-2-ol-induced *Burkholderia* sp. MAK1 cells. HPLC-MS analysis showed that pyridine was transformed into a single product whose molecular mass was 16 Da higher than that of the parent compound. The UV spectrum of the product was very similar to that of pyridine yet did not match with the spectra of 2-, The O's spectrum or ite ploduct was very similar to that of pyriamic yet dut not match with tite spectra of 2-7, 3-, or 4-hydroxy-substituted pyridines at position suggesting that the product of pyridine biotransformation spyridine-1-oxide (pyridine-N-oxide). The retention time, UV spectrum and ionisation profile of the bioconversion product matched those of analytical standard, pyridine-N-oxide, suggesting that Burkholderia sp. MAKI catalyzes pyridine oxidation at position 1. Induction of cells with pyridin-2-ol was necessary for the oxidation of pyridin-as well as for pyridin-2-ol and pyridin-2-amine transformation indicating that the same enzyme of Burkholderia sp. MAK1 is responsible for all these biotransformations.

A group of pyridines and pyrazines containing a methyl group attached to the aromatic ring at different posi-tions (Fig. 5) was studied as potential substrates for *Burkholderia* sp. MAK1. The test revealed that the whole cells of Burkholderia sp. MAK1 catalyzed the transformation of 2-methyl-, 3-methyl-, and 4-methylpyridine into corresponding N-oxides whose structures were confirmed by HPLC-MS using analytical standards (Table 3). Burkholderia sp. MAK1 was also capable of transforming di- and trimethyl pyridines, except those in which both positions adjacent to nitrogen were occupied.

Based on HPLC-MS analysis, the biotransformation of pyrazine resulted in the formation of two products with molecular masses that were 16 Da and 32 Da higher than that of the parent compound. ¹H and ¹³C NMR with molecular masses that were 16 Da and 32 Da higher than that of the parent compound. ¹H and ¹⁰C NMR analysis allowed identification of these products as pyrazine-1-oxide (¹H NMR (DMSO-d_a, ppm): 8–8.34-8.36 (m, 2H, CH), 8.54-8.57 (m, 2H, CH); ¹⁰C NMR (DMSO-d_a, ppm): 8= 134.85, 148.94) and pyrazine-1,4-dioxide (¹H NMR (DMSO-d_a, ppm): 8–8.28 (s, 4H, CH); ¹⁰C NMR (DMSO-d_a, ppm): 8=137.21).
Our research revealed that Burkholderia sp. MAK1 has also the ability to oxidize various methylpyrazines. For the oxidation of methylated pyrazines the single free position adjacent to either one of nitrogen atoms was a sufficient condition, e.g. the cells could oxidize 2,35-trimethylpyrazine, but not 2,35,5-tertamethylpyrazine. To date, only a few reports regarding the microbial N-hydroxylation of pyridines have been published. The formation of pyridine N-oxides has been observed in fungi Cuminghamella elegans ATCC 62669⁴, Verticillium sp. GF39⁴, and other fungit²² as well as in bacteria Methylococcus capsulatus²³ and Diaphorobacter sp. 15-51⁴³. Also, the purified a comatic percovenase from fungus Aerocube accept has been found to be active towards pyridine

the purified aromatic peroxygenase from fungus Agrocybe aegerita has been found to be active towards pyridine and its derivatives. In this context, the results of this study not only broaden our understanding of microbial transformation but also provide a versatile tool that can be used in a regioselective oxyfunctionalization of various pyridine derivatives

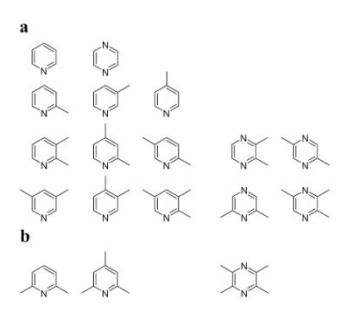


Figure 5. Pyridine, pyrazine and their methylated derivatives as substrates for the 2-hydroxypyridineinduced Burkholderia sp. MAK1 cells. (a) Substrate consumption occurs; (b) no reaction observed.

Substrate		Product			
Name	[M+H]+	[M+H]+	NMR	Name/Possible outcome	
Pyridine	80	96	-	Hydroxylated at the 1-position	
2-Methylpyridine	94	110	-	Hydroxylated at the 1-position	
3-Methylpyridine	94	110	-	Hydroxylated at the 1-position	
4-Methylpyridine	94	110	-	Hydroxylated at the 1-position	
Pyrazine	81	97 and 113	+	pyrazine-1-oxide and pyrazine-1,4-dioxide	

Table 3. The bioconversion features of pyridine and pyrazine derivatives for which reactions products were detectable. For the NMR analysis approximately 10 mg of purified bioconversion product was used.

Conclusions

In summary, whole cells of Burkholderia sp. MAK1 have high activity towards pyridin-2-amines and pyridin-2-ols, and are applicable for the synthesis of pyridin-5-ols from the corresponding substrates. Moreover, unsubstituted pyridine and pyrazine as well as their methylated derivatives can be converted into the corresponding N-oxides using pyridin-2-ol-induced Burkholderia sp. MAKI (Fig. 6). The approach presented here offers a promising alternative to chemical synthesis of hydroxylated pyridines.

Methods

Methods
Chemicals. Pyridin-2-amine, 2-chloropyridine, pyridine-2-carboxylic acid, pyridine-N-oxide, pyridin-3-ol, 2-aminopyridin-3-ol, 3-nitropyridin-2-amine, 2-hydroxy-6-oxo-1H-pyridine-4-carboxylic acid, pyrazine, pyridine-4-carboxylic acid and pyridine-2-a-dicarboxylic acid were purchased from Merck (Darmstadt, Germany). Pyridin-2-ol, pyrimidin-2-ol, 3-methylpyridine, 4-methylpyridine, 2-pyridylimethanol, pyridine-2-di-10-methylpyridine, 2-methylpyridine, 2-methylpyridine, 2-pyridylimethanol, pyridine-2-di-10-methylpyridine, 2-methylpyridine, 2-methylpyridine, 2-methylpyridine, 2-di-methylpyridine, 2-methylpyridine-2-mine, 3-methylpyridine-3-mine, pyridine-2-di-methylpyrazine, 2-di-methylpyrazine, 2-di-methylpyridine, 2-di-methylpy amine, 3-chloropyridin-2-amine, 4-chloropyridin-2-amine, 6-chloropyridin-2-amine, 3-bromopyridin-2-amine, 4-bromopyridin-2-amine, 6-bromopyridin-2-amine, 3-fluoropyridin-2-amine, 3-fluoropyridin-2

SCIENTIFIC REPORTS | 6:39129 | DOI: 10.1038/srep39129

Figure 6. The general scheme of oxyfunctionalization of pyridine and pyrazine derivatives using whole cells of *Burkholderia* sp. MAK1.

4-fluoropyridin-2-amine, 6-fluoropyridin-2-amine, 2-aminopyridin-4-ol, 3-methoxypyridin-2-amine, 6-methoxypyridin-2-amine, ethyl 2-aminopyridine-3-carboxylate, 2-aminopyrimidin-4-ol, 4-chloropyrimidin-2-amine, 4-bromopyridin-2-ol and 3-bromo-6-methylpyridin-2-ol were the products of Combi Blocks Inc (San Diego, 4-promopyriani-2-oi and 3-promo-e-mentylpyriani-2-oi were the products or Combi blocks inc (San Diego, USA). All reagents used in this study were of analytical grade. Nutrient agar (NA) medium and brain heart infusion (BHI) medium were obtained from Oxoid (Hampshire, UK). The 2-amino-3H-dipyrido[32,2-b;23'-e] [1,4] oxazine-3-one prepared by oxidation-dimerization of 2-amino-3-hydroxypyridine as described for 2-aminophenol⁴⁴, was a gift from Dr. J. Sarlauskas. The alkylated pyridones were synthesized according to the published

procedure".

1-Ethylpyridin-2(1*H*)-one. Yield 170 mg (69%), colourless oil. MS (ESI*): *m/z* 124.15 [M+H]*. ¹H NMR (CDCl₃, ppm): δ = 1.37 (t, *J* = 7.2 Hz, 3H, CH₃), 4.00 (q, *J* = 7.2 Hz, 2H, CH₃), 6.21 (td, *J* = 6.7, 1.4 Hz, 1H, CH), 6.61 (ddd, *J* = 9.1, 1.4, 0.8 Hz, 1H, CH), 7.29-7.37 (m, 2H, CH); ¹¹C NMR (CDCl₃, ppm): δ = 14.69, 44.96, 106.47, 120.96, 137.01, 139.46, 162.51

 $\begin{array}{l} 12096, [37.01, 139.46, [62.51.\\ 1.Propylpyridin-2(1H)-one. Yield 200 mg (73%), colourless oil. MS (ESI^+): <math>m/c$ 138.15 [M+H]+. 1 H NMR (DMSO-d_o, ppm): δ =0.95 (t, J=7.4 Hz, 3H, CH_J), 1.56–1.69 (m, 2H, CH_J), 3.75 (t, J=7.4 Hz, 2H, CH_J), 6.1 (t, J=6.7, 1.4 Hz, 1H, CH), 6.42 (ddd, J=9.1, 1.3, 0.6 Hz, 1H, CH), 7.35–7.46 (m, 1H, CH), 7.72 (ddd, J=6.7, 2.1, 0.6 Hz, 1H, CH); 1 C NMR (DMSO-d_o, ppm): δ =14.00, 29.23, 46.78, 105.55, 119.82, 138.93, 141.43, 162.15.
1. Butylpyridin-2(1H)-one. Yield 180 mg (60%), yellowish oil. MS (ESI^+): m/c 152.20 [M+H]+. 1 H NMR (DMSO-d_o, ppm): δ =0.90 (t, J=7.4 Hz, 2H, CH_J), 3.86 (t, J=7.4 Hz, 2H, CH_J), 6.19 (td, J=6.7, 1.4 Hz, 1H, CH), 6.36 (ddd, J=9.1, 1.4, 0.6 Hz, 1H, CH), 7.33–7.42 (m, H, CH), 7.35–7.21, 0.6 Hz, 1H, CH), 7.35–7.42 (m, 10.55), 120.02, 139.53, 140.13, 161.82.

Microbial cultures and cultivation conditions. EFA (g/l): K_3HPO₄ 10.0, KH₂PO₄ 4.0, yeast extract 0.5, (NH₂); So₄ 1.0, 2-hydroxypyridine 2.0, MgSO₄ × 7H₂O 0.2, salt solution 10 ml/l., pH 7.2; Salt solution (g/l): CaCl₂ × 2H₂O 2.0, MnSO₄ × 4H₂O 1.0, FeSO₄ × 7H₂O 0.5, all components were dissolved in 0.1N HCl and added in to EFA medium before cultivation; Koser mineral medium (g/l): NaCl 5.0, NH₄H₂PO₄ 1.0, K₃HPO₄ 1.0, MgSO₄ × 7H₂O 0.4. The final pH was adjusted to 7.0%. Koser agar medium was prepared adding agar to Koser mineral medium (15 g/l). Nutrient agar medium (g/l): 28.0; BHI (g/l): 37. All media and solutions were autoclaved at 1 arm for 30 min. at 1 atm for 30 min.

Bacteria were cultivated in liquid media with aeration at 30 °C.

For substrate specificity and bioconversion experiments *Burkholderia* sp. MAK1 was grown at 30 °C for 20 hours in 11 flasks containing 200 ml EFA medium. The cells were harvested by centrifugation and washed twice with 10 mM potassium phosphate buffer, pH 7.2.

Isolation of 2-hydroxypyridine utilizing microorganisms. $0.5\,\mathrm{g}$ of soil was suspended in $20\,\mathrm{ml}$ of Koser mineral medium. The aliquots $(10-100\,\mu\text{l})$ were spread on Koser agar plates supplemented with 0.1% 2-hydroxypyridine and clotrimazole $(20\,\mu\text{g/ml})$. Clotrimazole is known as cytochrome P450 inhibitor and was used to suppress growth of actinobacteria (e. g., Rhodococcus, Streptomyces, Mycobacterium) or fungi. After 3–5 days of aerobical cultivation at 30 °C the best growing colonies were selected for further work.

DNA analysis. DNA was extracted according to Woo $et\,al.^o$, 16S rRNA encoding genes were amplified using universal primers w001 and w002 o . The PCR product was cloned into the pT257RT plasmid (Thermo Fisher Scientific, Lithuania) and sequenced using M15/pUC (46) forward 22-mer and reverse 24-mer primers.

SCIENTIFIC REPORTS | 6:39129 | DOI: 10.1038/srep39129

16S rRNA sequence of MAK1 was analyzed using BLAST tool and The Ribosomal Database Project in the NCBI database. A phylogenetic tree was constructed and displayed using the neighbor-joining method with MEGA6⁴⁹. The Burkholderia sp. MAK1 16S rRNA gene sequence was deposited in GenBank under accession no. KU195413. Burkholderia sp. MAK1 was deposited to DSMZ German Culture Collection with accession no. DSM102049.

Bioconversion of pyridines, pyrimidines and pyrazines using the cells of Burkholderia sp. MAK1. 0.05 g of we biomass of Burkholderia sp. MAK1 cells was resuspended in 1 ml of 10 mM potassium phosphate bulker, pH 7.2. The suspension was supplemented with 15 mM glucose and 0.25 mM of corresponding properties. substrate and incubated at 30 °C. The process of the conversion was followed by HPLC-MS.

Isolation and characterization of bioconversion products. ~2 g of wet biomass of Burkholderia sp. MAK1 cells was resuspended in 100 ml of 10 mM potassium phosphate buffer, pH 7.2 supplemented with 15 mM of glucose and 0.25 mM of corresponding substrate and incubated at 30 °C. After bioconversion the cells of Burkholderia sp. MAK1 were separated by centrifugation. The supernatant liquid was vaporized to dryness under reduced pressure. The residue was dissolved in 5 ml of deionized water and purification of the product was carried out using reverse phase chromatography (12 g C-18 cartridge). Prior the purification the column was equilibrated with water. A mobile phase that consisted of water and methanol delivered in the gradient 10:0 — 10:5 elution mode. The collected fractions were analyzed by HPLC-MS. The fractions containing pure product were joined, and the solvent was removed under reduced pressure. ¹H NMR spectra were recorded in DMSO-d₀ or CDCl₀ on Bruker Ascend 400, 400 MHz, and ¹⁰C NMR were recorded on Bruker Ascend 400, 100 MHz. Chemical shifts are reported in parts per million relative to the solvent resonance signal as an internal standard. reported in parts per million relative to the solvent resonance signal as an internal standard.

HPLC-MS analysis. Before the analysis the cells were separated from the reaction mixture by centrifugation. The resultant supernatant was mixed with an equal part of actionitrile, centrifuged and analyzed using a high performance liquid chromatography system (CBM-20A controller, two LC-2020AD pumps, SIL-30AC auto sampler and CTO-20AC column oven; Shimadzu, Japan) equipped with a photo diode array (PDA) detector (SPD-M2OA Prominence diode array detector; Shimadzu, Japan) and a mass spectrometer (LCMS-2020, Shimadzu, Japan) ronmarca coole array detector; similarda, japani and a mass spectrometer (LCA95-2024), Similarda, Japani and a mass spectrometer (LCA95-2024), Similarda, Japani and with an ESI source. The chromatographic separation was conducted using a YMC Pack Pro column, 3×150 mm (YMC, Japan) at 40°C and a mobile phase that consisted of 0.1% formic acid water solution (solvent A), and acetonitrile (solvent B) delivered in the 0-60% gradient elution mode. Mass scans were measured from 210 up to m/z 700, at 350 °C interface temperature, 250 °C DL temperature, ±4,500 V interface voltage, neutral DL/Qarray, using N_2 as nebulizing and drying gas. Mass spectrometry data was acquired in both the positive and negative ionization mode. The data was analyzed using the LabSolutions LCMS software.

Activity assay of pyridine-2,5-diol 5,6-dioxygenase from Burkholderia sp. MAK1. Burkholderia sp. MAK1 was grown at 30 °C for 20 hours in two 150 ml flasks, one containing 25 ml EFA medium (pyridin-2-ol induced cells), other containing 25 ml EFA medium where pyridin-2-ol is substituted for succinate (uninduced cells, negative control). The cells were harvested by centrifugation, washed twice with 10 mM potassium phosphate buffer (pH 7.2), suspended in 5 ml of the same buffer and sonicated. In 1.5 ml tubes three separate reaction mixtures were combined: internal control (990 µl 10 mM potassium phosphate buffer, pH 7.2 and 10 µl 2 mg/ml pyridine-2,5-diol solution), negative control (890 µl 10 mM potassium phosphate buffer, pH 7.2, 10 µl 2 mg/ml pyridine-2,5-diol solution and 100 µl cell-free extract of uninduced cells) and sample (890 µl 10 mM potassium phosphate buffer, pH 7.2, 10 µl 2 mg/ml pyridine-2,5-diol solution and 100 µl cell-free extract of induced cells). 100µl of each reaction mixture was transferred to a 96 well plate and change in absorbance (\(\lambda_{\text{max}}\) 320 nm) per 30 minutes was measured. Overall change in absorbance was evaluated by subtracting noise data (internal and negative controls) from sample data. We were able to achieve 200–250 mU per 11 medium, where 1 enzyme unit (U) is an amount of enzyme that catalyzes depletion of 1μ mol pyridine-2,5-diol per minute. The measured molar extinction coefficient of pyridine-2,5-diol in ethanol was 9800 M⁻¹·cm⁻¹.

- References
 L. Loughlin, W. A., Tyndall, J. D. A., Glenn, M. P. & Fairlie, D. P. Beta-strand mimetics. Chem. Rev. 104, 6085–6117 (2004).
 2. Costantino, L. & Barlocco, D. Privileged structures as leads in medicinal chemistry. Curr. Med. Chem. 13, 65–85 (2006).
 3. Goldman, M. E. et al. Pyridinone derivatives specific human-immunodeficiency-virus type-1 reverse-transcriptase inhibitors with antiviral activity. Proc. Natl. Acad. Sci. USA 88, 6863–6867 (1991). 4. Li, Q., Mitscher, L. A. & Shen, L. L. The 2-pyridone antibacterial agents: bacterial topoisomerase inhibitors. Med. Res. Rev. 20,
- n, H. J. & Gademann, K. 4-Hydroxy-2-pyridone alkaloids: structures and synthetic approaches. Nat. Prod. Rep. 27, 1168–1185
- (2010).
 6. Desai, N. C., Rajpara, K. M. & Joshi, V. V. Synthesis of pyrazole encompassing 2-pyridone derivatives as antibacterial agents. Bioorg. Med. Chem. Lett. 23, 2714–2717 (2013).
- Med. Chem. Lett. 23, 2/14–2/17 (2013).

 7. Charrier, J. D. et al. Discovery and structure-activity relationship of 3-aminopyrid-2-ones as potent and selective interleukin-2

- Charrier, J. D. et al. Discovery and structure-activity relationship of 3-aminopyrid-2-ones as potent and selective interleukin-2 inducible T-cell kinase (Rib inhibitors, J. Mad. Chem. 54, 2341-235) (2011).
 Kusakabe, K. et al. Design, synthesis, and binding mode prediction of 2-pyridone-based selective CB2 receptor agonists. Bioorgan. Med. Chem. 21, 2045-2055 (2013).
 Urban, M., Pohl, R., Klepetarova, B. & Hocek, M. New modular and efficient approach to 6-substituted pyridin-2-yl C-nucleosides. J. Org. Chem. 17, 7322-7328 (2006).
 Tauraite, D., Raznasa, R., Mikalkenas, A., Serva, S. & Medeys, R. Synthesis of pyridone-based nucleoside analogues as substrates or abbituse of DNA analogues on Novel 2018 (1) 18 (1) 2172 (2016).

- 10. вазиляць, 1..., Кадапав, к., дикдикспая, л., эстуа, 5. & Meskys, К. Synthesis of pyridone-based nucleoside analogues as substrates or inhibitors of DNA polymerases. Nucleos Nucleot. Nucl. 35, 163–177 (2016).

 11. Rudra, A. et al. Bromopyridone nucleotide analogues, anoxic selective radiosensitizing agents that are incorporated in DNA by polymerases. J. Org. Chem. 80, 10675–10685 (2015).

 12. Wijmans, M. et al. 6-Amino-3-pyridinols: towards diffusion-controlled chain-breaking antioxidants. Angew. Chem. Int. Edit. 42, 4370–4373 (2003).

- Mase, T., Arima, H., Tomioka, K., Yamada, T. & Murase, K. Imidazo[2,1-b]benzothiazoles. 2. New immunosuppressive agents. J. Med. Chem. 29, 386-394 (1986).
 I. Lhassani, M. et al. Synthesis and antiviral activity of imidazo[1,2-a]pyridines. Eur. J. Med. Chem. 34, 271-274 (1999).
 Pires, M. J. D., Poeira, D. L. & Marques, M. M. B. Metal-catalyzed cross-coupling reactions of aminopyridines. Eur. J. Org. Chem. 33,

- Pires, M. J. D., Pocira, D. L. & Marques, M. M. B. Metal-catalyzed cross-coupling reactions of aminopyridines. Eur. J. Org. Chem. 33, 7197–7234 (2015).
 Odell, L. R. et al. Functionalized 3-amino-imidazo[1,2-a]pyridines: a novel class of drug-like Mycobacterium tuberculosis glutamine synthetase inhibitors. Bioorg. Med. Chem. Lett. 19, 4790–4793 (2009).
 Radulovic, N. et al. New 33-annelated coumarin derivatives synthesis, antimicrobial activity, antioxidant capacity, and molecular
- modeling, Monatsh, Chem. 137, 1477-1486 (2006).

- modeling. Monatsh. Chem. 137, 1477–1486 (2006).

 18. Behrman, E. I. Improved syntheses of 5-hydroxy-e-pyridones (2,5-dihydroxypyridines). Synthetic Commun. 38, 1168–1175 (2008).

 19. Moore, J. A. & Marascia, F. I. Heterocyclic studies. VII. The preparation and reactions of 2-amino-5-hydroxypyridines; the formation of an azaquimone, J. Am. Chem. Soc. 81, 6049–6065 (1999).

 20. Cai, L. S. et al. Synthesis and structure affinity relationships of new 4-(6-iodo-H-imidazo(1,2-alpyridin-2-yl)-N-dimethylbenzeneamine derivatives as ligands for human beta-amyloid plaques. J. Med. Chem. 50, 476–4758 (2007).

 21. Goranda, J. N., Korval, D. & Lankalapalli, R. S. An unusual synthesis of 2-pyridone and 3.5-dihydroxypyridine from a carbohydrate.
- Tetrahedron Lett. 54, 3230-3232 (2013).
- Tetuhedron Lett. 54, 3230–3232 (2013).

 2. Schewe, H., Mirata, M., A., Holmann, D., & Schrader, J. Biooxidation of monoterpenes with bacterial monooxygenases. Process Biochem. 46, 1885–1899 (2011).

 2. Schrewe, M., Julsing, M. K., Buhler, B. & Schmid, A. Whole-cell biocatalysis for selective and productive C-O functional group introduction and modification. Chem. Soc. Rev. 42, 6346–6377 (2013).

 2. Urlacher, J. B. & Girhard, M. Cytochrome P450 monooxygenases: an update on perspectives for synthetic application. Trends Biotechnol. 30, 26–36 (2012).

- Biotectimol. 39, 26–36 (2012).

 S. Nakano, H. et al. Purification, characterization and gene cloning of 6-hydroxynicotinate 3-monooxygenase from Pseudomonas fluorescens TNS. Eur. J. Biochem. 260, 120–126 (1999).

 S. Brandsch, R. Microbiology and biochemistry of nicotine degradation. Appl. Microbiol. Biotechnol. 69, 493–498 (2006).

 Zr. Kutanovas, S. et al. Biocomeresion of methylpyrazines and pyridlines using novel pyrazines-degrading microorganisms. Chemija 24,

- Kutanovas, S. et al. Isolation and characterization of novel pyridine dicarboxylic acid-degrading microorganisms. Chemija 27, 74–83
- 29. Colby, J., Stirling, D. I. & Dalton, H. The soluble methane mono-oxygenase of Methylococcus capsulatus (Bath). Its ability to
- Colly, J., Stirling, D. I. & Dalton, H. The soluble methane mono-oxygenae of Methylococcus capsulatus (Bath). Its ability to oxygenate n-alkanes, n-alkanes, ethers, and alicyclic, commantic and heterocyclic compounds. Biochem. J. 165, 995–902 (1977).
 Ullrich, K., Dolge, C., Kluge, M. & Hofrichter, M. Fyridine as novel substrate for regioselective oxygenation with aromatic percoxygenase from Agracybe acgeria. FEBS Lett. 582, 1400–1406 (2008).
 Mitsukura, K., Hayashi, M., Koshida, T. & Nagasawa, T. Oxdadation of aromatic N-heterocyclic compounds to N-oxides by Verticillians of Cyber 20 (18). Biosci. Bioreg. 115, 651–653 (2013).
 Cain, R. B., Houghton, C. & Wright, K. A. Microbial metabolism of the pyridine ring, Metabolism of 2- and 3-hydroxypyridines by the maleamate pathway in Achromobacter sp. Biochem. J. 140, 293–300 (1974).
 Xiasier, J. P., Feng, Y. & Bollag, J. M. Microbial netabolism of pyridine, quinoline, acridine, and their derivatives under aerobic and anaerobic conditions. Microbiol. Rev. 60, 483–498 (1996).
 O. Cloughlin, E., J. Sims, G. K. & Traina, S. J. Biodegradation of 2-methyl, 2-ethyl, and 2-hydroxypyridine by an Arthrobacter sp. isolated from subsurface sediment. Biodegradation 10, 93–104 (1999).
 S. Stanislasskien, R. et al. Construction of Expérichia col-Arthrobacter-Rhodococcus shuttle vectors based on a cryptic plasmid from Arthrobacter rhomb and investigation of their application for functional screening. FEMS Microbiol. Lett. 327, 78–86 (2012).
 S. Fetzner, S. Bacterial degradation of pyridine, include, quinoline, and their derivatives under different redox conditions. Appl. Microbiol. Biotechnol. 49, 237–250 (1998).
 Yatiekunas, J. Gasparavictute, R. Rutkiene, R., Tauraite, D. & Meskys, R. A. 2-hydroxypyridine catabolism pathway in Rhodococcus

- Microbiol. Biotechnol. 49, 237–250 (1998).
 7. Vatiekumas, I., Gasparavictute, R., Rutkiene, R., Tauraite, D. & Meskys, R. A. 2-hydroxypyridine catabolism pathway in Rhodococcus triodochrous strain PY11. Appl. Environ. Microbiol. 82, 1264–1273 (2015).
 8. Holmes, P. E., Rittebengs, C. & Kinackmuss, H. The bacterial oxidation of nicotine. 8. Synthesis of 2.3.6-trihydroxypyridine and accumulation and partial characterization of the product of 2.6-dihydroxypyridine oxidation. J. Biol. Chem. 247, 7628–7633 (1972).
 9. Tse, H. et al. Production of 2-aminophenoxazin-3-one by Staphylococcus aureus causes false-positive results in beta-galactosidase assays. J. Clin. Microbiol. 50, 5780–5782 (2012).

- assays. J. Clin. Microbiol. 50, 3780–3782 (2012).

 40. Arora, P. K. & Bae, H. Bacterial degradation of chlorophenols and their derivatives. Microb. Cell. Fact. 13, 31 (2014).

 41. Tally, T. et al. Microbial transformation of 2-amino-4-methyl-3-nitropyridine. J. Ind. Microbial Biotechnol. 39, 1789–1799 (2012).

 42. Parshikov, I. A., Netrusov, A. I. & Sutherland, J. B. Microbial transformation of azaarenes and potential uses in pharmaceutical synthesis. Appl. Microbiol. Biotechnol. 95, 871–888 (2012).

 43. Sun, J. Q. et al. Bacterial pyridine hydroxylation is ubiquitous in environment. Appl. Microbiol. Biotechnol. 98, 455–464 (2014).

 43. Nagaswan, H. T. & Guttmann, H. R. The oxidiation of 4-aminophenols by cytochrome c and cytochrome oxidase. I. Enzymatic oxidations and binding of oxidation products to bovine serum albumin. J. Biol. Chem. 234, 1593–1599 (1959).

 45. Kozikowski, A. P. Tueckmantel, W., Chellappan, S., Kellar, K. J. & Xiao, Y. 10-Substituted cytisine derivatives and methods of use thereof, vol. 2010/0048666 A. I. US2010.

- Interest. 70. 2010/09/09/00 Al. US2010.
 Koser, S. A. & Baird, G. R. Baterial destruction of nicotinic acid. J Infect Dis. 75, 250–261 (1944).
 Woo, T. H., Cheng, A. F. & Ling, J. M. An application of a simple method for the preparation of bacterial DNA. Biotechniques 13, 696–698 (1922).
- K. Godon, I. J. Zumstein, E., Dabert, P., Habouzit, F. & Moletta, R. Molecular microbial diversity of an anaerobic digestor as determined by small-subunit rDNA sequence analysis. Appl. Environ. Microbiol. 63, 2802–2813 (1997).
 Tamura, K., Stecher, G., Peterson, D., Fillpski, A. & Kumar, S. MEGA6: molecular evolutionary genetics analysis version 6.0. Mol. Biol. Evol. 30, 2725–2729 (2013).

Acknowledgements

The work was supported by European Social Fund (ESF) under the Human Resources Development Action Programme, the Global Grant measure, project No. VP1-3.1-\$MM-07-K-03-015. We are grateful to Dr. J. \$arlauskas for the valuable cooperation. We also thank Dr. L. Kalinienė for assistance with the preparation of the manuscript.

Author Contributions

R.M. conceived the study. R.G. isolated bacterial strain. J.S., J.V. and V.P. carried out bioconversion experiments. D.T. synthesized the substrates. J.S. and D.T. conducted the analysis of compounds. J.S., J.V., V.P., R.G., D.T. and R.M. analyzed the data and prepared the manuscript. All authors read and approved the final manuscript.

Additional Information
Supplementary information accompanies this paper at http://www.nature.com/srep

Competing financial interests: The authors declare no competing financial interests.

How to cite this article: Stankevičiūtė, J. et al. Oxyfunctionalization of pyridine derivatives using whole cells of Burkholderia sp. MAK1. Sci. Rep. 6, 39129; doi: 10.1038/srep39129 (2016).

Publisher's note: Springer Nature remains neutral with regard to jurisdictional claims in published maps and institutional affiliations.

This work is licensed under a Creative Commons Attribution 4.0 International License. The images or other third party material in this article are included in the article's Creative Commons license, unless indicated otherwise in the credit line; if the material is not included under the Creative Commons license, users will need to obtain permission from the license holder to reproduce the material. To view a copy of this license, visit http://creativecommons.org/licenses/by/4.0/

© The Author(s) 2016

Publication II

Petkevičius V, Vaitekūnas J, Stankevičiūtė J, Gasparavičiūtė R, Meškys R. Catabolism of 2-hydroxypyridine by *Burkholderia* sp. strain MAK1: a 2-hydroxypyridine 5-monooxygenase encoded by *hpdABCDE* catalyzes the first step of biodegradation. *Appl. Environ. Microbiol.* 2018, 84, e00387-18.

This material is licenced for reuse by American Society for Microbiology. All rights reserved.





Catabolism of 2-Hydroxypyridine by *Burkholderia* sp. Strain MAK1: a 2-Hydroxypyridine 5-Monooxygenase Encoded by *hpdABCDE* Catalyzes the First Step of Biodegradation

Vytautas Petkevičius, a Justas Vaitekūnas, a Jonita Stankevičiūtė, a Renata Gasparavičiūtė, a Rolandas Meškysa

*Department of Molecular Microbiology and Biotechnology, Institute of Biochemistry, Life Sciences Center, Vilnius University, Vilnius, Lithuania

ABSTRACT Microbial degradation of 2-hydroxypyridine usually results in the formation of a blue pigment (nicotine blue). In contrast, the Burkholderia sp. strain MAK1 bacterium utilizes 2-hydroxypyridine without the accumulation of nicotine blue. This scarcely investigated degradation pathway presumably employs 2-hydroxypyridine 5-monooxygenase, an elusive enzyme that has been hypothesized but has yet to be identified or characterized. The isolation of the mutant strain Burkholderia sp. MAK1 AP5 that is unable to utilize 2-hydroxypyridine has led to the identification of a gene cluster (designated hpd) which is responsible for the degradation of 2-hydroxypyridine. The activity of 2-hydroxypyridine 5-monooxygenase has been assigned to a soluble diiron monooxygenase (SDIMO) encoded by a five-gene cluster (hpdA, hpdB, hpdC, hpdD, and hpdE). A 4.5-kb DNA fragment containing all five genes has been successfully expressed in Burkholderia sp. MAK1 AP5 cells. We have proved that the recombinant HpdABCDE protein catalyzes the enzymatic turnover of 2-hydroxypyridine to 2,5dihydroxypyridine. Moreover, we have confirmed that emerging 2.5-dihydroxypyridine is a substrate for HpdF, an enzyme similar to 2,5-dihydroxypyridine 5,6dioxygenases that are involved in the catabolic pathways of nicotine and nicotinic acid. The proteins and genes identified in this study have allowed the identification of a novel degradation pathway of 2-hydroxypyridine. Our results provide a better understanding of the biodegradation of pyridine derivatives in nature. Also, the discovered 2-hydroxypyridine 5-monooxygenase may be an attractive catalyst for the regioselective synthesis of various N-heterocyclic compounds.

IMPORTANCE The degradation pathway of 2-hydroxypyridine without the accumulation of a blue pigment is relatively unexplored, as, to our knowledge, no genetic data related to this process have ever been presented. In this paper, we describe genes and enzymes involved in this little-studied catabolic pathway. This work provides new insights into the metabolism of 2-hydroxypyridine in nature. A broadrange substrate specificity of 2-hydroxypyridine 5-monoxygenase, a key enzyme in the degradation, makes this biocatalyst attractive for the regioselective hydroxylation of pyridine derivatives.

KEYWORDS 2-hydroxypyridine, 2-hydroxypyridine 5-monooxygenase, *Burkholderia* sp. MAK1, 2,5-dihydroxypyridine, 2,5-dihydroxypyridine 5,6-dioxygenase

pyridine and its derivatives are among the most abundant N-heterocyclic compounds in nature (1), including alkaloids, such as nicotine and mimosine, and many derivatives of nicotinic and picolinic acids (2). Pyridine and its derivatives are also produced in large quantities by the chemical industry as part of energy generation (e.g., from coal or shale oil production), pharmaceutical manufacture (e.g., isoniazid, cetylpyridinium chloride, and coramine), and agricultural activities (the herbicides diquat, paraquat, picloram, and fluridone) (3). The wastewater generated during the

Received 15 February 2018 Accepted 22 March 2018

Accepted manuscript posted online 30

Citation Petkevičius V, Valtekūnas J, Stankevičiūči J, Gasparavičiūre R, Meškys R. 2018. Catabolism of 2-hydroxypyridine 5monooxygenase encoded by hpdABCDE catalyzes the first step of biodegradation. Appl Environ Microbiol 84:e00387-18. https://doi.org/ 10.1138/ABMONBS.2.18

Editor Ning-Yi Zhou, Shanghai Jiao Tong University

Copyright © 2018 American Society for Microbiology. All Rights Reserved. Address correspondence to Vytautas

June 2018 Volume 84 Issue 11 e00387-18

Applied and Environmental Microbiology

FIG 1 Proposed degradation pathways of pyridine derivatives in bacteria through the formation of hydroxypyridines. Green arrows represent pathways or reactions for which appropriate genes and/or enzymes have been identified. Orange arrows show proposed pathways or reactions. The blue arrow represents spontaneous autooxidation. Triple arrows indicate more than one reaction.

aforementioned processes contains pyridine and pyridinecarboxylic acids, as well as amino-, chloro-, alkyl-, and hydroxypyridines (4). The heterocyclic nature of pyridine derivatives increases their solubility; therefore, they are easily transported through soil and contaminate groundwater (5). Due to their prevalence, toxicity, and mutagenic potential, pyridines are considered hazardous pollutants (6).

The microbial degradation of pyridine compounds usually involves the formation of hydroxylated intermediates (Fig. 1). Nevertheless, for decades, it was assumed that the biodegradation of pyridine did not include initial hydroxylation (1). However, more recent results oppose this theory. The data obtained by gas chromatography-mass spectrometry (GC-MS) methods suggest that Arthrobacter sp. strain KM-4 consumes pyridine via the formation of 2-hydroxypyridine (2HP) and 2,3-dihidroxypyridine (23DHP) (7). Likewise, MS analysis has shown the formation of dihydroxypyridines as metabolites of the pyridine degradation pathway in Rhodococcus sp. strain Chr9 (8), although no enzymes involved in these conversions have been identified thus far. In the case of phenol-degrading bacteria, the conversion of pyridine to pyridine-N-oxide (PNO) is catalyzed by the phenol monooxygenase (9). In Nocardia spp., the degradation of PNO begins with an enzymatic transformation of PNO to 2HP before undergoing further catabolism (10). Various forms of hydroxypyridines (2HP, PNO, 3-hydroxypyridine, and 4-hydroxypyridine) have been detected in urine samples of animals dosed with pyridine, suggesting that hydroxylation of pyridine is ubiquitous in nature (11). The most common hydroxylated intermediate in the degradation of pyridine derivatives appears to be 2.5-dihydroxypyridine (25DHP) (2). In the nicotinic acid degradation pathway, the formation of 25DHP from 6-hydroxynicotinic acid is catalyzed by the monooxygenase NicC (12). Two studies describe the formation of 25DHP from 6-hydroxy-3-succinoylpyridine catalyzed by monooxygenases HspB (13) and VppD (14). The occurrence of 25DHP has also

June 2018 Volume 84 Issue 11 e00387-18

been detected during the catabolism of picollinic acid (1) or 3-hydroxypyridine (15). However, the enzymes responsible for these biotransformations have not been identified so far. The best-studied 25DHP degradation pathway involves ring opening by 25DHP 5,6-dioxygenase, followed by the three-step catalytic cascade (maleamate pathway) leading to the formation of fumarate (16).

While guite a number of different bacteria (Arthrobacter, Rhodococcus, Achromobacter, and Nocardia spp.) have been found to degrade 2HP (1, 15, 17), neither enzymes nor genes implicated in this process have been extensively studied to date. The most researched degradation pathways of 2HP involve the formation of 2,3,6-trihydroxypyridine (THP). The THP intermediate autooxidizes spontaneously to form a blue pigment, 4,5,4',5'tetrahydroxy-3,3'-diazadiphenoquinone-(2,2') (18, 19). It has been proposed that THP originates through the oxidation of 2,5-dihydroxypyridine (25DHP), 2,6-dihydroxypyridine (26DHP), or 23DHP. However, the enzymes involved in these conversions are mostly unknown, and only the 26DHP 3-hydroxylase from Arthrobacter nicotinovorans (20) and HpvB monooxygenase from Arthrobacter sp. strain PY22 (21) have been identified to date. Most recently, it has been demonstrated that Rhodococcus sp. strain PY11 encodes a four-component dioxygenase, HpoBCDF, that transforms 2HP to 3,6-dihydroxy-1,2,3,6-tetrahydropyridin-2-one, which is further oxidized by HpoE to THP (22). Also, 2HP degradation without the formation of a blue pigment was observed. In three Achromobacter species, the degradation of 2HP resulted in an accumulation of maleamate, formic acid, ammonium, maleate, and fumarate, indicating the involvement of maleamate degradation pathway (15). The cell extracts of these bacteria also demonstrate 25DHP 5,6-dioxygenase activity, suggesting 25DHP to be a putative intermediate. However, the first step of 2HP degradation in this pathway remains enigmatic, since although the involvement of a putative 2HP 5-monooxygenase has been implied, neither the enzyme itself nor its gene have been identified/characterized thus far.

In our previous work (23), we demonstrated that *Burkholderia* sp. strain MAK1 cells pregrown in the presence of 2HP are able to hydroxylate various pyridine and pyrazine derivatives regioselectively. In this study, we present data on the genes and enzymes involved in the degradation of 2HP in *Burkholderia* sp. MAK1, a strain that uses 2HP as the sole source of carbon and energy without the formation of a blue pigment. The identified gene cluster *hpd* contains genes required for 2HP assimilation. The first steps of 2HP degradation in *Burkholderia* sp. MAK1 have been elucidated both by analysis of reaction products and identification of the enzymes responsible for these conversions.

RESULTS AND DISCUSSION

Identification of the gene cluster responsible for the catabolism of 2HP in Burkholderia sp. MAK1. The ability of the 2HP-induced Burkholderia sp. MAK1 cells to hydroxylate pyridines at the C-5 position suggested that 2HP was degraded via the formation of 25DHP. Later, we noticed that 2HP-induced Burkholderia sp. MAK1 cells turned deep blue when grown on agar plates with indole, whereas the color of uninduced cells remained unchanged. It is well known that the enzymatic synthesis of indigo dye from indole involves various types of mono- or dioxygenases (24). Therefore, we assumed that the degradation of 2HP by Burkholderia sp. MAK1 begins with the formation of 25DHP, catalyzed by a 2HP-inducible monooxygenase, which is also able to hydroxylate indole. Following this hypothesis, a mutant of Burkholderia sp. MAK1 in which the appropriate gene was disrupted would neither turn blue in the presence of indole nor be able to grow with 2HP as the sole carbon and energy source.

To generate random mutants, the competent cells of Burkholderia sp. MAK1 were transformed with the plasposon pTnMod-OKm' (25) by electroporation and then plated on EFA medium[10.0 g/liter K,PPO₄, 4.0 g/liter K,PPO₄, 0.5 g/liter yeast extract, 1.0 g/liter (NH₂)₂SO₄, 0.2 g/liter MgSO₄,7H₂O (pH 7.0)] containing 2HP (as an inducer), succinate (Suc; as a carbon source), kanamycin (Km), and indole (Ind). The first screening step involved the identification of the white colony-forming mutants among the blue-forming ones. Then, such mutants were transferred onto another 2HP-Suc-Km-Ind agar plate to ensure that the cells were kanamycin resistant and remained white. To

June 2018 Volume 84 Issue 11 e00387-18 aem.asm.org 3

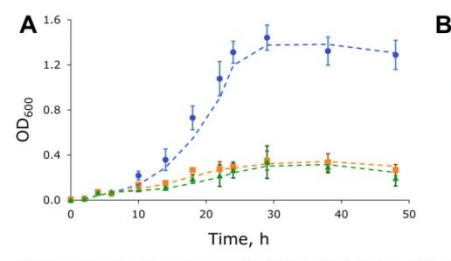




FIG 2 Growth kinetics and indigo dye production of wild-type Burkholderia sp. MAK1 and MAK1 ΔP5 mutant. (A) Blue circles, growth of wild-type bacterium in EFA medium containing 2HP (1.0 g/liter); orange squares, MAK1 ΔP5 mutant in EFA medium containing 2HP (1.0 g/liter); green triangles, wild-type bacterium in EFA medium without the carbon source. Data points are averages of the results from three experiments, and error bars show the standard deviation. Dashed lines represent trendlines using moving average data approximation (period = 2). (β) Burkholderia sp. MAK1 ΔP5 bacterium (on the left) and wild-type Burkholderia sp. MAK1 (on the right) grown on EFA medium supplemented with 2HP, succinate, and indole.

test their inability to consume 2HP, the mutant cells were transferred onto agar plates containing 2HP as the sole source of carbon and energy. In this manner, we were able to select a proper mutant, designated *Burkholderia* sp. MAK1 Δ PS, with no capacity to synthesize indigo dye (in the presence of indole and 2HP) or to degrade 2HP (Fig. 2).

To retrieve the transposon insertion site, the chromosomic DNA of the *Burkholderia* sp. MAKI ΔPS was digested with one of the restriction enzymes (Sall or Drail), both of which had recognition sites flanking a kanamycin resistance cassette, and was self-ligated. Thus, the recombinant circular DNA molecules containing a pMB1 ori sequence were produced, so that they could function as the plasmids in *Escherichia coli* and could be used for the transformation and screening. The insertion site flanking sequences (plasmids pSal_4 [5,714 bp] and pDra_1 [8,249 bp]) were determined applying a primer walking strategy. Merging these sequences resulted in a continuous DNA fragment. Then, the derived sequence was compared to that obtained from whole-genome sequencing. Notably, the analysis of the whole-genome sequencing data alone did not allow for the identification of 2HP assimilation genes. However, by combining the data from the analysis of kanamycin resistance cassette-flanking regions and whole-genome sequencing, the gene cluster (designated *hpd*) responsible for the degradation of 2HP in *Burkholderia* sp. MAK1 (Fig. 3B) was identified.

Bioinformatic analysis of the hpd gene cluster. The hpd gene cluster is a 13-kblong DNA fragment containing 12 open reading frames (Table 1). Four genes show high sequence similarity to those encoding the catabolism of 25DHP (25DHP 5,6-dioxygenase, N-formylmaleamate deformylase, maleamate amidase, and maleate isomerase) in nicotineand nicotinate-degrading bacteria (12–14). This indicates that in Burkholderia sp. MAK1, 2HP is catabolized via the formation of 25DHP and through the maleamate pathway (Fig. 3), Also, the presence of the aforementioned genes supports the hypothesis that 2HP is being directly hydroxylated to form 25DHP. The maleamate pathway begins with the dioxygenolysis of 25DHP to N-formylmaleamic acid, catalyzed by 25DHP 5,6dioxygenase (12). HpdF of Burkholderia sp. MAK1 shows a significant similarity to the well-characterized dioxygenases, such as NicX (55%) from Pseudomonas putida KT2440, Hpo (41%) from Pseudomonas putida S16, and VppE (41%) from Ochrobactrum sp. strain SJY1, suggesting that it likely is a 25DHP 5,6-dioxygenase. In addition, HpdF possesses the canonical 2-His-1-carboxylate (H265, H316, and D318) metal-binding motif found in the classical extradiol ring cleavage dioxygenases. The hydrolysis of N-formylmaleamic acid to maleamic and formic acids is catalyzed by N-formylmaleamate deformylase, a member of α/β -hydrolase-fold superfamily. HpdG from *Burkholderia* sp. MAK1 has homology to the enzymes from the α/β -hydrolase-fold superfamily and shows 30%

June 2018 Volume 84 Issue 11 e00387-18

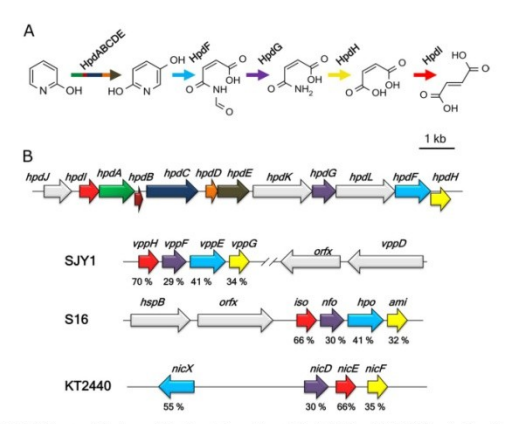


FIG 3 (A) Proposed 2-hydroxypyridine degradation pathway in Butkholderia sp. MAK1. (B) Organization of the hpd gene cluster. hpdABCE, 2HP 5-monoxygenase (green hpdAB, dark red hpdB), dark blue hpdC), can brown hpdB] arrows, hpdf. 2SDHP 5-dioxygenase (sprein, hpdG, Mornymhaelmante deform) lase (purple); hpdH, maleamate amidase (yellow); hpdf, melaste isomerase (red). hpdL (chaperone), hpdL (chaperone), hpdL (chaperone) are colored the same as in well-characterized pyridine derivative-degrading bacteria (Cchroboctrum sp. SV1). Pseudomonas putdue sigN 5-diox SV1, and in a city service of the same as in well-characterized pyridine derivative-degrading bacteria (Cchroboctrum sp. SV1). Pseudomonas putdue sigN 6-diox sigN 6

similarity to the well-studied N-formylmaleamate deformylases Nfo (13) and NicD (12). The next step in the biodegradation pathway is the conversion of maleamate to maleic acid catalyzed by maleamate amidase, a member of the cysteine hydrolase superfamily. In the hpd gene cluster, the corresponding enzyme has been found to be encoded by hpdH. The degradation pathway of 2HP ends with the isomerization of maleic acid to fumaric acid, a Krebs cycle intermediate. In the case of Burkholderia sp. MAK1, the isomerization activity has been assigned to HpdI, as it shows a significant homology to the maleate cis/trans-isomerase, an enzyme belonging to the Asp/Glu racemase superfamily. Three genes (hpdJ, hpdI, and hpdK) from the hpd locus appear to be indirectly involved in the biodegradation of 2HP and have been associated with transcription regulation, protein folding, and transport. Based on the results of bioinformatics

TABLE 1 Functional annotation of hypothetical proteins encoded in hpd gene cluster

Protein			Superfamily designation information		
	Size (amino acids)	Putative function	Specific hit/conserved domain	Accession no	
HpdJ	345	Transcription regulator	HTH_AraC	cl26290	
Hpdl	233	Maleate isomerase	Asp Glu race	cl00518	
HpdA	348	2HP 5-monooxygenase subunit	Ferritin-like	cl00264	
HpdB	105	2HP 5-monooxygenase regulatory subunit	MmoB/DmpM	PF02406	
HpdC	491	2HP 5-monooxygenase catalytic subunit	Ferritin_like	cl00264	
HpdD	118	Ferredoxin	Thioredoxin_like	cl00388	
HpdE	404	NADH-ubiquinone oxidoreductase	NADH_4Fe-4S	cl26507	
HpdK	555	Permease	SLC5-6-like sbd	cl00456	
HpdG	285	N-Formylmaleamate deformylase	Abhydrolase_1	cl26327	
HpdL	535	Chaperone	Chaperonin_like	cl02777	
HpdF	348	25DHP 5,6-dioxygenase	Peptidase_M29	cl19596	
HpdH	307	Maleamate amidase	Cysteine hydrolases	cl00220	

June 2018 Volume 84 Issue 11 e00387-18

analysis, the hypothetical 2HP 5-monooxygenase of Burkholderia sp. MAK1 is a soluble diiron monooxygenase (SDIMO) encoded by a five-gene locus (hpdA, hpaB, hpdC, hpdD, and hpdE). The family of SDIMOs can be divided into the following five major groups: phenol hydroxylases, soluble methane monooxygenases, four-component alkene/aromatic monooxygenases, alkane/alkene monooxygenases, and tetrahydrofuran monooxygenases (26). The BLAST analysis revealed similarity between hpdA and toluene monooxygenase β -subunit. In the case of the gene product of hpdB, however, homology searches returned only a few low-similarity hits, one of which was a putative phenol hydroxylase. Based on a Pfam search. HpdB of Burkholderia sp. MAK1 has been predicted to belong to the Mmob/DmpM family, which mostly consists of methane monooxygenase regulatory proteins. The protein encoded by hpdC shows similarity to the toluene monooxygenase α -subunit, which harbors a carboxylate-bridged diiron center at the active site. According to the literature, SDIMOs form a dimeric (bi- or tri-component) hydroxylase complex, $\alpha_2\beta_2\gamma_2$ or $\alpha_2\beta_2$ (27). Based on the results of bioinformatics analysis, hpdC and hpdA of Burkholderia sp. MAK1 code for the α - and β -subunits, respectively, whereas the hpdB-encoded protein possesses regulatory function. Most SDI-MOs contain a sulfur-iron cluster and flavin adenine dinucleotide (FAD)-dependent oxidoreductase that shuttles electrons from NADH to a catalytic complex, as well as a small Rieske protein that mediates electron transfer between oxidoreductase and catalytic complex. In the case of the hpd gene cluster, these functions have been assigned to hpdE and hpdD, respectively. The multiple-amino-acid sequence alignment of HpdC with various well-studied α -subunits of SDIMOs revealed that these proteins share a set of conservative carboxylate-bridged diiron center-forming amino acids (E120, E150, H153, E211, E245, and H248), an observation that has been supported by the tertiary structure model of HpdC (see Fig. S1 in the supplemental material). Despite these similarities, the phylogenetic analysis revealed that HpdC likely differs from any known SDIMOs, as it appears to occupy a distinct branch in the phylogenetic tree (see Fig. 4A). Notably, homology searches with the HpdC amino acid sequence have returned only low-similarity hits. The closest matches (which all were putative proteins from Gram-positive bacteria) shared 41% amino acid (aa) sequence identity with HpdC, while the similarity between HpdC and other characterized homologous proteins was <35%. The remaining Burkholderia sp. MAK1 monooxygenase genes. hpdA, hpdB, hpdD, and hpdE, show even lower similarity to their characterized counterparts (Fig. 4B). Also, as seen in Fig. 4B, the arrangement of the Burkholderia sp. MAK1 hpdABCDE gene cluster differs profoundly from that of bacteria representing other SDIMO groups. Taken together, all these findings illustrate how unusual and unique is the hpdABCDE gene cluster in Burkholderia sp. MAK1.

The bioinformatics analysis of the hpd gene cluster revealed homologues of the characterized enzymes involved in the catabolism of 25DHP. In Burkholderia Sp. MAK1, the hypothetical 2HP 5-monooxygenase is encoded by the hpdABCDE gene cluster and is only distantly related to SDIMOs from other bacteria. SDIMOs are usually found in xenobiotic-degrading microorganisms, where they usually catalyze the first steps of the degradation of xenobiotics by hydroxylating the substrate (26, 27). To date, a number of SDIMOs capable of hydroxylating pyridine derivatives (8, 9) have been described in the literature. However, to our knowledge, no SDIMO enzymes directly involved in the biodegradation of pyridine and its derivatives have been reported thus far.

qPCR analysis of the hpdABCDE gene cluster. To confirm that the identified hpdABCDE genes were indeed expressed in response to 2HP, quantitative PCR (qPCR) experiments were performed using total RNA extracted from the 2HP-induced cells of MAK1, as described in Materials and Methods. The reverse transcription-PCR (RT-PCR) produced PCR products of the expected size (Fig. 5A). A comparison of hpdABCDE mRNA synthesis levels between 2HP-grown Burkholderia sp. MAK1 cells (induced conditions) and succinate-grown cells (no induction) was made. The results revealed that the transcription of hpdABCDE genes increased 100-fold in the presence of 2HP (Fig. 5B); hence, HpdABCDE synthesis was shown to be specifically induced by growth on 2HP.

June 2018 Volume 84 Issue 11 e00387-18

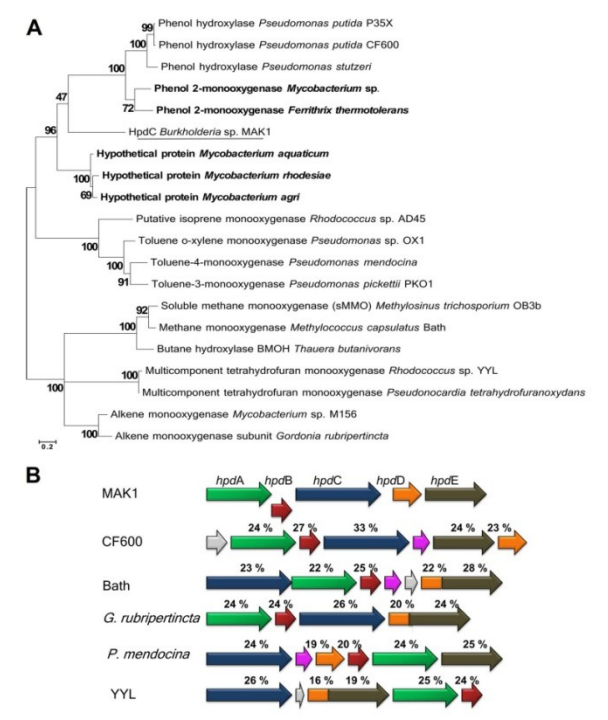


FIG 4 Phylogenetic analysis of hpdABCDE genes. (A) The phylogenetic tree of SDIMO α -subunits. The tree was generated using the maximum likelihood method with 500 bootstrap iterations. The scale bar represents 0.20 substitutions per site. The five closest BLAST his of HpdCar erg given in bold. (B) Structural alignment between representatives of all five SDIMO groups and the hpdABCDE duster. Identities (%) of amino acid sequence between hpdABCDE and homologous proteins are indicated under the corresponding ORFs. Blue arrows, α -subunits; generarrows, β -subunits; portion oxidoreductated under the corresponding ORFs. Blue arrows, freedoxins; brown arrows, NADH-sibiquinone oxidoreductases; gray arrows, putative or unknown-function genes.

Cloning and expression of hpdABCDE and hpdF genes in E. coli. Since the genes and enzymes implicated in the maleamate pathway are well described (12–14), we have concentrated our investigation on the apparent 2HP hydroxylation to 25DHP, presumably catalyzed by HpdABCDE, and the following ring opening of 25DHP potentially driven by HpdF. The overexpression of HpdF was successfully achieved by transforming E. coli BL21(DE3) or Rosetta(DE3)pLySS cells with the plasmid HpdF_pET. SDS-PAGE analysis revealed that the recombinant HpdF (theoretical mass, 38 Kba) was expressed as a soluble protein (Fig. S2A), and the cells harbored an active 25DHP dioxygenase (specific activity, 0.54 \pm 0.1 nmol - min^1 \cdot mg^-1 of cell [wet weight]). To obtain a 2HP hydroxylase, the hpdABCDE cluster was cloned as a continuous DNA fragment into the pET-28b plasmid vector. The resulting recombinant plasmid was then used to transform

June 2018 Volume 84 Issue 11 e00387-18

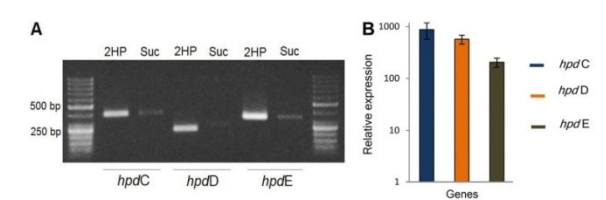


FIG 5 Qualitative (A) and quantitative (B) RT-PCR analysis of the expression of hpdABCDE genes. Strain MAK1 was cultivated in liquid EFA medium supplemented with either 1.0 g/liter 2 HP (induced conditions) or 1.0 g/liter succinate (Suc; no induction) as a single source of carbon. Primers were designed to amplify the regions in hpdC, hpdD, and hpdE genes. The data are presented as relative RNA amounts calculated from the threshold cycles using the threshold cycle of 158 RNA as reference. Bars show the increase in the expression of the hpdC, hpdD, and hpdE genes under 2HP induction compared to growth without 2HP (on succinate). The averages of three independent runs are presented.

E. coli BL21(DE3) and Rosetta(DE3)pLysS cells. The expression of the recombinant proteins was observed even though the proteins were found mainly in an insoluble fraction (Fig. S2B), and no enzyme activity was detected. By lowering the cultivation temperature to 16°C, the fraction of a soluble protein was increased, although the monooxygenase activity remained undetected.

Identification of catalytic properties of HpdABCDE and HpdF proteins. Since E. coli cells appeared to be an unsuitable host for the expression of HpdABCDE, Burkholderia sp. MAK1 ΔP5 cells were considered as an alternative. We tested pBBR1MCS plasmids (28) as suitable expression vectors and were satisfied with their transformation efficiency and stability in Burkholderia sp. MAK1 ΔP5 cells. However, the Plac promoter used in these vectors seemed to be inactive in this host, as no significant fluorescence was detected in bacteria harboring plasmid gfp_pBBR1MCS-1 containing the gfp gene downstream of the P_{lac} promoter (data not shown). Hence, the arabinose-inducible P_{BAD} promoter was inserted, since it was successfully used for protein expression in the Burkholderia genus (29). Plac promoter elements of pBBR1MCS-1 were cut out with the restriction endonucleases Vspl and Sacl and replaced with a PCR amplicon containing the P_{BAD} promoter, araC regulator, and terminator sequences from the pBAD24 vector (30). Thus, a broad-host-range arabinose-inducible expression vector, pBAD-MCS-1, was generated (Fig. 6A). The activity of the P_{BAD} promoter was successfully tested by cloning the gfp gene into the pBAD-MCS-1 (gfp_pBAD-MCS-1) vector and transforming the Burkholderia sp. MAK1 cells with this plasmid (data not shown).

Encouraged by these results, we cloned the hpdABCDE cluster as a continuous DNA fragment into the pBAD-MCS1 vector (plasmid HpdABCDE_pBAD-MCS-1). Burkholderia sp. MAK1 ΔP5 cells transformed with this plasmid were grown in liquid EFA medium, and the expression of the recombinant proteins was induced with arabinose (final concentration, 0.2%). The SDS-PAGE analysis revealed the presence of the recombinant proteins in cell extracts (Fig. 6B), though a major portion of these proteins were synthesized as inclusion bodies. However, the most noticeable effect of the expression of HpdABCDE was observed on agar plates. When plated on medium containing succinate, 2HP, and arabinose, both the transformed cells and the medium turned bright green at first. Later, both turned deep brown and, finally, to black. In the case of Burkholderia sp. MAK1 ΔP5 cells plated on the same medium, as expected, no such change in color was observed. Since a freshly prepared aqueous solution of 25DHP exhibits the same color change during incubation under aerobic conditions, it was a strong indication that recombinant HpdABCDE catalyzes 2HP turnover to 25DHP. To confirm this, a more detailed analysis was carried out. First, the biomass of Burkholderia sp. MAK1 Δ P5 cells carrying the plasmid HpdABCDE_pBAD-MCS-1 was prepared, as described in Materials and Methods. Then, the intact cells were transferred to a reaction

June 2018 Volume 84 Issue 11 e00387-18

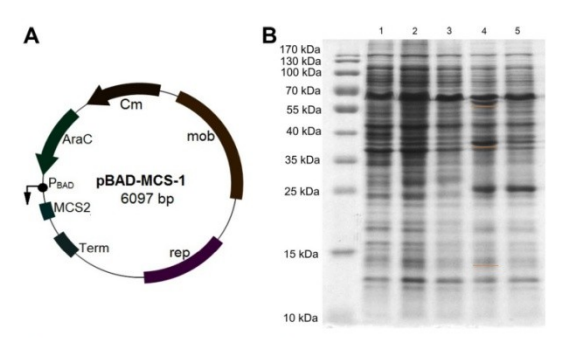


FIG 6 (A) Map of the plasmid vector pBAD-MCS-1. (B) SDS-PAGE analysis of HpdABCDE overexpression in Burkholderia sp. MAK1 ΔPS cells. Lanes 1 to 3, free-cell extracts of Burkholderia sp. MAK1 grown on succinate (lane 1), and on 2HP (lane 2, total fraction; lane 3, soluble fraction). Lanes 4 and 5, extracts of Burkholderia sp. MAK1 ΔPS/HpdABCDE, pBAD-MCS-1 and supplemented with O2% arabinose (lane 4, total fraction; lane 5, soluble fraction). Orange underlines indicate recombinant proteins.

mixture containing 2HP, and the UV spectra were recorded at fixed time intervals. The time-dependent decline of 2HP absorbance at 290 nm and the formation of a new compound with an absorbance peak at 320 nm were observed (Fig. 7). Then, this conversion mixture was analyzed by high-performance liquid chromatography mass spectrometry (HPLC-MS), where a 2HP-specific peak (retention time, 5 min 12 s; m/2 96) disappeared, and a new one (retention time, 3 min 8 s; m/2 112) was detected. An increase in mass by 16 Da indicated a typical monooxygenase activity, i.e., the incorporation of one oxygen atom. To evaluate the regioselectivity of the hydroxylation, a

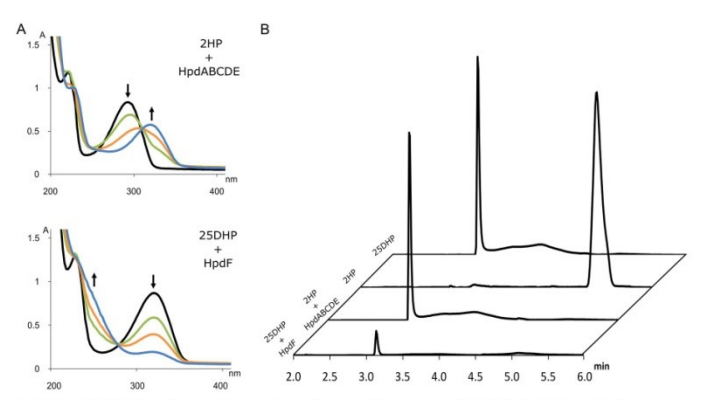


FIG 7 2HP and 25DHP biotransformation *in vivo* with recombinant cells [Burkholderia sp. MAK1 ΔP5/HpdABCDE_pBAD-MCS-1 and E. coli Rosetta(DE3)plys/S/HpdF_pET]. (A) The progress of the reaction was monitored using a UV-Vis spectrophotometer, initial spectra showed by black curves, after 1 h of incubation (green), after 2 h (orange), and after 3 h (blue). (B) The end products of biotransformation reaction were analyzed by HPLC and are presented as stacked HPLC chromatograms (310 nm).

June 2018 Volume 84 Issue 11 e00387-18 aem.asm.org 9

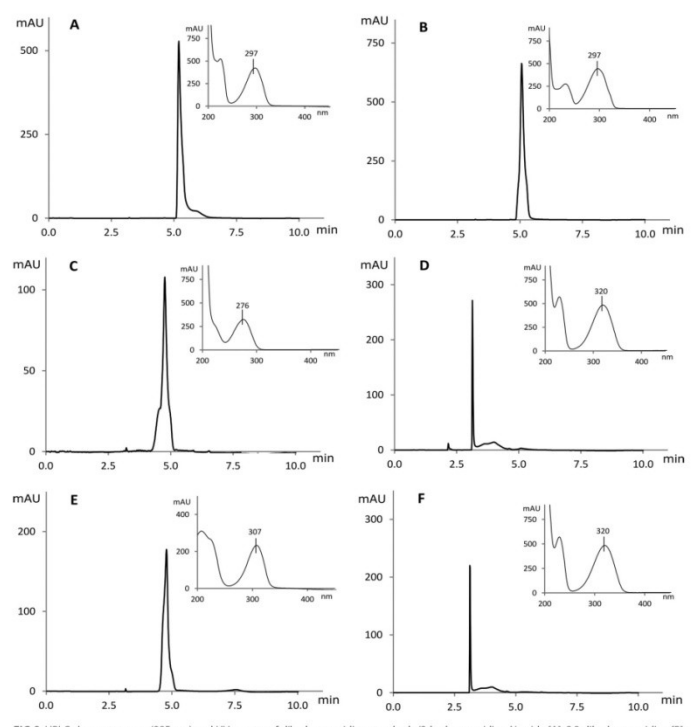


FIG 8 HPLC chromatograms (295 nm) and UV spectra of dihydroxypyridine standards (2-hydroxypyridine N-oxide (A), 2,3-dihydroxypyridine [B), 2,4-dihydroxypyridine [C), 2,5-dihydroxypyridine [D], 2,5-dihydroxypyridine [D] and conversion product of 2HP (F) using Burkholderia sp. MAK1 APS whole cells carrying hydraEQDE_BBAD-WCST_blasmid, and, mill-absorbance units.

chromatogram of the conversion product was compared with those of dihydroxypyridine standards (Fig. 8). The properties (retention time and absorbance spectrum) of the conversion product were found to exactly match those of 25DHP. These results confirmed that when *Burkholderia* sp. MAK1 ΔP5 cells were carrying a plasmid with *hpdABCDE* monooxygenase genes, they produced an active enzyme and efficiently hydroxylated 2HP to 25DHP. Although the enzyme activity of *Burkholderia* sp. MAK1 ΔP5 carrying HpdABCDE_pBAD-MCS-1 does not surpass that of the wild-type bacterium (0.75 ± 0.12 mol - min · · · · mg · · 1 compared to 1.1 ± 0.15 mol · min · · · · · mg · · 1 of cell [wet weight], respectively), such a system offers a desirable advantage, the production of detectable hydroxylated intermediates. It should be noted that the formation of 25DHP has never been tracked in the wild-type *Burkholderia* sp. MAK1 bacterium. As 25DHP was readily used up by heterologously expressed Hpdf (Fig. 7), we speculated that under 2HP-induced growth conditions, *Burkholderia* sp. MAK1 cells expressed genome-encoded Hpdf, which

June 2018 Volume 84 Issue 11 e00387-18

reduced 25DHP to an imperceptible concentration. The HpdF-catalyzed dioxygenolysis would also explain why, during our previous work, a big portion of possible conversion products remained undetected. Notably, no such obstacle was encountered when Hpd-ABCDE was expressed in *Burkholderia* sp. MAK1 ΔP5. Here, bacteria were grown without 2HP and, as a result, the expression of the genome-encoded HpdF was disabled. This not only led to the detection of 25DHP but also allowed us to perform HpdABCDE-catalyzed conversions (such as hydroxylation of 3-fluoropyridin-2-amine, 6-fluoropyridin-2-ol, 3-chloropyridin-2-ol, 3-bnoropyridin-2-ol, 3-methylpyridin-2-ol, and 2-hydroxy-6-methylpyridin-3-carbonitrile [Fig. S3]), all of which had been unsuccessfully attempted previously using 2HP-induced wild-type *Burkholderia* sp. MAK1. Therefore, the *Burkholderia* sp. MAK1 ΔP5/HpdABCDE_pBAD-MCS-1 system not only provided evidence of 2HP catabolism but also proved to be a superior biocatalyst, as opposed to the wild-type *Wurkholderia* Sp. MAK1.

Diversity of pyridine derivative-attacking oxygenases. Aromatic and aliphatic compounds (hydrocarbons) are devoid of functional groups and therefore exhibit a low chemical reactivity (31). Aerobic utilization of various hydrocarbons as organic growth substrates by microorganisms generally involves oxidizing enzymes (32). Pyridine derivatives, despite their heterocyclic nature, appear to follow this rule as well. Although the proposed pathways for the catabolism of pyridines predict the participation of oxygenases, only a limited number of the putative biocatalysts responsible for these conversions have been identified to date. These include the following nicotine and nicotinic acid degradation enzymes: 6-hydroxynicotinate 3-monooxygenase NicC from Pseudomonas nutida KT2440 (12), 6-hydroxy-3-succinovlpyridine 3-monooxygenase HspB from Pseudomonas putida S16 (13), and another 6-hydroxy-3-succinovlpyridine 3-monooxygenase VppD from Ochrobactrum sp. SJY1 (14). The catabolism of 2HP or closely related compounds in different bacteria is started by the following structurally different enzymes: the four-component 2HP dioxygenase HpoBCDF from Rhodococcus sp. PY11 (22), the 26DHP 3-hydroxylase from Arthrobacter nicotinovorans (20), the two-component 2HP monooxygenase HpyB from Arthrobacter sp. PY22 (21), or the 2-hydroxypyridine 5-monooxygenase encoded by hpdABCDE from Burkholderia sp. MAK1, characterized in this work. Although only a small fraction of possible biocatalysts has been identified, it is clear that bacteria code for a variety of different oxygenases that initialize the degradation of pyridine derivatives. The structural diversity of oxygenases with the same specificity is not new to the microbial world. A good example is the aerobic degradation of toluene that can be initiated by at least five different pathways. Monooxygenase-driven hydroxylation may occur at all three positions on the benzene ring (ortho, meta, and para) as well as at the methyl group, while dioxygenases catalyze incorporation of both oxygen atoms releasing toluene-cis-1,2-dihydrodiol (33). All of these conversions are catalyzed by structurally and functionally different enzymes. The reason behind this phenomenon may be the abundance of the toluene sources. Toluene is found naturally in petroleum and coal. It is a major component of gasoline and is also produced by the burning of organic materials (31). Toluene is also produced industrially for use as a solvent and in the production of various chemicals (32). In addition, toluene is produced and emitted by plants (33). All of this makes toluene obtainable in different ecological niches that are occupied by diverse bacteria. which employ different enzymes to initiate the assimilation of toluene. The pyridine derivatives are also abundant in nature. Both natural and anthropogenic sources contribute to the presence of pyridines in the environment.

In the presence of a new growth substrate, bacteria may not necessarily adapt their own enzymatic repertoire via the duplications of corresponding genes and their subsequent mutations. In addition, bacteria constantly borrow genetic material by horizontal gene transfer (31). The hpd gene cluster is likely to have been recently horizontally transferred into Burkholderia MAKI for the following reasons. First, all of the closest homologues of hpd cluster genes are not from the Burkholderia genus. Second, the first enzyme of the pathway, HpdABCDE monooxygenase, is very unusual among SDIMOs.

June 2018 Volume 84 Issue 11 e00387-18

TABLE 2 Bacterial strains used in this study

Strain	Genotype or characteristics of the strain ^a	Source or reference
Burkholderia sp. MAK1 (DSM 102049)	2HP-degrading bacterium	39
Burkholderia sp. MAK1∆ P5	Mutant of Burkholderia sp. MAK1, which is unable to consume 2HP	This study
E. coli DH5α	F ⁻ endA1 glnV44 thi-1 recA1 relA1 gyrA96 deoR nupG purB20 ϕ 80dlacZ Δ M15 Δ (lacZYA-argF)U169, hsdR17(r_v - m_v +), λ -	Thermo Fisher Scientific Lithuania
E. coli BL21(DE3)	F ompT gal dcm lon $hsdS_B(r_B^- m_B^-) \lambda(DE3 [laci lacUV5-T7p07 ind1]$ $sam7 nin5]) [malB^+]_{K=12}(\lambda^5)$	Novagen, Germany
E. coli Rosetta(DE3)pLysS	F ⁻ ompT gal dcm lon $hsdS_8(r_8^- m_8^-) \lambda(DE3 [lacl lacUV5-T7p07 ind1 sam7 nin5]) [mal8+]K-12(\lambda^2) pLysSRARE[T7p20 ileX argU thrU tyrU glyT thrT argW metT leuW proL orip15a] (Cm')$	Novagen, Germany

^oCm^r, chloramphenicol resistance.

It exhibits only a very low sequence identity (~30%) with other known proteins and features a unique genetic architecture. Last, there is no experimental evidence of the direct involvement of SDIMOs in the biodegradation of pyridine derivatives. Most likely, the monooxygenase genes have been acquired by horizontal transfer and have been recruited by the appropriate lower pathway (maleamate pathway) for cleavage of hydroxylated products. We hypothesize that Burkholderia sp. MAK1 may have acquired either the entire hpd cluster or only the hpdABCDE genes from other bacteria, and the novel enzymes may have been recruited to serve in a preexisting maleamate pathway. Over time, these new catabolic genes may have been modified, allowing utilization of an alternative carbon source, such as 2HP. The results of HpdABCDE overexpression in Burkholderia sp. MAK1 ΔP5 may also be attributed to the "external origin" of the hpd cluster. It is possible that in the presence of 2HP, the wild-type bacteria produced a sufficient, albeit small, amount of enzymes needed to assimilate 2HP. When the expression of HpdABCDE was induced from a plasmid, the protein synthesis machinery of *Burkholderia* sp. MAK1 ΔP5 cells was not able to overcome the overproduction of "foreign" proteins, which became misfolded and ended up insoluble.

Overall, the discovery of HpdABCDE monooxygenase is a major contribution to our understanding of the initial steps of degradation of pyridine derivatives in bacteria and the diversity of enzymes that govern this process. This study has identified the genetic locus corresponding to a long-elusive 2HP 5-monooxygenase and thus has added an important piece to the puzzle of the biodegradation of pyridine derivatives in nature.

Conclusions. A gene cluster, hpd, from Burkholderia sp. MAK1 containing all the necessary genes for the degradation of 2HP has been identified. We show that the 2HP biodegradation pathway starts with the hydroxylation of 2HP to 25DHP catalyzed by the 2-hydroxypyridine 5-monooxygenase encoded by hpdABCDE, a gene encoding an enzyme (HpdABCDE) that shows similarity to soluble diiron monooxygenases, which participate in the biodegradation of various aromatic and aliphatic pollutants but have never been implicated in the biodegradation of pyridines. The next step in the catabolic pathway is the ring opening of 25DHP. This reaction is catalyzed by 25DHP 5,6dioxygenase HpdF, which is very similar to enzymes found in the catabolic pathways of nicotine and nicotinate. Notably, no 25DHP 5,6-dioxygenase has been implicated in the 2HP degradation pathway to date. After the ring opening, the degradation process possibly proceeds via the so-called maleamate pathway, since all genes associated with this pathway have homologues in the hpd cluster. Our study not only provides evidence of the new degradation pathway of 2HP but also deepens our understanding of the microbial biodegradation of pyridine and its derivatives in nature. A broad-range substrate specificity allows the recommendation of HpdABCDE to be used as a regioselective biocatalyst for the synthesis of the hydroxylated pyridine derivatives.

MATERIALS AND METHODS

Bacterial strains, chemicals, and standard techniques. The bacterial strains used in this study are sited in Table 2. Burkholderia cells were cultivated at 30°C in liquid EFA medium [10.0 g/liter K,HPO, φ.0. g/liter KH,PO, φ.0 S g/liter yeast extract, 1.0 g/liter (NH_φ)₂O_D, φ.2 g/liter MgSO₄?H₃O (pH 7.0)] supple-

June 2018 Volume 84 Issue 11 e00387-18

TABLE 3 Primers used in this study

Primer name	Primer sequence (5'→3') ^a	Use
Vsp_F_BAD	AACATTAATGTCTGATTCGTTACC	Designing pBAD-MCS-1
Sac_R_BAD	ATGAGCTCGAGTTTGTAGAAACG	Designing pBAD-MCS-1
P5_Hind_R	TTAAGCTTTCAAGCGTCAGCCCGCAAGGGTTCTC	Cloning
P1_Pcil_F	TAACATGTCAGCACGGTCAAGCTGGTCC	Cloning
HpdF_F_Nco	ATCCATGGGCTCCTTAAGCGATGCAG	Cloning
HpdF_R_Hind	ACTAAGCTTTCATGCCATCACCTCATCG	Cloning
TnModSekv_F	GCAACACCTTCTTCACGAGG	Sequencing
TnModSekv_R	GTTCCTGGCCTTTTGCTGGC	Sequencing
P4M_R	GCCGACCACTGGCAAGGCGG	Sequencing
CB1F2	GCGAACACATTGCCATT	Sequencing
CB2F2	TCATTCCTTCGCCATCGTTCAG	Sequencing
Cont84R2	CTTCCAGCCTGACGATCACA	Sequencing
diox1_R	TTGCTCAACGATTATATGGACG	Sequencing
Hinc_R	ATCGACGTGGCGACGCAGG	Sequencing
Groel_F	ATACATATGAGCGTTAAGCGGATGG	Sequencing
MAK_Tat_F	GTATCACGGGGGCAAGTTCATCTGC	Sequencing
MAK_Rsa_F	ACATCGCACTGATGCTCCTCGG	Sequencing
P3Mut_F	TCTATCGCGAGTATGTGCGC	RT-PCR
P3Mut_R	AACGGGTCGCCGGAGAACAG	RT-PCR
P4Mut_F	GCCGACCACTGGCAAGGCGG	RT-PCR
P4Mut_R	ACGCGGAGAAGCACAGATAG	RT-PCR
P5Mut_F	GGGGGGGAGGCTTACCGGG	RT-PCR
P5Mut_R	AGCCCGCGGAGAAGAAACCG	RT-PCR
Frrs	GATTAGATACCCTGGTAGTCC	RT-PCR, 16S RNA
Rrrs	GTTGCGGGACTTAACCCAAC	RT-PCR, 16S RNA

^aRestriction sites are underlined.

mented with salt solution (2.0 g/liter Cacl₂2H₂O, 1.0 g/liter MnSO₄4H₂O, 0.5 g/liter FeSO₄7H₂O, all components were discolved in 0.1 M HCl) and with an appropriate carbon source (1.0 g/liter succinate or 1.0 g/liter 2HP). Burkholderia cells transformed with plasmids were cultivated on agar plates containing EFA medium. The medium that was used to cultivate transformed Burkholderia cells was also supplemented with the appropriate antibiotics (50 µg/ml kanamycin and 20 µg/ml chloramphenicoli. E. coli cells carrying recombinant plasmids were cultivated in LB (10 g/liter tryptone, 5 g/liter yeast extract, 10 g/liter NGO 10 37 g/liter brinh heart infusion (BHI) medium supplemented with the appropriate antibiotics (50 µg/ml kanamycin, 20 µg/ml chloramphenicol, or 100 µg/ml ampicillin). Electroporation was used to introduce plasmid DNA.

Qualitative and quantitative RT-PCR. Burkholderia sp. MAK1 cells were cultivated in EFA medium containing 1.0 g/lifer succinate or 1.0 g/lifer 2HP as the sole source or carbon until the culture reached an optical density at 600 nm (OD $_{coo}$) of 0.3. Total RNA was isolated using a 2R fungal/bacterial RNA MicroPep kit (Zymo Research Corporation). Copy DNA synthesis was carried out using the Maxima H Minus first-strand CDNA synthesis kit (Thermo Fisher Scientific, Lithuania), QPCR was conducted in a 2-ja reaction mixture containing 12.5 μ l of Maxima SYRB green/ROX qPCR master mix (2×) (Fermentas, Lithuania), 200 nM each primer (see Table 3), —50 ng of cDNA, and water up to 25 μ l. qPCR amplification was performed using a 7500 Fast real-time PCR system (Applied Biosystems, USA). The first step in qPCR was initial denaturation at 95°C for 10 min, followed by 35 cycles of 95°C for 15 s, 62°C for 30 s, and 72°C for 30 s. For quantitative enalysis, fluorescence data were recorded after the annealing step. All experiments were carried out three times. To verify the absence of DNA in the RNA samples, the procedure was performed without the reverse transcriptase step. The threshold cycle (G) (threshold value, 0.05) values were obtained using 7500 Software version 2.06. Relative target RNA analysis was performed using the $\Delta \Delta C_r$ algorithm and 165 RNA as a reference for normalization.

Plasmids and primers. The plasmids and primers used in this study are listed in Tables 3 and 4. Primers were ordered from Metabion, Germany. All the targeted genes were amplified by PCR using either Tag or Phusion (Thermo Fisher Scientific, Lithuania) DNA polymerase, according to the manufacturer's recommendations. The blunt-ended amplicons were cloned into the pJETI_ZPlunt vector, while sticky-ended amplicons were cloned into pTZ57R/T. Before recloning into expression vectors, the gene sequences were confirmed by DNA sequencing (Macropan The Netherlands).

vectors, the gene sequences were confirmed by DNA sequencing (Macrogen, The Netherlands). Induction of recombinant protein synthesis. E. coli Rosesta(DE3)pLysS cells transformed with plasmid HpdF_pET were grown in BHI or LB medium containing kanamycin (final concentration, 4 μ g/ml) at 30°C until the OD $_{000}$ reached 0.5 to 0.6. Then, the medium was supplemented with isopropyl-thio- β -2-galactopyranoside (β PTG; final concentration, 1 mM) and FeSO $_{\alpha}$ 7H, O (final FeT ** concentration, 1 mM) an

Burkholderia sp. MAK1 ΔP5 cells carrying the HpdABCDE_pBAD-MCS-1 plasmid were grown for about 40 h at 30°C in EFA medium containing 0.1% succinate, 0.2% arabinose, and 20 μg/ml chloramphenicol. Also, FeSO_x7H₂O was added twice, at the beginning of bacterial growth and after 20 h of cultivation, to a final concentration of 100 μM.

June 2018 Volume 84 Issue 11 e00387-18

TABLE 4 Plasmids used in this study

Plasmid	Plasmid characteristics ^a	Source or reference
pJET1.2/blunt	Apr ori CoIE1 eco47IR, high copy-no. cloning vector	Thermo Fisher Scientific, Lithuani
pTZ57R/T	Apr ori ColE1 lacZα, high copy-no. cloning vector	Thermo Fisher Scientific, Lithuani
pET-28b	pBR322-derived ColE1, T7 lac promoter, Kmr, protein expression vector	Novagen, Germany
pRSFDuet-1	RSF1030-replicon, T7 lac promoter, two MCSs, Kmr, protein expression vector	Novagen, Germany
pCDFDuet-1	CloDF13 replicon, T7 lac promoter, two MCSs, Smr, protein expression vector	Novagen, Germany
pBAD24	ColE1 ori, Apr, araC promoter, protein expression vector	Invitrogen
pBBR1MCS-1	pBBR1-derived, Cm ^r , lacZα, broad-host-range vector	28
pBAD-MCS-1	Amplicon containing regulatory elements of pBAD24 was amplified by PCR using primers Vsp_F_BAD and Sac_R_BAD, digested with Vspl and Sacl, and cloned into pBBR1MCS vector	This study
HpdF_pET	hpdF gene was amplified by PCR using HpdF_F_Nco and HpdF_R_Hind primers, digested with Ncol and Hindlll, and cloned into pET-28b vector	This study
HpdABCDE_pET	Monooxygenase gene cluster was amplified by PCR using P1_Pcil_F and P5_Hind_R primers, digested with Pcil and Hindlll, and cloned into pET-28b vector	This study
HpdABCDE_pBAD-MCS-1	pET_ HpdABCDE plasmid was digested with Xbal and HindIII, monooxygenase gene containing fragment was isolated, and cloned into pBAD-MCS-1 vector	This study
pART3-qfp	Escherichia coli-Arthrobacter shuttle vector	40
gfp_pBAD-MCS-1	pART3-gfp plasmid was digested with Xbal and HindIII, gfp gene containing fragment was isolated and cloned into pBAD-MCS-1 vector	This study
gfp_pBBR1MCS-1	pART3-gfp plasmid was digested with KpnI and HindIII, gfp gene containing fragment was isolated and cloned into pBBR1MCS-1 vector	This study
pSal_4	2HP degradation genes containing plasmid obtained during transposon mutagenesis	This study
pDra_1	2HP degradation genes containing plasmid obtained during transposon mutagenesis	This study

[&]quot;Apr, apramycin resistance; Kmr, kanamycin resistance; MCS, membrane contact sites; Smr, streptomycin resistance.

Biotransformation of pyridine derivatives. After protein synthesis induction, the cells were harvested by centrifugation and then washed twice with 50 mM potassium phosphate buffer (pH 7.0). In total, 0.005 g of wet biomass was resuspended in 1 ml of potassium phosphate buffer, and the resulting suspension was supplemented with the appropriate substrate at 0.25 to 1.0 mM and incubated at 30°C. The conversion process was monitored periodically by recording the UV-Vis spectrum of the substrate, as well as by performing HPLC-MS analysis.

HPLC-MS analysis. The parameters and conditions used in HPLC-MS analysis of biotransformation mixtures were described in our previous work (23).

mixtures were described in our previous work (25).

Whole-genome sequencing. The sequencing and subsequent assembly of the Burkholderia sp. MAK1 genome was performed by BaseClear (Leiden, The Netherlands). The quality-filtered Illiumina FAFT0 sequences 3,398,321 reads were assembled into a number of contig sequences. The analysis was performed using ABy55 version 1,51. The contigs were linked and placed into scaffolds based on the alignment of the 200,298 Pacific reads. Alignment was performed with BLASR. The de novo assembly statistics are the following: total number of scaffolds, 355 (maximum scaffold size, 2.9 Mb; minimum, 306 bp; average, 352 kb; number of spaps, 530; and total coverage, 1,25 Mb.

Gene sequence analysis and protein tertiary structure modeling. The deduced amino acid sequences of the proteins encoded by the had locus were searched against the NCBI database using BLAST (34). Protein functions were assigned based on a sequence similarity search against the NCBI Conserved Domain Database (35). Phylogenetic analyses and the multiple-sequence alignment were conducted using MEGA version 7 (36). The model of the Hpdc subunit was generated using the 1-TASSER server (37), while visualizations were made using the PyMOL 1.7.1.3 software (38).

**Accession number(s). The sequence of the JPP degradation cluster hpd of Burkholderia sp. MAKI

Accession number(s). The sequence of the 2HP degradation cluster hpd of Burkholderia sp. MAK1 was deposited in GenBank under the accession number MF957200.

SUPPLEMENTAL MATERIAL

Supplemental material for this article may be found at https://doi.org/10.1128/AEM .00387-18.

SUPPLEMENTAL FILE 1, PDF file, 0.7 MB.

ACKNOWLEDGMENTS

This research was funded by the European Social Fund according to the activity "Improvement of researchers' qualification by implementing world-class R&D projects" of measure no. 09.3.3-LMT-K-712 [grant no. DOTSUT-34(09.3.3-LMT-K712-01-0058/LSF-600000-58)].

We thank L. Kalinienė for assistance with the preparation of the manuscript.

June 2018 Volume 84 Issue 11 e00387-18

- 1. Kaiser JP, Feng Y, Bollag JM. 1996. Microbial metabolism of pyridine, quinoline, acridine, and their derivatives under aerobic and anaerobic
- conditions. Microbiol Rev 60:483–498.

 2. Fetzner S. 1998. Bacterial degradation of pyridine, indole, quinoline, and their derivatives under different redox conditions, Appl Microbiol Bio-
- technol 49:237–250. https://doi.org/10.1007/s002530051164.

 3. Padoley KV, Mudliar SN, Pandey RA. 2008. Heterocyclic nitrogenous pollutants in the environment and their treatment options–an overview. Biore-
- Sims GK, O'Loughlin EJ, Crawford RL. 1989. Degradation of pyridines in the environment. Crit Rev Environ Contr 19:309–340. https://doi.org/10 1080/10643388909388372
- .TIOUV/100433889V930037 &.
 S. Kuhn EP, Suflita JM. 1989. Microbial degradation of nitrogen, oxygen and sulfur heterocyclic compounds under anaerobic conditions: studies with aquifer samples. Environ Toxicol Chem 8:1149–1158. https://doi.org/10 1002/etc.5620081207
- Richards DJ, Shieh WK. 1986. Biological fate of organic priority pollutants in the aquatic environment. Water Res 20:1077–1090. https://doi.org/10 1016/0043-1354(86)90054-0
- 7. Khasaeva F, Vasilyuk N, Terentyev P, Troshina M, Lebedev A. 2011. A novel soil bacterial strain degrading pyridines. Environ Chem Lett 9:439–445. https://doi.org/10.1007/s10311-010-0299-6. 8. Sun JQ, Xu, L, Tang YQ, Chen FM, Liu WQ, Wu XL. 2011. Degradation of pyridine by one *Rhodococcus* strain in the presence of chromium
- (VI) or phenol. J Hazard Mater 191:62-68. https://doi.org/10.1016/j at.2011.04.034
- 9. Sun JQ, Xu L, Tang YQ, Chen FM, Zhao JJ, Wu XL. 2014. Bacterial pyridine hydroxylation is ubiquitous in environment, Appl Microbiol Biotechnol 98:455-464. https://doi.org/10.1007/s00253-013-4818-9.

 10. Shukla OP, Kaul SM. 1986. Microbiological transformation of pyridi
- N-oxide and pyridine by Nocardia sp. Can J Microbiol 32:330-341.
- N-oxide and pyridine by Nocardia sp. Can J Microbiol 32:330–341. https://doi.org/10.1139/M86-05. 11. Damani LA, Crooks PA, Shaker MS, Caldwell J, D'Souza J, Smith RL. 1982. Species differences in the metabolic C- and N-oxidation, and N-methylation of ["Clpyridine in vivo. Xenobiotica 12:527–534. https://doi.org/10.3109/0049852509038931. 12. Jiménez JI, Canales A, Jiménez-Barbero J, Ginalski K, Rychlewski L, García
- J., Díaz E. 2008. Deciphering the genetic determinants for aerobic nicotinic acid degradation: the *nic* cluster from *Pseudomonas putida* KT2440. Proc Natl Acad Sci U S A 105:11329–11334. https://doi.org/10 1073/pnas.0802273105.
- .1073/pnas.0802273105.
 13. Tang H, Yao Y, Wang L, Yu H, Ren Y, Wu G, Xu P. 2012. Genomic analysis of *Pseudomonas putida*: genes in a genome island are crucial for nicotine degradation. Sci Rep 2:377–385. https://doi.org/10.1038/srep00377.
 14. Yu H, Tang H, Zhu X, Li Y, Xu P. 2015. Molecular mechanism of nicotine degradation by a newly isolated strain, *Octrobactum sp.* strain SJY1 Appl Environ Microbiol 81:272–281. https://doi.org/10 1128/AFM 02265-14
- .1128/AEM.UZ.60-14.

 15. Cain RB, Houghton C, Wright KA. 1974. Microbial metabolism of the pyridine ring. Metabolism of 2- and 3-hydroxypyridines by the maleamate pathway in *Achromobacter* sp. Biochem J 140:293–300.
- Yao Y, Tang H, Ren H, Yu H, Wang L, Zhang W, Behrman JE, Xu P. 2013. Iron(II)-dependent dioxygenase and N-formylamide deformylase catalyze the reactions from 5-hydroxy-2-pyridone to maleamate, Sci Rep 3:3235. https://doi.org/10.1038/srep03235.

 17. Semėnaitė R, Gasparavičiūtė R, Duran R, Precigou S, Marcinkevičienė L,
- Bachmatova I, Meškys R. 2003. Genetic diversity of 2-hydroxypyridine-
- degrading soil bacteria. Biologija 2:27–29.

 18. Kolenbrander PE, Weinberger M. 1977. 2-Hydroxypyridine metabolism and pigment formation in three *Arthrobacter* species. J Bacteriol 132: 51-59
- Gupta RC, Shukla OP. 1975. Microbial metabolism of 2-hydroxypyridine. Indian J Biochem Biophys 12:296-298.
- Indian J Biochem Biophys 12:296–298.
 20. Baitsch D, Sandu C, Brandsch R, Igloi GL. 2001. Gene cluster on pAO1 of Arthrobacter nicotinovorans involved in degradation of the plant alkaloid nicotine: cloning, purification, and characterization of 2,6-dilydroxypytidine 3-hydroxylase. J Bacteriol 183:5262–5267. https://doi.
- .org/10.1128/JB.183.18.5262-5267.2001. 21. Stanislauskiene R, Gasparaviciute R, Vaitekunas J, Meskiene R, Rut-

- kiene R, Casaite V, Meskys R. 2012. Construction of Escherichia coli-Arthrobacter-Rhodococcus shuttle vectors based on a cryptic plasmid from Arthrobacter rhombi and investigation of their application for functional screening. FEMS Microbiol Lett 327:78 – 86. https://doi.org. 10.1111/j.1574-6968.2011.02462.x.
- 10.1111/J.1574-998.ZU11.02402.X.
 Valtekünas J, Gasparaviciute R, Rutkiene R, Tauraite D, Meskys R. 2015. A 2-hydroxypyridine catabolism pathway in Rhodococcus rhodochrous strain PY11. Appl Environ Microbiol 82:1264–1273. https://doi.org/10 1128/AFM 02975-15
- . 1128/aEM.U29/5-15. Stankevičiütė J, Vaitekūnas J, Petkevičius V, Gasparavičiūtė R, Tauraitė D, Meškys R. 2016. Oxyfunctionalization of pyridine derivatives using whole cells of *Burkholderia* sp. MAK1. Sci Rep 6:39129. https://doi.org/10.1038/
- 24. Han XH, Wang W, Xiao XG. 2008. Microbial biosynthesis and biotransformation of indigo and indigo-like pigments. Sheng Wu Gong Cheng Tue Bao 24:921–926. (In Chinese.) https://doi.org/10.1016/S1872 -2075(08)60043-6.
- Dennis JJ, Zylstra GJ. 1998. Plasposons: modular self-cloning minitrans Dennis JS, Jyana G. 1936. This posters in the Colonial serious metalling posterior poson derivatives for rapid genetic analysis of Gram-negative bacterial genomes. Appl Environ Microbiol 64:2710–2715.
 Leahy JG, Batchelor PJ, Morcomb SM. 2003. Evolution of the soluble
- diron monoxygenases. FEMS Microbiol Rev 27:449–479. https://doi.org/10.1016/S0168-6445(03)00023-8.

 Notomista E, Lahm A, Di Donato A, Tramontano A. 2003. Evolution of
- bacterial and archaeal multicomponent monooxygenases. J Mol Evol S6:435–445. https://doi.org/10.1007/s00239-002-2414-1. Kovach ME, Elzer PH, Hill DS, Robertson GT, Farris MA, Roop RM, Jr,
- Peterson KM, 1995. Four new derivatives of the broad-host-range clonreterson NM. 1993. Four new derivatives of the Broad-nost-range clon-ing vector pBBR1MCS, carrying different antibiotic-resistance cassettes. Gene 166:175–176. https://doi.org/10.1016/0378-1119(95)00584-1. 29. Lefebre MD, Valvano MA. 2002. Construction and evaluation of plasmid
- Leteore MJ, Valvano MA. 2002. Construction and evaluation or plasmid vectors optimized for constitutive and regulated gene expression in Burkholderia cepacia complex isolates. Appl Environ Microbiol 68: 5956–5964. https://doi.org/10.1128/AEM.68.12.5956-5964.2002.
- Guzman LM, Belin D, Carson MJ, Beckwith J. 1995. Tight regulation, modulation, and high-level expression by vectors containing the arabinose PBAD promoter. J Bacteriol 177:4121–4130. https://doi. org/10.1128/jb.177.14.4121-4130.1995.
- Widdel F, Musat F. 2010. Diversity and common principles in enzymatic activation of hydrocarbons, p 984–1004. *In* Timmis KN (ed), Handbook of
- hydrocarbon and lipid microbiology. Springer, Berlin, Heidelberg, Germany.

 32. Fuchs G, Boll M, Heider J. 2011. Microbial degradation of aromatic compounds-from one strategy to four. Nat Rev Microbiol 9:803–816. https://doi.org/10.1038/nrmicro2652.
- https://doi.org/10.1056/hrmicro2052. Parales RE, Parales JV, Pelletier DA, Ditty JL. 2008. Chapter 1 diversity of microbial toluene degradation pathways. Adv Appl Microbiol 64:2–43. https://doi.org/10.1016/S0065-2164(08)00401-2. 34. Pearson WR. Lipman DJ. 1988. Improved tools for biological sequence
- Yearson WK, Lipman DJ. 1988. Improved tools for biological sequence comparison. Proc Natl Acad Sci U S A 85:2444–2448.
 Marchler-Bauer A, Lu S, Anderson JB, Chitsaz F, Derbyshire MK, DeWeese-Scott C, Fong JH, Geer LY, Geer RC, Gonzales NR, Gwadz M, DeWeese-Scott C, Fong JH, Geer LY, Geer RC, Gonzales NR, Gwadz M, Hurvitz DJ, Jackson JD, Re Z, Lanczycki CJ, Lu F, Marchler GH, Mullokandov M, Omelchenko MV, Robertson CL, Song JS, Thanki N, Yamashita RA, Zhang D, Zhang N, Zheng C, Bysurs HS. 2011. CDO: a Conserved Dollan Database for the functional annotation of proteins. Nucleic Acids Res 39:D225–D229. https://doi.org/10.1093/nar/gkq1189.

 Kumar S, Stecher G, Tamura K, 2016. MESQA?: Molecular Evolutionary
- Kumar S, Stecher G, Tamura R. 2016. MEGAT: Molecular Evolutionary Genetics Analysis version 7.0 for bigger datasets. Mol Biol Evol 33: 1870–1874. https://doi.org/10.1093/molbev/msw054.
 Zhang Y, 2008. ITASSER sever for protein 30 structure prediction. BMC Bioinformatics 940. https://doi.org/10.1186/1471-2105-9-40.
 DeLano WL. 2002. The PyMOL molecular graphics system on World Wide Web. http://www.pymol.org

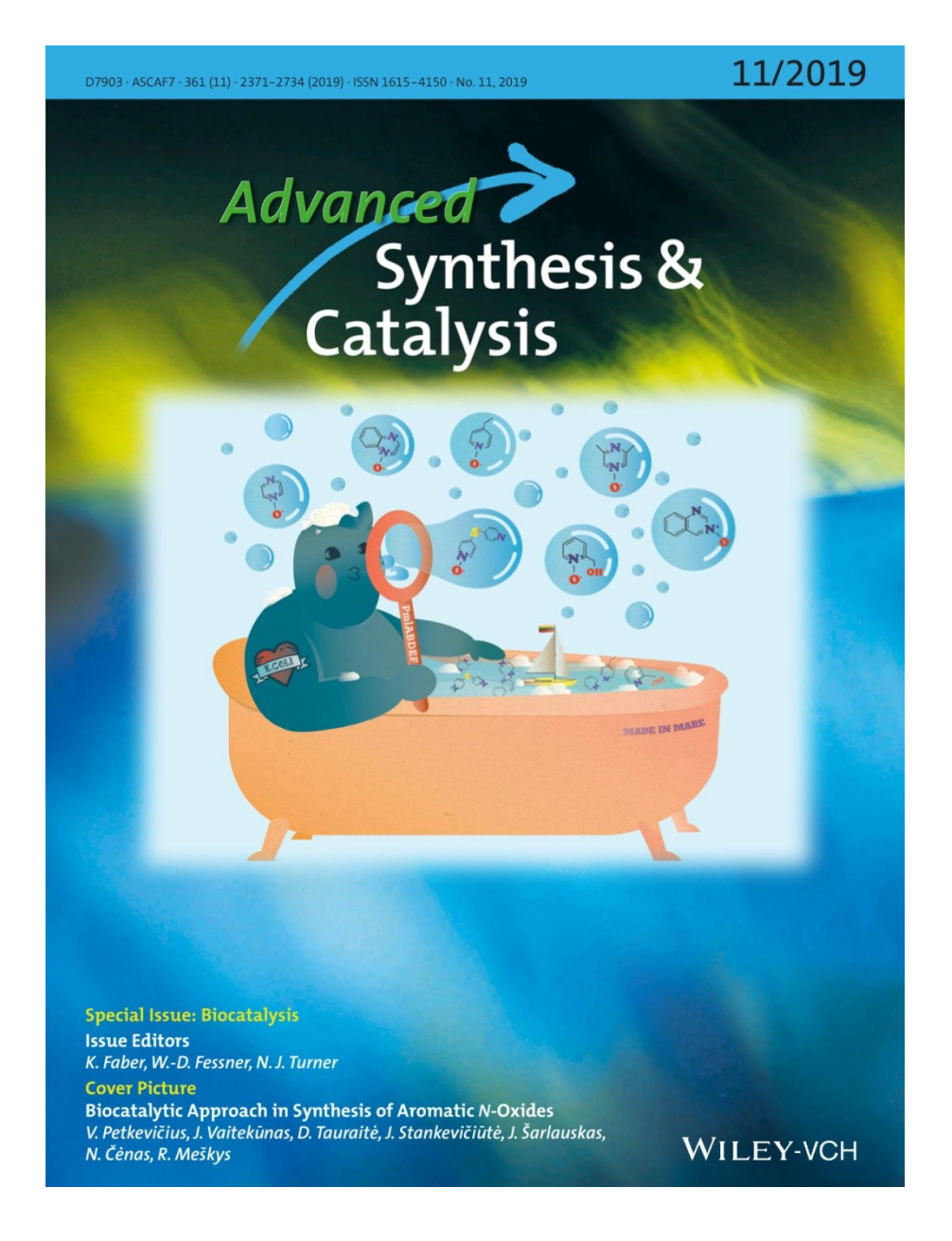
- Gasparavičiūtė R, Kropa A, Meškys R. 2006. A new Arthrobacter strain utilizing 4-hydroxypyridine. Biologija 4:41–45.
 Kutanovas S, Stankeviciute J, Urbelis G, Tauraite D, Rutkiene R, Meskys R. 2013. Identification and characterization of a tetramethylpyrazine catabolic pathway in *Rhodococcus jostii* TMP1. Appl Environ Microbiol 79 3649–3657. https://doi.org/10.1128/AEM.00011-13.

Publication III

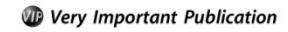
Petkevičius V, Vaitekūnas J, Tauraitė D, Stankevičiūtė J, Šarlauskas J, Čėnas N, Meškys R. A biocatalytic synthesis of heteroaromatic *N*-oxides by whole cells of *Escherichia coli* expressing the multicomponent, soluble di-iron monooxygenase (SDIMO) PmlABCDEF. *Adv. Synth. Catal.* 2019, 361, 2456-2465.

.

This material is licenced for reuse by John Wiley & Sons, Inc. All rights reserved.







A Biocatalytic Synthesis of Heteroaromatic N-Oxides by Whole Cells of Escherichia coli Expressing the Multicomponent, Soluble Di-Iron Monooxygenase (SDIMO) PmlABCDEF

Vytautas Petkevičius, a.* Justas Vaitekūnas, Daiva Tauraitė, a Jonita Stankevičiūtė, a Jonas Šarlauskas, b Narimantas Čėnas, b and Rolandas Meškysa

Department of Molecular Microbiology and Biotechnology, Institute of Biochemistry, Life Sciences Center, Vilnius University, Saulėtekio 7, Vilnius LT-10257, Lithuania Tel: +37052234386

Fax + 37052687009

E-mail: vytautas.petkevicius@bchi.vu.lt

Department of Xenobiotics Biochemistry Institute of Biochemistry, Life Sciences Center, Vilnius University, Saulétekio 7, Vilnius LT-10257, Lithuania

Manuscript received: November 5, 2018; Revised manuscript received: December 5, 2018; Version of record online:

Supporting information for this article is available on the WWW under https://doi.org/10.1002/adsc.201801491

Abstract: Aromatic N-oxides (ArN-OX) are desirable biologically active compounds with a potential for application in pharmacy and agriculture industries. As biocatalysis is making a great impact in organic synthesis, there is still a lack of efficient and convenient enzyme-based techniques for the production of aromatic N-oxides. In this study, a recombinant soluble di-iron monooxygenase (SDIMO) PmlABCDEF overexpressed in Escherichia coli was showed to produce various aromatic N-oxides. Out of 98 tested Nheterocycles, seventy were converted to the corresponding N-oxides without any side oxidation products. This whole-cell biocatalyst showed a high activity towards pyridines, pyrazines, and pyrimidines. It was also capable of oxidizing bulky N-heterocycles with two or even three aromatic rings. Being entirely biocatalytic, our approach provides an environmentally friendly and mild method for the production of aromatic N-oxides avoiding the use of strong oxidants, organometallic catalysts, undesirable solvents, or other environment unfriendly reagents.

Keywords: Biocatalysis; chemoselectivity; nitrogen heterocycles; oxidation; regioselectivity; soluble di-iron monoxygenase

Introduction

Various N-heteroaromatic compounds are widely used as starting materials in diverse chemical syntheses.[1] However, unsubstituted N-heterocycles are rather inert molecules that are challenging to modify chemically. One of the approaches for their functionalization is N-oxidation, which increases their reactivity with either electrophilic and nucleophilic agents.[2] In fact, the chemistry and applications of aromatic N-oxides have been receiving increased attention over the last two decades due to their usefulness as potential anticancer, antibacterial, antihypertensive, antiparasitic, anti-HIV, anti-inflammatory, herbicidal, neuro-

protective, and procognitive agents.[3,4] ArN-OX are useful as protecting groups, auxiliary agents, oxidants, ligands in metal complexes and catalysts.[5] Also, ArN-OX have been shown to be useful in energetic materials applications such as propellants, explosives, and pyrotechnics. [6] The most common approach for the synthesis of these compounds employ oxidation by peroxy acids^[7] or hydrogen peroxide.^[8] Although these reagents are rather inexpensive, they are dangerous to handle and produce significant amount of waste. Hydrogen peroxide-mediated oxidation has been improved by using transition metal catalysts, which form highly reactive oxo or peroxymetal species. Most commonly used metals include rehnium, [9] ruthe-

Adv. Synth. Catal. 2019, 361, 1-11 These are not the final page numbers! 77

Wiley Online Library

© 2019 Wiley-VCH Verlag GmbH & Co. KGaA, Weinheim



nium, [10] manganese, [11] and tungsten, [12] The main drawback of these methods is a possible product contamination with potentially hazardous metals. The alternatives include condensation reactions, various ring transformations, rearrangements and cycloadditions, [13,14] These reactions, however, are relatively unspecific and often complicated. Most recently, Mo/P-catalyzed oxidation [15] and 2,2,2-trifluoroacetophenone/H₂O₂ based oxidation [16] have been introduced as promising new methods. They were shown to be chemoselective and operated under mild reaction conditions. Nonetheless, a practically useful biocatalytic method to synthesize ArN–OX has yet to be developed.

There are several reports on biological N-oxidation of N-heterocycles. Among the isolated enzymes methane monooxygenase^[17] and cytochrome P450^[18] as well as Rhodococcus jostii TMP1 cells^[19] have been shown to oxidize N-heterocycles with a presumed formation of N-oxides; however, further studies have not been elaborated. Other efforts to exploit enzymes or cells for the synthesis of N-oxides involved peroxygenase from Agrocybe aegerita, ^[20] cyclohexanone monooxygenase from Lysobacter antibioticus, ^[21] and whole cells of Verticillium sp. GF39^[22] and Burkholderia sp. MAK1. ^[23] The main shortcomings of those biocatalysts include low productivity, inconvenient atypical microorganisms, and narrow range of substrates. Thus a practically useful biocatalytic method to synthesize ArN–OX has yet to be developed.

In this study, we report that monooxygenase PmlABCDEF recombinantly expressed in *E. coli* is highly functional *N*-oxidizing biocatalyst. The optimized whole cell bioconversions produced a controllable, productive and green method for the synthesis of ArN-OX (Scheme 1). We demonstrated a broad

Scheme 1. Synthesis of aromatic N-oxides using PmlABC-DEF monoxygenase producing E. coli cells as biocatalyst. This process requires atmospheric oxygen as an oxidant. X= C or N, n=1 or 2.

substrate specificity of this enzyme testing close to a hundred of different compounds, thus surpassing the scale of previous studies. Our approach proved to be chemoselective as it can be used for the molecules bearing oxidation-sensitive functional groups. Also, this method provides regioselectivity as only specific mono N-oxides are formed.

Results and Discussion

Selection of ArN-OX Producing Enzyme

SDIMOs are a group of enzymes that hydroxylate various aromatic compounds enabling bacteria to assimilate them. [24] Because of their broad substrate range and chemo-, stereo-, regioselectivity they are attractive enzymes for biocatalysis.[25] We previously reported that the cells of Burkhoderia sp. MAK1 are capable of transforming certain pyridine derivatives to the corresponding *N*-oxides.^[23] Later, the genes responsible for this activity were identified as a new type of SDIMOs. [26] However, recombinant expression of this monooxygenase in different hosts did not produce active enzyme, while wild-type Burkhoderia sp. MAK1 cells were a troublesome biocatalyst to work with. Convinced that particular SDIMOs are able to catalyze N-oxidation, we sought for ones functional in the E. coli cells. Thus, we explored the DNA sequences of our collection of various oxygenases obtained from metagenomes looking for an occurrence of SDIMOs. Hence, seven clones displaying sequence similarities to SDIMOs were selected. Initial experiments showed that one clone designated as p577 A was capable of oxidation of pyridine. After the full DNA sequence of plasmid p577 A was obtained, a 4.5 kb gene cluster of six open reading frames was identified and entitled as pmlABCDEF. PmlABCDEF shared overall ~80% amino acid sequence identity with butylphenol monooxygenase from Pseudomonas putida, an enzyme of the SDIMO group (Table S1).

Optimization of PmIABCDEF Production

To proceed with a bioconversion experiments, our initial goal was to maximize the expression of PmlABCDEF as well as biomass production of the recombinant cells. Thus, pmlABCDEF was amplified by PCR as a continuous DNA fragment and cloned into a protein expression vector, creating the pET_PmlABCDEF plasmid. E. coli BL21 (DE3) and E. coli Rosetta(DE3)pLysS cells carrying aforementioned plasmid (PML and PML_Ros respectively) were used for further studies. The recombinant cells were grown in nutritionally rich medium (LB or BHI) with glucose at 37°C. After addition of IPTG bacteria strains were transferred to 30°C overnight induction.

Adv. Synth. Catal. 2019, 361, 1-11 Wiley Online Library

© 2019 Wiley-VCH Verlag GmbH & Co. KGaA, Weinheim

These are not the final page numbers! 77



SDS-PAGE analysis revealed that PmlABCDEF was produced mainly as insoluble proteins. Consequently, cultivation temperatures were lowered maintaining 30°C for the growth stage and 20°C for protein expression. This process drastically increased production of PmlABCDEF as soluble proteins (Figure S1). Regarding the medium, there were no significant differences between BHI or LB media in terms of protein or biomass production. Also, final concentration of IPTG did not significantly enhanced PmlABCDEF expression as 0.5 mM of IPTG seemed to reach the saturation. Since no distinguished difference in an oxidation activity of PML and PML Ros strains was observed, for further studies PML was used as PML Ros was vulnerable to cell lysis during bioconversion.

Investigation on Substrate Scope of PML

The initial bioconversion experiments showed that PmlABCDEF strain was able to oxidize pyridine and pyrazine. Using HPLC-MS the end products of the reactions were identified as pyridine-1-oxide and pyrazine-1-oxide, accordingly, by comparison with the analytical standards. Further, we tried to elucidate the substrate scope of PML (Table 1). The experiments were carried out on an analytical scale in 1 mL reaction volume using whole-cell PML and 1 mM substrate at 30°C overnight. Among 98 tested N-aromatic compounds, 70 were shown to be converted by various conversion degree into products whose molecular mass increased by 16 Da (HPLC-MS data in Supporting information).

The derivatives of pyridine comprised a significant part of the examined compounds. Pyridines harboring small aliphatic groups (2a, 3a, 4a, 5a, 6a, 8a, 9a) were fully converted by PML. The exceptions were 2.6-dimethylpyridine (7a) and 2.4.6-trimethylpyridine (10a), as they possess two o-substituents with respect to nitrogen which possibly hinders the attack. From known biocatalyst only Burkholderia sp. MAK [12] appeared to possess a very similar preference for alkylated pyridines. Peroxygenase from Agrocybe aegeriu also acted on those compounds, however side-products of methyl group oxidation were present. [20] Alkylated pyridines did not fall into substrate scope of Verticillium sp. GF39 cells. [21] however, the N-oxides were proposed to be formed when Rhodococcus jostii TMP1 [19] was used for conversion of 3-methyl- and 3-ethylpyridine, 2,3-dimethyl-, 3,5-dimethyl-, and 2,3,5-trimethylpyridine.

Other favorable substrates for PML included those bearing hydroxymethyl (12a, 13a, 14a), methoxy (15a) and cyano moieties (30a, 31a). It appears that the electron-donating or -accepting properties of the substituents in the 3rd and 4rd positions of pyridine ring did not affect the reaction yield. One of the factors

which significantly lowered the reaction yield might be a pyridine/pyridone tautomerism of 2-hydroxypyridine and its derivatives (compounds 17a, 19a, 20a). The same factor, including a possible 2-aminopyridine/ pyridinimine tautomerism might be responsible for the absence of reactivity in the case of 2-mercaptopyridine, 2,3-dihydroxypyridine, 2,4-dihydroxypyridine, 4hydroxypyridine, 2-amino-3-hydroxypyridine, and an decreased activity towards 2-amino derivatives 21 a. 22a, 26a, 27a, 28a. Another important factor decreasing the reactivity might be the presence of a negative charge, because all pyridine carboxylic acid as well as pyridine-2,6-dicarboxylic acid were not oxidized by PML. In fact, pyridinecarboxylic acids were not transformed by peroxygenase from Agrocybe aegerita, Verticillium sp. GF39 and Burkholderia sp. MAK1 cells as well. [20,22,23]

The halogenated and especially polyhalogenated N-heteroaromatics are known to be difficult to oxidize. [17] The electron withdrawing effect of halogens reduces the nucleophilicity of the ring nitrogen as well as the reactivity towards m-CPBA, H₂O₂. HOF-CH₂CN and other generated electrophilic oxygen species. Enzymes from the SDIMOs group usually employ iron-peroxo complex in the active center, [58] thus not surprisingly PML does not catalyze N-oxidation of 2,6-dichloropyridine, 2,6-difluoropyridine and 3,5-dibromopyridine. Only 2-chloropyridine was converted to a corresponding N-oxide.

We also investigated diazine compounds as potential substrates. Methylpyrazines (34a, 35a, 36a) were shown to be excellent substrates with the exception of 2.3.6-trimethylpyrazine (37a) which o-substituents might hinder accessibility to nitrogen atom. PML also oxidized the molecules such as 5-methyl-6,7-dihydro-5H-cyclopenta[b]pyrazine (38a) or acetylpyrazine (39a) containing complex substituents. All four tested pyrimidines (43a, 44a, 45a, 46a) were converted in high yields to the corresponding N-oxides. Interestingly, some of acceptable diazine substrates possessed amino group, halogen atom or both, in contrast, these substituents in pyridines impeded the catalysis. Pyridazine (40a) and its derivatives (41a, 42a) were not as acceptable substrates as pyrazines and pyridines. A plausible explanation for such behavior is the difference in the electron densities around the nitrogen atoms. In fact, pyridazine possess the lowest basicity as well as nucleophilicity of all tested diazines (pyrazine > pyrimidine > pyridazine) which makes it less chemically reactive towards electrophilic interac-Compounds that were completely inactive included tetramethylpyrazine, pyrido[2,3-b]pyrazine, 2-hydroxypyrimidine and 2,3,6-tetrahydropyridazine-3.6-dione

Regarding two-ring heterocycles several of them also fell into the range of PML substrates. Unsubstituted compounds like quinoline (47a), isoquinoline

Adv. Synth. Catal. 2019, 361, 1-11 Wiley Online Library

© 2019 Wiley-VCH Verlag GmbH & Co. KGaA, Weinheim



 $\textbf{Table 1.} \ \ \text{The compounds used as substrates by PML. The conversion (\%) was estimated by the consumption of the substrate (initial concentration - 1 mM).}$

Substrate [%] Substrate [%] Substrate [%] Substrate [%] N >99	141	concentration - 1 in	1,1,1,						
1a 2a 3a 4a 4a 1a 2a 3a		Substrate	[%]	Substrate	[%]	Substrate	[%]	Substrate	[%]
5a 6a 7a 8a 8a		> N	99		>99		>99		>99
5a 6a 7a 8a Sa Sa Sa Sa Sa Sa Sa		1a		2a		3a		4a	
9		~ >	99		>99		18		>99
9a 10a 11a 12a OH >99		5a		6a		7a		8a	
OH >99		×	99		9	T	55	OH	>99
13a		9a				11a		12a	
OH 71		OH >	99	OH	>99		>99	(N)OH	53
17a 18a 19a 20a 17a 18a 20a 17a 18a 20a 17a 18a 20a 17a 24a 24a 17a 25a 26a 27a 28a 17a 28a 17a 25a 26a 27a 28a 17a 28a 28a 17a 29a 30a 31a 32a 17a 3a		13a		14a		15a		16a	
22a 23a 24a O ₂ N NH ₂ 22 NC NH ₂ 57 NH ₂ 25 CI N NH ₂ >99 24a 24a O ₂ N NH ₂ 22 NC NH ₂ 57 NH ₂ 25 CI N NH ₂ 16 25a 26a 27a 28a CN S99 N S99 N S99 N S99 N S99 N S99 N S99 N S99			33	OH	71	CN OH	13		11
21a		17a		18a		19a		20a	
22		N NH ₂	38		52	[N] NH2	83	NH ₂	>99
29a 30a 31a 32a N >99 N >99 N >99 N >99 N >99		NH ₂	22	IN NH2		NH ₂	25	NH ₂	16
29a 30a 31a 32a N >99 N N >99 N N >99 N >99 N >99 N N >99 N N >99 N N N N		200							
N >99 N >99 N >99 N >99		N CI	80		>99		>99		80
		29a		30a		31a		32a	
33a 34a 35a 36a		N >	99	$\binom{N}{N}$	>99		>99		>99
		33a		34a		35a		36a	

Adv. Synth. Catal. 2019, 361, 1–11 Wiley Online Library 4
These are not the final page numbers! 77

© 2019 Wiley-VCH Verlag GmbH & Co. KGaA, Weinheim



N 6	N 68	N 43	N 22
N 18	NH2 30	N >99	CI N >99
41a	42a	43a	44a
N >99 N NH ₂	N_N >99	89 47a	N 85
454	400	7/0	400
N 77	○ 67	>99	71 N
49a	50a	51a	52a
N 85	N >99	N 87	38 N
53a	54a	55a	56a
N 9 57a	N—————————————————————————————————————	N 17 H 59a	N 15
N N 10	N NH ₂ 27	N N 8 63a	N N 14 H 64a
77 NO ₂	S >99	78 N 67a	N 44
97 69a N	70a N >99	-	, , , , , , , , , , , , , , , , , , , ,

Adv. Synth. Catal. 2019, 361, 1–11 Wiley Online Library 5
These are not the final page numbers! 77

© 2019 Wiley-VCH Verlag GmbH & Co. KGaA, Weinheim



Table 2. The list of synthesized and purified N-oxides.

Substrate	Productivity [mgL ⁻¹ h ⁻¹]	Product	Yield [%]
Pyridine (1a)	39.6	Pyridine-1-oxide (1b)	75
4-Cyanopyridine (31 a)	15.0	4-Cyanopyridine-1-oxide (31b)	68
4-Ethylpyridine (9a)	15.4	4-Ethylpyridine-1-oxide (9b)	64
2-Chloropyridine (29a)	4.3	2-Chloropyridine-1-oxide (29b)	43
2-Hydroxymethylpyridine (12a)	10.4	2-Hydroxymethylpyridine -1-oxide (12b)	78
Pyrazine (33a)	40.0 and 480*	Pyrazine-1-oxide (33b)	82
2,6-Dimethylpyrazine (36a)	25.8	3,5-Dimethylpyrazine-1-oxide (36b)	48
Quinoxaline (52 a)	4.3	Quinoxaline-1-oxide (52b)	66
5,6,7,8-Tetrahydroquinoxaline (55a)	5.4	5,6,7,8-Tetrahydroquinoxaline-1-oxide (55b)	45
Isoquinoline (48a)	5.1	Isoquinoline-2-oxide (48b)	64
1-Methylisoquinoline (49a)	5.1	1-Methylisoquinoline-2-oxide (49b)	42
4-(Pyridin-4-ylsulfanyl)pyridine (66a)	17.0	4-(Pyridin-4-ylsulfanyl)pyridine-1-oxide (66b)	81
4-(1,3-Oxazol-5-yl)pyridine (69 a)	6.5	4-(1,3-Oxazol-5-yl)pyridine-1-oxide (69b)	75
Quinazoline (54a)	12.2	Quinazoline-3-oxide (54b)	67

^{*}reaction was performed in 1 L bioreactor

(48a), quinoxaline (52a), 1,5-naphtyridine (53a) and quinozaline (54a) were transformed at high conversion yields. Their derivatives with one alicyclic ring (50a, 51a, 55a) or methyl group (49a) also possessed good reactivity. However, PML did not catalyze Noxidation of 2-methylquinoline like of 2,6-dimethylpyridine or tetramethylpyrazine, as well as of 6,7dihydro-5*H*-isoquinolin-8-one, 4-aminoquinoline, 11*H*-indeno[1,2-b]quinoxalin-11-one. From the aforementioned biocatalysts only *Verticillium sp.* GF39 cells were shown to utilize two-ring heterocycles. The three-ring containing N-heterocycles 57a, 58a, and 59a were poor substrates for PML, and only the trace amounts of putative monoxides were detected by HPLC-MS. The exception was acridine (56a), which at 0.5 mM concentration underwent a substantial conversion to a possible acridine-10-oxide. To our best knowledge, only Lysobacter antibioticus[21] catalyzed the N-oxidation of three-ring N-heterocycles (phenazine). As expected, PML did not transformed 1,10-phenanthroline, the Fe-chelating agent, which rapidly colored reaction mixture in red inhibiting the catalysis. The two-ring compounds with two or three nitrogen atoms (57a, 60a, 62a) prominent starting materials for synthesis of anticancer 1,4-di-N-oxides 16 were poor substrates for PML, except compound 52 a. A low bio-convertability was observed in the case of compounds 63a and 64a as well. The derivatives not transformed at all included nicotine, nicotinamide, 3bromopyrazolo[1,5-a]pyrimidine, bis(pyridin-2-yl) ethane-1,2-dione, 1-(4-pyridyl)piperidine, 2-(pyridin-2-yl)pyridine, pyrazolo[1,5-a]pyrimidine. However, a group of complex substrates harboring two rings such as 4-(4-nitrobenzyl)pyridine (65a), 4-(pyridin-4-ylsulfanyl)pyridine (66a), 3-(pyrrol-1-yl)pyridine (67a), 4-(pyridin-4-yl)pyridine (68a). 4-(1,3-oxazol-5-yl) pyridine (69a) and 2-phenylpyridine (70a) were converted at high yields.

Overall, PML displayed an extraordinary wide substrate range towards N-heterocyclic compounds that made it prominent among the previously reported biocatalysts. Pyridines were among the most acceptable substrates. Pyrazines and pyrimidines were also oxidized by PML in high conversion yields, while conversion rates of pyridazines where considerably lower. Molecules featuring two six-membered rings were moderate substrates, although mostly not as productive as compounds with a single six-membered ring. The largest molecules that were oxidized by PML consisted of three six-membered rings, albeit only traces of oxidation products were detected. This observation suggested that PML biocatalytic activity declined as substrates size and complexity increased. The particular features of undesirable substrates include two ortho-substituents, carboxy-, hydroxy- and amino-groups or halogen atoms.

Biocatalytic Synthesis of ArN-OX

For the preparative scale synthesis of N-oxides we selected 14 compounds (Table 2) that reflect the elucidated substrate space of PML or are challenging to produce by conventional methods. Pyridine (1a), pyrazine (33a) and their derivatives represented the simplest single-ring heterocycles containing one and two nitrogen atoms. These included 4-ethylpyridine (9a), 2-chloropyridine (29a), 4-cyanopyridine (31a), 2-hydroxymethylpyridine (12a), and 2,6-dimethylpyrazine (36a). Other compounds served as diverse two-ring systems, some of them possessing alicyclic or systems, some of them possessing alicyclic or (52a), 5.6.7.8-tetrahydroquinoxaline (55a), isoquino-

Adv. Synth. Catal. 2019, 361, 1–11 Wiley Online Library

© 2019 Wiley-VCH Verlag GmbH & Co. KGaA, Weinheim



line $(48\,a)$, 1-methylisoquinoline $(49\,a)$, quinazoline $(54\,a)$, 4-pyridin-4-ylsulfanylpyridine $(66\,a)$, and 4-(1,3-oxazol-5-yl)pyridine $(69\,a)$.

The preparative scale synthesis was performed in 200 mL reaction volume for 24 h utilizing 1.0-10.0 mM of appropriate substrate. Pyrazine and pyridine were the most productive substrates found so far. Both were completely converted to corresponding monoxides after 24 h of exposure with PML using 10 mM as a final concentration. The production yields of 75% for pyridine-1-oxide and 82% for pyrazine-1oxide with respective productivities of 39.6 mg L⁻¹h⁻ and 40.0 mg L⁻¹h⁻¹, were achieved. This is tenfold greater than productivities reached by using Burkholderia sp. MAK1 (3.8 mg L⁻¹h⁻¹ for pyridine-1-oxide and 3.9 mg L⁻¹h⁻¹ for pyrazine-1-oxide). [23] On the other hand, Verticillium sp. GF39 cells were reported to possess respectable productivities: 79.5 mg L⁻¹ h⁻¹ for 1-methylisoquinoline-2-oxide, 10.5 mg L-1 h-1 for pyridine-1-oxide, $61.0 \text{ mg L}^{-1}\text{h}^{-1}$ for 2-methylpyridine-1-oxide, $76.9 \text{ mg L}^{-1}\text{h}^{-1}$ for quinoline-1-xide and $5.1 \text{ mg L}^{-1}\text{h}^{-1}$ for isoquinoline-2-oxide. However, the narrow substrate range of this biocatalyst severely limits its application.

Notwithstanding that the N-oxides of 9a, 29a, 31a can be synthesized chemically in a variety of ways, [9.15,30] the PML-catalyzed synthesis is an attractive 'green' alternative. The chemical synthesis of mono-N-oxides from compounds possessing two nitrogen atoms (33 a, 36 a, 52 a, 54 a, 55 a) and especially for pyrazine derivatives is challenging as dioxides may form as well. [27.31] Usually the side reactions are avoided by adding an equimolar amount of the oxidizing agent and conducting the reaction at low temperatures. [32] Besides aromatic mono-N-oxides preparation, our method is suitable for a regioselective synthesis. Earlier reported N-oxidations of 2,6-dimethylpyrazine (36a) resulted in a mixture of 3,5dimethylpyrazine-1-oxide and 2,6-dimethylpyrazine-1-oxide [33,34] Our method yields a product, which was detected as a single peak in HPLC-MS, and ¹H NMR and 13C NMR analysis confirmed it as 3,5-dimethylpyrazine-1-oxide (36b). An oxidation of quinazoline (54a) also gave only one product which was identified as quinazoline-3-oxide (54a). Besides, we have synthesized mono-N-oxides of 5-methyl-6,7-dihydro-5H-cyclopenta[b]pyrazine (38a) and 2-amino-4-chloropyrimidine (44a). However, ¹H NMR and ¹³C NMR analysis did not revealed the exact structure of the final product.

For compounds containing reactive substituents, e.g., 12a, 66a, 69a exposure to typical oxidizing agents (m-CPBA, H₂O₂, trifluoroperoxyacetic acid, HOF-CH₃CN) may modify the substituent as well. Although recently chemoselective methods^[15,16] have been introduced, they are not entirely environment-friendly. PML-catalyzed approach also was shown to

be chemoselective, hence 2-hydroxymethylpyridine was converted to a single product (12b) without traces of possible pyridine-2-carbaldehyde or pyridine-2-carboxylic acid. Moreover, 4-(pyridin-4-ylsulfanyl) pyridine was transformed to the corresponding mono-N-oxide 66b avoiding the formation of a sulfoxide. Finally, oxidation of 4-(1,3-oxazol-5-yl)pyridine resulted in N-oxide in the pyridine ring (69b), while attack on a substituent oxazole ring was not observed. Undoubtedly, such conversions are challenging for the standard chemical approaches.

The biocatalytic synthesis of pyrazine-1-oxide was also performed on a multi-gram scale in 1 L bioreac-The supplementation of pyrazine (800 mg, 10 mmol) together with glucose (1.8 g, 10 mmol) owas executed periodically, once in two hours. In total, 2.4 g of pyrazine was utilized in 6 h. Compared with the conversion in flasks, this technique increased the productivity tenfold, from $40.0 \text{ mg L}^{-1} \text{ h}^{-1}$ to $480 \text{ mg L}^{-1} \text{ h}^{-1}$. It also allowed reaching gram-scale synthesis of 33b in a few hours (Figure S2). We assumed that the observed increase in productivity was caused by enhanced supplementation of oxygen, which was crucial for the PmlABCDEF catalytic activity. It was previously demonstrated that a proper level of oxygen saturation was essential for various oxygenase-catalyzed processes conducted in bioreactors. [35] Indeed, this example suggested that conducting PML-catalyzed N-oxidation in bioreactor should increase productivity in the case of other substrates as

Conclusions

PmlABCDEF, belonging to the SDIMO group, serves as a novel biocatalyst for synthesis of aromatic Noxides with high conversion yields (70-100%). Furthermore, most of those N-oxides have not been previously prepared using a biocatalytic approach. In addition, to best of our knowledge, the synthesis of 4-(pyridin-4-ylsulfanyl)pyridine-1-oxide and 4-(1,3-oxazol-5-yl)pyridine-1-oxide has not been documented neither by biocatalytic nor chemical approach. The presented method is efficient and scalable making a gram-scale synthesis feasible in a few hours. Our method stands out as being biocatalytic, environmentally friendly, productive as well as being regioand chemoselective. Moreover, further improvements of the biocatalyst are possible via a directed evolution of the PmlABCDEF oxygenase.

Experimental Section

Materials

2-Hydroxypyridine, 2-hydroxypyrimidine, 2-aminopyrimidine, 2-methylpyridine, 3-methylpyridine, 4-methylpyridine,

Adv. Synth. Catal. 2019, 361, 1–11 Wiley Online Library

© 2019 Wiley-VCH Verlag GmbH & Co. KGaA, Weinheim



2-hydroxymethylpyridine, 2-mercaptopyridine, 2-hydroxy-3bromopyridine, 2-hydroxy-3-methylpyridine, 2,3-dihydroxy-pyridine, 2,4-dihydroxypyridine, 2,3-dimethylpyridine, 2,4dimethylpyridine, pyridine-2-carboxylic acid, pyridine-4-carboxylic acid, pyridine-2,6-dicarboxylic acid, 2,6-dimethylpyridine, 3,5-dimethylpyridine, 2,3,5-trimethylpyridine, acetylpyrazine, 2,3-dimethylpyrazine, 2,5-dimethylpyrazine, 2,6dimethylpyrazine, 2,3,5-trimethylpyrazine, tetramethylpyrazine, 2-(2-hydroxyethyl)pyridine, pyridazine, 3-methylpyridazine, 6,7-dihydro-5*H*-cyclopenta[b]pyridine, 5-methyl-6,7-dihydro-5H-cyclopenta[b]pyrazine, quinoxaline, tetrahydroquinoxaline, isoquinoline,1-methylisoquinoline, 2-methylquinoline, 5,6,7,8-tetrahydroisoquinoline, 1,2,3,6-tetra-2,4-diamino-6-methyl-1,3,5hydropyridazine-3,6-dione, 2,4,6-triamino-1,3,5-triazine, 1H-pyrrolo[2,3-b] pyridine, 1H,2H,3H-pyrrolo[2,3-b]pyridine, 8-acetyl-5,6,7,8tetrahydroquinoline, nicotine, nicotinamide, 1,5-naphtyridine, 2,6-difluoropyridine, 3-bromopyrazolo[1,5-a]pyrimidine, bis(pyridin-2-yl)ethane-1,2-dione, 4,7-phenanthroline, 1-(4-pyridyl)piperidine, imidazo[1,2-a]pyrazine, norharmane, quinazoline, 4-phenylpyrimidine, 3,5-dibromopyridine, 2-amino-3-hydroxypyridine, 2-phenylpyridine, 2-(pyridin-2-yl) pyridine, 4-(pyridin-4-yl)pyridine, acridine, 1,10-phenanthroline, phenazine were obtained from Sigma-Aldrich (Munich, Germany). 2-Chloropyridine, 2,6-dichloropyridine, pyridine-1-oxide, 3-hydroxypyridine, 2-amino-3-nitropyridine, 2-aminopyridine, pyrazine, quinoline were purchased from Merck (Darmstadt, Germany). Indole, 4-ethylpyridine, 4-(4-nitrobenzyl)pyridine 4-cyanopyridine 3-cyanopyridine 2.46-trimethylpyridine, 3-hydroxymethylpyridine, 4- hydroxymethylwere from Fluka (Buchs, 4-hydroxypyridine Switzerland). The compounds including 2-hydroxy-3-fluoro-pyridine, 2-amino-3-chloropyridine, 2-amino-4-chloropyrimidine were the products of Combi Blocks Inc (San Die-4-(4-pyridinylsulfanyl)pyridine, ylmethyl)pyridine, 4-(1,3-oxazol-5-yl)pyridine, 6,7-dihydro-5H-isoquinolin-8-one were purchased from FluoroChem (Hadfield, UK), 4-methoxypyridine was ordered from Bide Pharmatech (Shanghai, China), and 6-amino-3-cyanopyridine, 2-amino-5-chloropyridine, 2-amino-5-bromopyridine, 2-amino-6-methylpyridine, 3-aminopyridazine, 2-amino-4,6-dimethylpyrimidine, 2,4-diamino-1,3,5-triazine, 3-amino-5,6-dimethyl-1,2,4-triazine were from TCI EUROPE N.V. (Belgium)

Bacterial Strains and Growth Conditions

 $E.\ coli\ DH5\alpha$ (Thermo Fischer Scientific, Lithuania) was used as a host for gene cloning. $E.\ coli\ BL21$ (DE3) and $E.\ coli\ Roseta(DE3)pLysS$ (Novagen, Germany) were chosen as hosts for recombinant protein production. All bacterial strains were routinely grown in Luria-Bertani (LB) broth at 3γ°C, supplemented with kanamycin (100 μgmL $^{-1}$) or chloramphenicol (20 μgmL $^{-1}$) if necessary. Composition of media was as follows: LB (g/L) – tryptone (Formedium, UK) 10.0, yeast extract (Merck, Germany) 5.0, NaCl (Fluka, Switzerland) 5.0; brain heart infusion broth (BHI), (Oxoid, UK) – 37.0. All media were adjusted to pH = 7.2 and autoclaved at 1 atm for 30 min.

Metagenomic Libraries

DNA from soil and sediment samples were isolated by using "ZR Soil Microbe DNA MidPrep^{NA**} (Zymo Research, Germany). Metagenomic libraries were constructed using a pUC19 vector as described. Soil The oxygenases producing hits forming blue colonies were screened by the spreading transformed *E. coli* cells on LB agar supplemented with 1 mM of indole. The plasmid DNA was isolated from each positive clone and the cloned fragment was partially sequenced from both ends.

Construction of pET PmlABCDEF

The oligonucleotide primers phe. xba_F (5'-actatetagagettectgaacegtggtg-3') and phe_hind_R (5'-aattaagetttegaategettgga-acge-3') were ordered from Metabion, Germany. The primers were designed to amplify monoxygenase gene and its ribosomal binding site on p577 A plasmid. The amplification was performed using a Phusion Green Hot Start II High-Fidelity PCR Master Mix (Thermo Fischer Scientific, Lithuania) aaccording to the manufacturer's instructions. The PCR amplicon was hydrolyzed with XbaI and HindIII (Thermo Fischer Scientific, Lithuania) and ligated to the properly digested protein expression vector pET-28b (Novagen, Germany). Standard methods and techniques were employed for DNA manipulations (plasmid transformation, screening, isolation). In the final plasmid (designated pET_PmIABCDEF), the cloned gene was checked by sequencing (Macrogen, Netherlands). The new strains harboring pET_PmIABCDEF plasmid were named PML (E. coli BL21 (DE3)) and PML_Ros (E. coli Rosetta(DE3)pLysS) (Table 3).

Induction Conditions of PmlABCDEF Monooxygenase

PML and PML_Ros strains were cultivated at 30°C on a rotary shaker at 180 pm in 1 L Erlenmeyer flasks containing either 200 mL LB, or BHI medium supplemented with corresponding antibiotic. The broth was additionally supplemented with glucose (to a final concentration of 1.0%) to prevent basal recombinant protein expression. The incubation continued until OD $_{800}$ reached 0.5–0.8. Then the culture was supplemented with isopropyl β -D-1-thiogalactopyranoside (IPTG) to a final concentration of 0.5 mM and placed at $20\,^{\circ}\text{C}$ on a rotary shaker at 180 rpm overnight.

Bioconversions of N-heterocycles using whole Cells of PMI.

After induction, cells were separated from the medium by centrifugation (4000 g for 5 min). Then the biomass (3.0–4.0 g of wet weight) was washed twice with 10 mM potassium phosphate buffer (pH=7.0) and transferred to 1 L Erlenmeyer flasks containing 200 mL of the same buffer and 1.0–10.0 mM of the appropriate substrate. The reaction was carried out at 30 $^{\circ}$ C on a rotary shaker at 180 rpm. After 8 h of incubation, reaction mixture was supplemented with glucose (5 mmol) and the conversion was continued over-

Adv. Synth. Catal. 2019, 361, 1–11 Wiley Online Library

© 2019 Wiley-VCH Verlag GmbH & Co. KGaA, Weinheim



Table 3. Plasmids and strains used in this study.

Plasmid or strain	Relevant characteristics	Source or reference
Plasmid		
p577 A pET-28b	pUC19/HindIII + 9 kb metagenomic DNA insert containing $pmlABCDEF$ gene pBR322-derived ColE1, T7 lac promoter, Km', protein expression vector	This study Novagen, Germany
pET_ pmlABCDEF	Recombinant pET-28b containing pmlABCDEF gene	This study
Strain		
E. coli DH5α	F^ endA1 glnV44 thi-1 recA1 relA1 gyrA96 deoR nupG purB20 q80dlacZ Δ M15 Δ (lacZYA-argF)U169, hsdR17(r_{\kappa}^-m_{\kappa}^+), \lambda^-	Thermo Fischer Scientific, Lithuania
E. coli BL21 (DE3)	F ⁻ ompT gal dcm lon $hsdS_B(r_B^-m_B^-)$ λ (DE3 [lac1 lacUV5-T7p07 ind1 sam7 nin5]) $[malB^+]_{K-12}(\lambda^8)$	Novagen, Germany
E. coli Rosetta (DE3)pLysS	\vec{F} - $ompT$ gal dem lon $hsdS_n(r_n m_n)$ $\lambda(DE3 \{lac1\ lac1V5-T7p07\ ind1\ sam7\ nin5\}\}$ $[malB\]_{k:12}(\Lambda^3)$ $pLysSRARE[T7p20\ ileX\ argU\ thrU\ tyrU\ glyT\ thrT\ argW\ metT\ leuW\ proL\ or_{ists}](Cm^4)$	Novagen, Germany
PML PML_Ros	E. coli BL21 (DE3) harboring pET_PmlABCDEF E. coli Rosetta(DE3)pLysS harboring pET_PmlABCDEF	This study This study

night for a total of 24 h or until 15-50 mg of the selected substrate was completely consumed.

The conversion in a Biostat® B plus bioreactor was accomplished utilizing PML biomass from collected from 2.L of growth medium. The reaction was carried out in 1.L of 10 mM potassium phosphate buffer (pH=7.0) and started with 10 mmol of pyrazine. The bioconversion was monitored by TLC, and portions of 10 mmol of pyrazine were periodically added after observing significant depletion of the substrate. The temperature was kept at 30°C, and pH was maintained at 6.8-7.0 by auto-equilibration with 0.2 M NaOH. Oxygen saturation (pO₂) was kept at 80-95% level by passing air (3 atm) through the reaction mixture and vigorous stirring (400 rpm). Glucose (portions of 10 mmol) was added periodically alongside substrate. The conversion process was controlled using the BioPAT® MFCS/ DA 3.0 software.

Isolation of N-oxides

The reaction mixture was separated from biomass by centrifugation (4000 g for 30 min). The volume of the supernatant was reduced under vacuum to a volume of 10–15 mL and it was transferred to the separation funnel. Then water phase was washed with equivalent volume of ethyl acctate at least three-four times. The organic phases were combined and dried by anhydrous Na,SO₈. The resulting solution was evaporated under reduced pressure to give a final product, N-oxide. All isolation stages were monitored by TLC. The purity of the final product was verified by high-performance liquid chromatography-mass spectrometry (HPLC-MS) and the chemical structure was confirmed by nuclear magnetic resonance (MMR) spectroscopy.

The reaction mixture from bioreactor was also separated from biomass by centrifugation (4000 g for 60 min). Then the supernatant was completely dried out under reduced pressure. The resulting debris was several times gently washed with 5 mL of warm ethyl acetate. Then organic phases were combined and dried by anhydrous $\rm Na_2SO_4$, the solution was evaporated under vacuum to give a final product.

Calculation of Bioconversion Parameters

A conversion is expressed as $((I_a-F_a)/I_a)^x$ 100%, where $I_a=$ initial amount of a substrate before the conversion, F_a- final amount of a substrate after conversion. The substrate amount was determined by integrating the absorbance area (254 nm) of a particular peak in HPLC chromatogram. If no substrate was left, the conversion is defined as complete (>99%). Productivity is an expected amount of N-oxide (mg) produced in 1 L reaction mixture under optimum conditions per 1 h.

HPLC-MS Analysis

Before the analysis the cells were separated from the reaction mixture by centrifugation. The resulting supernatant was mixed with an equal part of acetonitrile, centrifuged and analyzed using a high performance liquid chromatography system. HPLC-MS analysis was performed using a high performance liquid chromatography system (Shimadzu, Japan) equipped with a photo diode array (PDA) detector and a mass spectrometer (LCMS-2020, Shimadzu, Japan) equipped with an ESI source. The data was analyzed using the LabSolutions LCMS software.

Adv. Synth. Catal. 2019, 361, 1–11 Wiley Online Library 9

These are not the final page numbers!

© 2019 Wiley-VCH Verlag GmbH & Co. KGaA, Weinheim



¹H NMR and ¹³C NMR

NMR spectra were recorded in DMSO-d₆ on an Ascend 400: ¹H NMR - 400 MHz, ¹³C NMR - 100 MHz (Bruker, USA). Chemical shifts (b) are reported in ppm relative to the solvent resonance signal as an internal standard.

GenBank Accession Number(s)

The sequence of the p577 A clone containing pmlABCDEF gene cluster was deposited in GenBank under the accession number MK037457.

Acknowledgements

This research was funded by the European Social Fund according to the activity 'Improvement of researchers' qualification by implementing world-class R&D projects Measure No. 09.3.3-LMT-K-712 (grant No. DOTSUT-34(09.3.3-LMT-K712-01-0058/LSS-600000-58)). This research was performed in cooperation with the INMARE consortium.

References

- [1] J. Alcazar, D. Oehlrich, Future Med. Chem. 2010, 2, 169-176.
- [2] J. Clayden, N. Greeves, S.G. Warren, Organic Chemistry, Oxford University Press, 2012, 2, 730–731
- [3] A. M. Mfuh, O. V Larionov, Curr. Med. Chem. 2015, 22, 2819-2857
- [4] J. Balzarini, M. Stevens, E. De Clercq, D. Schols, C. Pannecouque, J. Antimicrob. Chemother. 2005, 55, 2, 135-138.
- [5] Y. Shaker, Arkivoc. 2001,1, 242–248.
- [6] D. E. Chavez, in: Heterocyclic N-oxides (Eds.: O. V. Larionov, B. Maes, J. Cossy, S. Polanc), Springer, 2017,
- [7] H. P. Kokatha, P. F. Thomson, S. Bae, V. R. Doddi, M. K. Lakshman, J. Org. Chem. 2011, 76, 7842–7848.
- [8] H. S. Mosher, L. Turner, A. Carlsmith, Org. Synth. 1963, 4, 828-830.
- [9] C. Coperet, C. H. Adolfsson, V. T. Khovong, K. A. Yudin, B. K. Sharpless, J. Org. Chem. 1998, 63, 1740-
- [10] P. Veerakumar, S. Balakumar, M. Velayudham, K. L. Lu, S. Rajagopal, Catal. Sci. Technol. 2012, 2, 1140-1145.
- [11] A. Thellend, P. Battioni, W. Sanderson, D. Mansuy,
- Synthesis. 1997, 12, 1387–1388.
 [12] D. Sloboda-Rozner, P. Witte, P. L. Alsters, R. Neumann, Adv. Synth. Catal. 2004, 346, 339-345.

- [13] A. W. Chucholowski, S. Uhlendorf, Tetrahedron Lett. 1990. 31. 1949-1952.
- [14] R. Nesi, D. Giomi, S. Papaleo, S. Turchi, J. Org. Chem. 1992, 57, 3713-3716.
- O. V. Larionov, D. Stephens, A. M. Mfuh, H. D. Arman, A. S. Naumova, G. Chavez, B. Skenderi, Org. Biomol. Chem. 2014, 12, 3026-3036.
- [16] D. Limnios, C. G. Kokotos, Chem. Eur. J. 2014, 20, 559-563.
- [17] J. Colby, D. I. Stirling, H. Dalton, Biochem. J. 1977, 165,
- [18] L. A. Damani, P. A. Crooks, M. S. Shaker, J. Caldwell, J.
- D'souza, R. L. Smith, Xenobiotica. 1982, 12, 527-534. [19] S. Kutanovas, R. Rutkienė, D. Tauraitė, R. Meškys, Chemija 2013 24 67-73
- [20] R. Ullrich, C. Dolge, M. Kluge, M. Hofrichter, FEBS Lett. 2008, 582, 4100-4106.
- [21] Y. Zhao, G. Qian, Y. Ye, S. Wright, H. Chen, Y. Shen, F. Liu, L. Du, Org. Lett. 2016, 18, 2495-2498.
- [22] K. Mitsukura, M. Havashi, T. Yoshida, T. Nagasawa, J. Biosci. Bioeng. 2013, 115, 651-653.
- [23] J. Stankevičiūtė, J. Vaitekūnas, V. Petkevičius, R. Gasparavičiūtė, D. Tauraitė, R. Meškys. Sci. Rep. 2016, 6, 39129.
- [24] J. G. Leahy, P. J. Batchelor, S. M. Morcomb, FEMS Microbiol. Rev. 2003, 27, 449-479.
- [25] D. E. Torres Pazmiño, M. Winkler, A. Glieder, M. W. Fraaije, J. Biotechnol. 2010, 146, 9-24.
- V. Petkevičius, J. Vaitekūnas, J. Stankevičiūtė, R. Gasparavičiūtė, R. Meškys, Appl. Environ. Microbiol. 2018 84 00387-18
- [27] M. Carmeli, S. Rozen, J. Org. Chem. 2006, 71, 5761-5765.
- [28] C. E. Tinberg, S. J. Lippard, Biochemistry. 2009, 48, 12145-12158
- [29] H. J. Soscún, M. A. Hinchliffe, J. Mol. Struct. 1994, 304, 109-120. [30] R. T. Shuman, P. L. Ornstein, J. W. Paschal, P. D.
- Gesellchen, J. Org. Chem. 1990, 55, 738-741.
- [31] S. Rozen, A. Shaffer, Org. Lett. 2017, 19, 4707-4709. [32] F. Roudesly, L. F. Veiros, J. Oble, G. Poli, Org. Lett.
- 2018, 20, 2346-2350. [33] B. Klein, J. Berkowitz, J. Am. Chem. Soc. 1959, 81,
- 5160-5166. [34] J. S. Dickschat, H. Reichenbach, I. Wagner-Dobler, S. S.
- Novel, Eur. J. Org. Chem. 2005, 18, 4141-4153. [35] W. A. Deutz, J. B. van Beilen, B. Witholt, Curr. Opin. Biotechnol. 2001, 12, 419-425.
- [36] N. Urbelienė, S. Kutanovas, R. Meškienė, R. Gasparavičiūtė, D. Tauraitė, M. Koplūnaitė, R. Meškys. Microb. Biotechnol. 2018. doi: 10.1111/1751-7915.13316.

Adv. Synth. Catal. 2019, 361, 1-11 Wiley Online Library

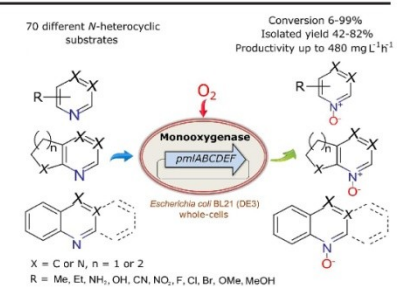
© 2019 Wiley-VCH Verlag GmbH & Co. KGaA, Weinheim

FULL PAPER

A Biocatalytic Synthesis of Heteroaromatic N-Oxides by Whole Cells of Excherichia coli Expressing the Multicomponent, Soluble Di-Iron Monooxygenase (SDIMO) PmlABCDEF

Adv. Synth. Catal. 2019, 361, 1-11

V. Petkevičius*, J. Vaitekūnas, D. Tauraitė, J. Stankevičiūtė, J. Šarlauskas, N. Čėnas, R. Meškys



Publication IV

Petkevičius V, Vaitekūnas J, Vaitkus D, Čėnas N, Meškys R. Tailoring a soluble diiron monooxygenase for synthesis of aromatic *N*-oxides. *Catalysts*. 2019, 9(4), e356.





Article

Tailoring a Soluble Diiron Monooxygenase for Synthesis of Aromatic *N*-oxides

Vytautas Petkevičius ^{1,*}, Justas Vaitekūnas ¹, Dovydas Vaitkus ¹, Narimantas Čėnas ² and Rolandas Meškys ¹

- Department of Molecular Microbiology and Biotechnology, Institute of Biochemistry, Life Sciences Center, Vilnius University, Saulétekio 7, LT-10257 Vilnius, Lithuania; justas vaitekunas@bchi.vu.lt (J.V.); dovydas.vaitkus07@gmail.com (D.V.); rolandas.meskys@bchi.vu.lt (R.M.)
- Department of Xenobiotics Biochemistry, Institute of Biochemistry, Life Sciences Center, Vilnius University, Saulétekio 7,LT-10257 Vilnius, Lithuania; narimantas.cenas@bchi.vu.lt (N.Č.)
- * Correspondence: vytautas.petkevicius@bchi.vu.lt

Received: 18 March 2019; Accepted: 3 April 2019; Published: 12 April 2019



Abstract: The aromatic N-oxides have received increased attention over the last few years due to their potential application in medicine, agriculture and organic chemistry. As a green alternative in their synthesis, the biocatalytic method employing whole cells of Escherichia coli bearing phenol monooxygenase like protein PmlABCDEF (from here on – PML monooxygenase) has been introduced. In this work, site-directed mutagenesis was used to study the contributions of active site neighboring residues 1106, A113, G109, F181, F200, F209 to the regiospecificity of N-oxidation. Based on chromogenic indole oxidation screening, a collection of PML mutants with altered catalytic properties was created. Among the tested mutants, the A113G variant acquired the most distinguishable N-oxidations capacity. This new variant of PML was able to produce dioxides (quinoxaline-1,4-dioxide, 2,5-dimethylpyrazine-1-dioxide) and specific mono-N-oxides (2,3,5-trimethylpyrazine-1-oxide) that were unachievable using the wild type PML. This mutant also featured reshaped regioselectivity as N-oxidation shifted towards quinazoline-1-oxide compared to quinazoline-3-oxide that is produced by the wild type PML.

Keywords: soluble diiron monooxygenase; aromatic *N*-oxides; protein engineering; biocatalysis; mutagenesis

1. Introduction

Biocatalysis has become an attractive alternative to chemical synthesis because of its exceptional selectivity, high efficiency and ability to produce relatively pure compounds. The number of biotransformation processes applied on a commercial scale is constantly increasing [1]. The usage of biocatalysts in synthesis also avoids the need for the blocking and deblocking steps often found in organic counterparts and usually are performed under mild conditions [2]. The majority of currently used enzymes in biocatalysis are hydrolases and transferases, though various oxygenases recently have been attracting tremendous interest as well [3]. These enzymes are able to hydroxylate various non-activated hydrocarbons regio- and stereospecifically, thus accomplishing chemical transformations that are of a significant challenge in synthetic chemistry [4]. Oxygenases catalyze a wide variety of reactions including activation of sp³ hybridized C atoms, epoxidation of C=C double bonds, aromatic hydroxylation, N-oxidation, deamination and dehalogenation, Baeyer-Villiger oxidation, as well as N-, O- and S-dealkylation [5]. These enzymes can accept a diversity of substrates, including fatty acids, terpenes, steroids, prostaglandins, mono-aromatic, poly-aromatic and heteroaromatic compounds, as well as alkanes, alkenes, organic solvents, antibiotics, pesticides, carcinogens and

Catalysts 2019, 9, 356; doi:10.3390/catal9040356

www.mdpi.com/journal/catalysts

Catalysts 2019, 9, 356 2 of 14

toxins, thus suggesting their application in pharmacology, agriculture and bioremediation [6]. In fact, the most extensively studied cytochrome P450s together with Rieske oxygenases, flavin-dependent monooxygenases, iron- and α -ketoglutarate-dependent dioxygenases have been applied to the synthesis of chemicals on a preparative scale [5]. Nevertheless, alternative types of oxygenases are also intensely studied. In particular, soluble diiron monooxygenases (SDIMOs) have been actively studied for a number of years. The family of SDIMO enzymes is composed of aromatic/alkene monooxygenases, phenol monooxygenases, soluble methane monooxygenases (sMMO), alkene monooxygenases, and propane monooxygenases together with tetrahydrofuran monooxygenases [7,8]. SDIMOs are threeor four-component enzyme systems which contain: i) a dimeric hydroxylase protein composed of two or three subunits in an $(\alpha\beta\gamma)_2$ or $(\alpha\beta)_2$ quaternary structure, ii) an nicotinamide adenine dinucleotide (NADH)oxidoreductase with an N-terminal chloroplast-type ferredoxin domain and a C-terminal reductase domain with flavin adenine dinucleotide (FAD) and nicotinamide adenine dinucleotide phosphate (NAD(P))-ribose binding regions, iii) a small effector or coupling protein with no prosthetic groups, and in some cases, iv) a Rieske-type ferredoxin protein. The active site of protein complex is located within the largest α subunit; it contains a carboxylate-bridged diiron center usually coordinated by four glutamate and two histidine residues [8]. The substrate space of those enzymes encompasses alkylated phenols, aromatic heterocycles, alkanes and alkenes of a variable length, polychlorinated hydrocarbons and other hazardous pollutants indicating their potential for bioremediation applications [9]. Taken together with favorable kinetic parameters and possible regio-, stereoselectivity, the SDIMOs emerge as candidates in various biocatalysis applications [10]. Most recently we have demonstrated that an enzyme of SDIMO family could also be employed to catalyze a different type of oxidation as phenol monooxygenase like (PML) monooxygenase transformed numerous nitrogen-containing aromatic compounds to the corresponding N-oxides [11]. N-oxidation is commonly used in the chemistry of N-heteroaromatics to increase their reactivity for further modifications [12]. In addition, N-oxides alone are desirable compounds in pharmacy, catalysis, agriculture and pyrotechnics [13]. Despite the array of available chemical methods for N-oxides synthesis, biocatalytic approaches are limited and incomplete. To date, only PML catalyzed transformations have been demonstrated as a productive and green alternative to existing chemical techniques. However, an inclusive toolbox of biocatalysts for targeted and efficient preparation of desired N-oxides is still under development. Therefore, both directed evolution and rational design were successfully used to identify amino acids responsible for SDIMO regioselectivity and to improve their activity toward natural and artificial substrates is a promising way to improve an existing toolbox

Thus, in this study, we analyzed sequence-structure-function based relationships in well-studied SDIMOs to create the specific PML mutants. An indirect chromogenic screening method based on indole oxidation was used to select mutants featuring new catalytic properties relative to wild type enzyme. We have successfully isolated variants of PML with altered regiospecificity for N-oxidation, increased substrate range or capacity to produce aromatic di-N-oxides.

2. Results and Discussion

2.1. Identification of Target Amino Acids for Mutagenesis

The PML monooxygenase shares high sequence homology to SDIMO group of phenol monooxygenases. PML shows 86% amino acids similarity to butylphenol monooxygenases from Pseudomonas putida, the closest basic local alignment search tool (BLAST) hit with known function. This PML enzyme was isolated from our collection of various oxygenases obtained from metagenomes, and its sequence is submitted to NCBI under accession number MK037457. PmlABCDEF shares all similarities to a typical SDIMO. The core of hydroxylase is composed of PmlD, PmlB and PmlE, which stand for α,β and γ subunits, respectively. PmlF is an NADH oxidoreductase, while PmlA and PmlC most likely perform regulatory functions. The carboxylate-bridged diiron center is buried within a

Catalysts 2019, 9, 356 3 of 14

catalytic PmlD subunit. The wild type PML has been introduced as a novel biocatalyst for oxidation of N-heteroaromatic compounds [11]. It has been demonstrated that under optimal conditions (30 °C, pH 7.0, 24 h, 1 mM substrate concentration) specific mono-N-oxides are formed (Table 1).

The possible hotspots for mutagenesis were deduced from the MSA (multi-sequence alignment) of characterized SDIMOs (Figure 1) and the structural model of PML (Figure 2). Our first goal was to try to expand the hydrophobic pocket adjacent to the active site of PML. We expected that enlarging the active center cavity would produce mutants with preferences for bulkier and more complex substrates. Three phenylalanine residues (F181, F200, F209) situated near the diiron center in our 3D model (Figure 2) were considered as an appropriate target since previous reports indicated that amino acids in these positions have potential to change substrate specificity as well as regio- and stereospecificity [15-17]. Semiconservative phenylalanine (F181 in PML sequence; F176 in toluene 3-monooxygenase (T3MO) [18], toluene-o-xylene monooxygenase (ToMO) [15,19], toluene 4-monooxygenase (T4MO) [20]; F185 in butane monooxygenase (BMO) [21]; F172 in propene monooxygenase (PMO) [16]; F188 in soluble methane monooxygenase (sMMO) [22]; F181 in toluene 2-monooxygenase (TOM) [23,24]; F191 in HpdABCDE (Hpd) [25]) was shown to be important in determining the size of the acceptable substrate in ToMO and T4MO. Other addressed positions regulated regio- (F196 in T4MO) and stereospecificity (V188 in PMO) [16,20]. This hotspot varies among SDIMOs, from large aromatic residues like phenylalanine (F196 in T3MO and ToMO, F200 in TOM, F210 in Hpd) to small residues like glycine (G205 in BMO and G208 in sMMO). The corresponding position in PML is occupied by F200. Finally, mutagenesis of F205 in ToMO and T4MO demonstrated the importance of this residue, because the decreased volume of a side-chain (F205L, F205I, F205G) changed regioselectivity of the enzyme or an affinity to the specific substrate. Other SDIMOs also employ hydrophobic/aromatic residues in the analogous site (F205 in T3MO, I214 in BMO, L197 in PMO, I217 in sMMO, F209 in TOM, F219 in Hpd), including PML, which possesses F209. Keeping these data in mind, three bulky hydrophobic semiconservative amino acids of PML (F181, F200 and F209) were chosen for the site-directed mutagenesis to alanines by a classical method (Section 4, Tables 2 and 3).

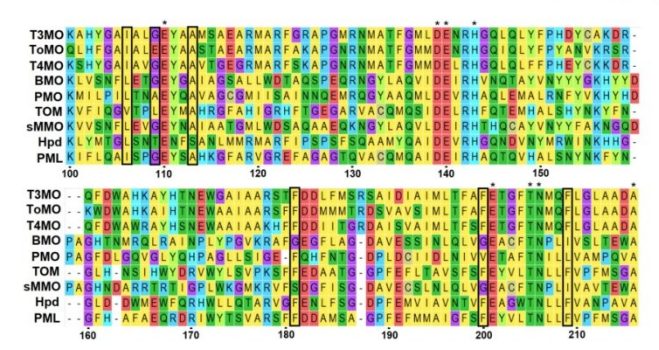


Figure 1. The protein sequence alignment between well-studied SDIMOs α subunits. Toluene 3-monooxygenase (T3MO) of Ralstonia picketii PKO-1, toluene-o-xylene monooxygenase (ToMO) of Pseudomonas stutzeri OX1, toluene 4-monooxygenase (T4MO) from Pseudomonas mendocina KR1, butane monooxygenase (BMO) from Thauera butanivorans, propene monooxygenase (PMO) from Mycobacterium sp. M156, toluene 2-monooxygenase (TOM) from Burkholderia cepacia G4, soluble methane monooxygenase (sMMO) from Methylococcus capsulatus Bath, 2-hydroxypyridine 5-monooxyganase HpdABCDE (Hpd) from Burkholderia sp. MAK1, PmlABCDEF (PML). The numeration is based on PML protein sequence.

Catalysts 2019, 9, 356 4 of 14

We obtained both single mutants (F181A, F200A, F209A) and double mutants (F181A/F200A, F181A/F209A, F200A/F209A) of the PML monooxygenase. Then those mutants were tested for N-oxidation capabilities. However, only two variants (F200A and F209A) were able to transform pyridine, pyrazine, quinoxaline, quinazoline, and 2,5-dimethylpyrazine into corresponding N-oxides while the rest of mutants lost this activity completely. We tested F200A and F209A mutants towards a number of larger substrates (acridine, phenazine, 4,7-phenantroline, norharmane). Those compounds were poor substrates for PML and only a minor amount of N-oxides were detected after transformation using wild type enzyme [11]. We assumed that an enlarged active site pocket of F200A and F209A mutants would result in an increased conversion compared to the wild type PML. However, the tested mutants did not possess enhanced N-oxidation capacity of bulkier substrates. Actually, these variants seemed to retain a substrate scope of the parental enzyme with some loss in efficiency of conversion (Table 1). Similar observations were made with other monooxygenases. The equivalent mutations decreasing the volume of an active center in ToMO (F176L, F176L, F196A, F205G) showed an altered regiospecificity for phenol, toluene or naphthalene [15,19]. However, mutants also were less efficient as the productivity and $k_{cat}\ dropped$ for all variants. Even more, T4MO variants F176A and F196G completely lost the activity toward toluene, trichloroethane and butadiene [26]. In fact, one of the most recent studies on SDIMO engineering revealed that only the combination of saturation mutagenesis at those positions produced the best results in terms of reshaped regioseletivity and productivity [17].

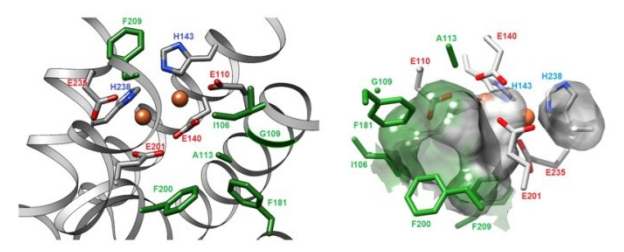


Figure 2. Two different representations of the 3D model of PmID active site. Ribbon model (on the left) shows amino acids of interest as sticks in the helix bundle, while surface model (on the right) represents a hydrophobic pocket in the active site. The carboxylate-bridged diiron center presented in Corey-Pauling-Koltun (CPK) coloring, amino acids chosen for mutagenesis displayed in green. Orange spheres represent two iron atoms.

2.2. The Selection of PML Mutants Based on Chromogenic Screening

Next, we targeted other important amino acids around the active center and cross-checked with the literature anticipating more significant changes in PML substrate specificity. Three residues in PML, namely I106, A113, and G109 were selected for saturation mutagenesis for the following reasons: (i) so-called substrate gate permits the substrate to enter the active site; usually its component is an aliphatic hydrophobic amino acid (L110 in sMMO; L91 in PMO; L107 in BMO; I100 in T4MO, T0MO, T3MO; V106 in T0M; L116 in Hpd). Its substitution into a smaller residue (alanine) resulted in a relaxed regiospecificity and accessibility for larger substrates. Equally well, its replacement by a larger phenylalanine residue induced a preference for smaller substrates or even impeded the activity [22–24]. Based on MSA, the corresponding position in PML is I106; (ii) another selected hotspot in PML is A113, which is conserved in almost all analyzed sequences (A117 in sMMO; A98 in PMO; A114 in BMO; A107 in T4MO, T0MO, T3MO; A113 in T0M). This site was shown to be decisive in substrate orientation and binding [16,18,27,28]; (iii) an additional hotspot crucial for enzyme regioselectivity, which exhibits a great variability, e.g., E103 in T0MO [15,19], A94 in PMO [16], and G103 in T4MO [20,29] and T3MO [18].

Catalysts 2019, 9, 356 5 of 14

Glycines are also present in BMO and sMMO (G110 and G113, respectively), although there are no data on their mutagenesis. The equivalent residue in TOM is I109, while Hpd bears T119. The corresponding amino acid in PML monooxygenase is G109.

To select potentially improved/changed enzymes from the library of mutants a convenient method was required. Aforementioned studies used a direct screening based on transformation of the appropriate substrate. The nylon membrane assay was used to visually inspect the color development by the end products (hydroquinone, resorcinol, catechol and their derivatives) produced by different mutants [19]. The PML similar approach seemed impractical as the majority of the potential N-oxides likely are not intensely colorful and would not stain bacterial colonies. However, SDIMOs are able to convert indole into a variety of pigments (indigo, indirubin, isoindigo) and colorful hydroxyindole derivatives (isatin, 6-hydroxyindole, 7-hydroxyindole). On the other hand, an altered indole oxidation specificity after the mutagenesis of TOM, ToMO and T4MO, induced the formation of different pigments [17,30,31]. It enabled the selection of distinct mutants on the base of diverse color development. We hypothesized that PML mutants with an altered oxidation regiospecificity of indole might possess different N-oxidation patterns as well. Hence, in total, nineteen differently colored colonies were selected (Figure 3). Five distinct coloration patterns were observed in the case of the I106 library. Sequencing of individual hits revealed that three different enzymes were created. I106N was selected two times, 106E was selected one time, and I106C also was selected two times. In addition, I106A mutant was created by site-direct mutagenesis separately. From the A113 library, we were able to distinguish five differently hued colonies. Sequence analysis of hits uncovered them as A113G (two times), A113V (one time) and A113F (two times). The G109 library produced the greatest coloration variety as nine different variants were selected in total. They were identified as G109M, G109Q, G109H (one time) and G109L, G109K, G109T (two times). Then those new enzymes were tested for their catalytic properties towards various N-heteroaromatic compounds.

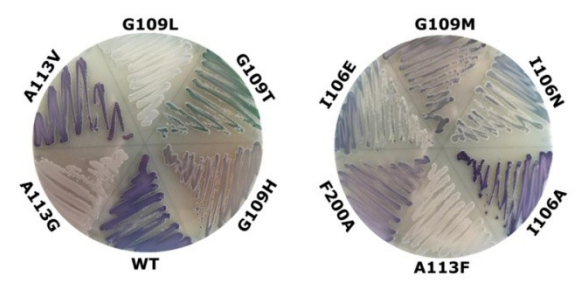


Figure 3. The formation of indigo-like pigments by isolated PML mutants. Only the most distinguishable variants are presented. Luria-Bertani (LB) plates were supplemented with 0.5 mM indole.

2.3. Elucidation of Properties of the Most Prominent Mutant A113G

In order to simplify the analysis of generated mutants, we avoided the use of a wide variety of previously identified wild type PML substrates [11] and concentrated on the compounds that could yield some notable end products. Those included various diazines and triazines to investigate the possibility of multiple N-oxidation, asymmetric compounds for potential regioselectivity shift, and some bulky derivatives that were barely oxidized by the wild type PML. From all tested mutants, the A113G variant gained the most distinctive catalytic properties (Figure 4). In particular, the A113G mutant was able to produce several di-N-oxides which were not characteristic for the parental PML. The A113G variant transformed quinoxaline to the mixture of two products. One compound (molecular

Catalysts 2019, 9, 356 6 of 14

mass increased by 16 Da) was previously identified as quinoxaline-1-oxide [11]. The other product (molecular mass increased by 32 Da) was separated and purified in this work (Figure 4A). The Nuclear Magnetic Resonance (NMR) as well as ultraviolet (UV) spectra of the compound matched those of quinoxaline-1,4-dioxide, a prominent starting material for the synthesis of anticancer agents [13]. The similar outcome was observed for 2,5-dimethylpyrazine, which was converted to the mixture of 2,5-dimethylpyrazine-1-oxide, as in the case of the wild-type PML [11], and to a new compound 2,5-dimethylpyrazine-1,4-dioxide (Figure 4B). In contrast, parental PML produced specific dioxide solely with pyrazine (Figure 4C) and only after prolonged exposure (48 h instead of 24 h) and lower substrate concentration (0.5 mM instead of 1.0 mM).

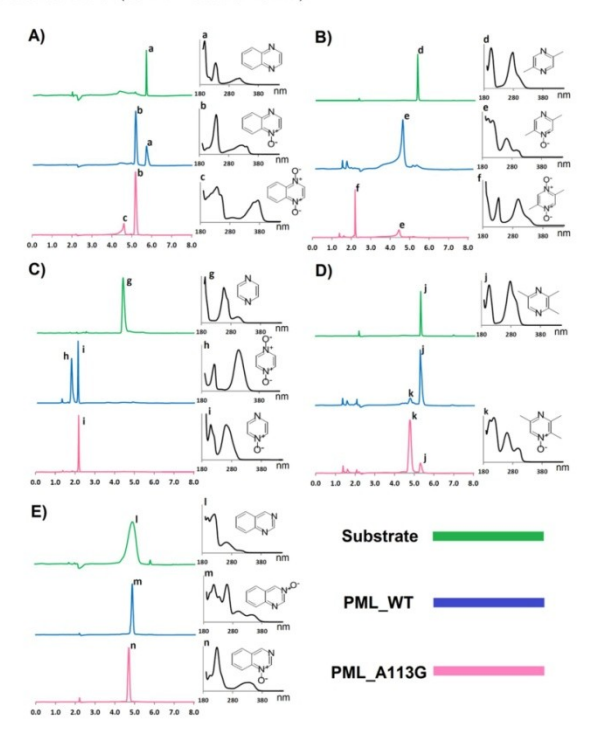


Figure 4. The analysis of the conversion reactions catalyzed by the wild type PML and the A113G mutant. Conversions conducted at 30° C for 24 h. The initial concentration of substrate was 1.0 mM. The end products were analyzed by high-performance liquid chromatography (HPLC). A) quinoxaline (345 nm); B) 2,5-dimethylpyrazine (277 nm); C) pyrazine (282 nm); D) 2,3-5-trimethylpyrazine (260 nm); E) quinazoline (320 nm). Lowercase letters relate the appropriate peak in HPLC to its corresponding ultraviolet (UV) spectra.

Catalysts 2019, 9, 356 7 of 14

In addition, this mutant was able to almost completely convert 2,3,5-trimethylpyrazine (Figure 4D) to a single compound (92% conversion using 1.0 mM of a substrate), which was later identified as 2,3,5-trimethylpyrazine-1-oxide. Production of latter by the wild type enzyme barely reached 6% conversion. The most distinct feature of the A113G mutant was the changed regioselectivity of N-oxidation. Quinazoline was oxidized by parental PML to quinazoline-3-oxide exclusively [11]. However, the A113G mutant transformed this substrate to the product with different retention time and UV spectra (Figure 4E), which indicated the formation of a new compound. After isolation and NMR analysis (Supplementary Materials), the product was confirmed as quinazoline-1-oxide, demonstrating a shift of oxygen attack from N3 to N1 position.

2.4. Impact of the Active Site Neighboring Amino Acids in PML Mutants

The A113 position appeared to be decisive in determining the substrate specificity. This position appears to be conservative in all well-studied monooxygenases, suggesting that it offers some evolutionary advantage. It seems that the variance in molecular volume at this site plays a key role. We showed that alanine-to-glycine substitution resulted in broadened and reshaped N-oxidation capabilities (Table 1). When this position was occupied by a bulkier residue (mutant A113V), the oxidation of quinoxaline and 2,3,5-trimethylpyrazine was completely suppressed. A larger substitute (A113F variant) constrained the catalysis even more since the A113F mutant just barely oxidized pyrazine, quinazoline and 2,5-dimethylpyrazine. In SDIMOs, residues acting as substrate gate were previously shown to be a major factor controlling substrate accessibility and reaction regioselectivity. However, in our study, an equivalent residue I106 of PML did not appear as important as was expected. The I106A mutant lacks leucine side-chain as a possible substrate size and entrance regulating factor. Nevertheless, there were no significant changes in oxidation patterns relative to wild type counterpart except for the lost ability to produce pyrazine-1,4-dioxide. Some other variants (I106E, I106N, I106C) also mostly retained the substrate scope of the parental enzyme, suggesting that I106 position was not critical for PML activity towards nitrogen heterocycles. Another hotspot G109 produced a variety of different PML mutants. G109M and G109Q variants apparently maintained N-oxidation features of primary PML except for the 2,3,5-trimethylpyrazine conversion. Mutants G109K, G109T and G109H additionally lost the capacity to form pyrazine-1,4-dioxide. Surprisingly, the G109L variant acquired almost exceptional ability to oxidize 2,3,5-trimethylpyrazine with a good yield, 89%, despite a possibly increased molecular volume of the hydrophobic pocket. This is apparently conflicting with the properties of A113G. On the other hand, the effect of G109 modification might be indirect, as it affects the neighboring E110 which is one of the active site constituents.

Most mutations in PML seemed to act as the determinants in substrate binding or access which resulted in the decrease of the conversion efficiency for certain compounds, though led to the surge of the transformation for others. Contrary, modifications in the reviewed SDIMOs often resulted in mutants with altered regioselectivity for hydroxylation. In our case, the shift in regiospecificity was detected only for N-oxidation of quinazoline. However, this phenomenon may be more variable using the series of compounds with a larger number of nitrogen atoms and their different surroundings. It is possible that by using substituted quinazolines, asymmetric diazines or other nitrogen-containing aromatics, these PML mutants would exhibit a broad range of different catalytic pathways. Moreover, the future modification of residues at PML active site vicinity might produce entirely diverse biocatalysts. Profoundly different from well-studied SDIMO, the monooxygenase HpdABCDE from Burkholderia sp. MAK1 serves as a good illustration. This enzyme not only transforms certain pyridines into corresponding N-oxides, but also hydroxylates 5-position of 2-hydroxy- and 2-aminopyridine derivatives [32]. This indicates that the residues encompassing the active site of SDIMO enzymes not only determine the pathways of N-oxidation, but also may influence the hydroxylation of N-heteroaromatic ring.

8 of 14

Catalysts 2019, 9, 356

Table 1. N-oxidation capabilities of PML mutants. Mono-N-oxide conversion * is calculated based on the consumption of the substrate. High degree of conversion (>70%) is labeled by '++'; conversion below 10% is depicted by '+' sign; transformations without traceable product indicated by '-: The ability to form a corresponding di-N-oxide is marked as 'Yes'.

		Z Z		z z		z z	\		
	1- <i>N</i> → 0	$1,4-N \rightarrow 0$	1-N → O	$1,4-N \rightarrow 0$	$1-N \rightarrow 0$	3-N → O	$1-N \rightarrow 0$	$1,4-N \rightarrow 0$	$1-N \rightarrow 0$
PML WT	++	Yes	++	,	1	++	++		+
A113G	++	Yes	++	Yes	++		++	Yes	++
A113V	+	Yes				+	++		
A113F	+			,		+	+	•	
I106A	++		+	,	,	++	++	,	,
I106E	+		++	•		+	++		
I106N	++	Yes	+	,		++	++	,	
I106C	+	Yes	++	,	٠	+	++	,	
G109M	++	Yes	++	,	,	+	++	,	,
G109L	++		++			+	++		+
G109K	++		++	,		++	++	,	
G109T	+		+			++	++		
G109Q	++	Yes	++	,		+	++	,	
G109H	+		+	,	,	+	+		
F181A				,					
F200A	++		+	,		+	++		
F209A	+		+			++	++		
F181A/F200A	,		,	,	,	,	,	,	,
F181A/F209A				,					
F200A/F209A									

* For conversions the whole cells of E. coli BL-21 bearing different PML mutants were used. The experiments were carried out in 10 mL reaction volume containing the appropriate substrate (1 mM) at 30°C for 24 h.

Catalysts 2019, 9, 356 9 of 14

3. Conclusions

Overall, we have demonstrated that altering the specific set of amino acids in PML affected regiospecificity of the oxygenase reaction, changed catalytic parameters or expanded range of possible substrates. We successfully applied a chromogenic screening method based on the formation of indigo-like pigments as an indirect selection platform for PML mutants with changed N-oxidation capabilities. This study strongly contributes to the field of SDIMOs and is a promising precedent exploiting further opportunities for biooxidation of N-heteroaromatic compounds by these versatile catalysts.

4. Materials and Methods

4.1. DNA Primers Used in this Study

Primers used in this study were ordered from Metabion, Munich, Germany. They were designed to amplify DNA sequence in pET_pmlABCDEF plasmid flanked by restriction sites of Sall and NheI restriction endonucleases.

Table 2. DNA sequence of the primers.

Primer Name	Primer Sequence (5' \rightarrow 3' Direction)	Use
PheP1_Sal_F	acgcatcgtcgacgacctctttgcc	Cloning
PheP3_Nhe_R	gtacagggctagcatgaactggtgg	Cloning
PheP3_I106A	aagatctttctgcaggccgccagccctggcgaatattc	Transforming I106 to A106
PheP3_I106A_R	gaatattcgccagggctggcggcctgcagaaagatctt	Transforming I106 to A106
PheP3_I106_SM	aagatetttetgeaggeeNNNageeetggegaatatte	Saturation mutagenesis of I106
PheP3_I106_SM_R	gaatattcgccagggctNNNggcctgcagaaagatctt	Saturation mutagenesis of I106
PheP3_G109_SM	gccatcagccctNNNgaatattccgcg	Saturation mutagenesis of G109
PheP3_G109_SM_R	cgcggaatattcNNNagggctgatggc	Saturation mutagenesis of G109
PheP3_ A113_SM	cctggcgaatattccNNNcacaagggctttg	Saturation mutagenesis of A113
PheP3_ A113_SM_R	caaagcccttgtgNNNggaatattcgccagg	Saturation mutagenesis of A113
PheP3_F181A_F	gtggcccgctcgttcgccgacgatgccatgag	Transforming F181 to A181
PheP3_F181A_R	ctcatggcatcgtcggcgaacgagcgggccac	Transforming F181 to A181
PheP3_F200A_F	ggcgatcggcttctccgccgaatatgtcctgacc	Transforming F200 to A200
PheP3_F200A_R	ggtcaggacatattcggcggagaagccgatcgcc	Transforming F200 to A200
PheP3_F209A_F	cctgaccaacctgctggctgtgcccttcatgtcc	Transforming F209 to A209
PheP3_F209A_R	ggacatgaagggcacagccagcaggttggtcagg	Transforming F209 to A209

4.2. Plasmids and Strains Used in This Study

In our previuos work [11], plasmid p577A was selected as a *N*-oxidation-possitive clone from metagenomic collection of various oxygenases and sequenced. PmlABCDEF gene cluster was cloned to pET-28b expression vector (Novagen, Germany) to yield plazmid pET_pmlABCDEF.

Table 3. The characteristics of the strains and plasmids.

Plasmid Or Strain	Relevant Characteristics	Source Or Reference
Plasmid		
p577A	pUC19/HindIII + 9 kb metagenomic DNA insert containing pmlABCDEF gene	[11]
pET_pmlABCDEF	Recombinant pET-28b containing pmlABCDEF gene	[11]
Strain		
E. coli DH5α	F^- endA1 glnV44 thi-1 recA1 relA1 gyrA96 deoR nupG purB20 $φ80dlacZ\Delta$ M15 $\Delta(lacZYA-argF)$ U169, hsdR17($r_K^-m_K^{-+}$), λ^-	Thermo Fischer Scientific, Vilnius, Lithuania
E. coli BL21 (DE3)	F ⁻ ompT gal dcm lon $hsdS_B(r_B^-m_B^-)$ $\lambda(DE3$ [lacI lacUV5-T7p07 ind1 sam7 nin5]) [malB ⁺] _{K-12} (λ^S)	Novagen, Darmstadt, Germany

Catalysts 2019, 9, 356 10 of 14

4.3. Site-Directed and Saturation Mutagenesis

Polymerase chain reaction (PCR) was conducted in 25 µl of the reaction mixture containing 12.5 µL of Phusion Green Hot Start II High-Fidelity PCR Master Mix (Thermo Fischer Scientific, Vilnius, Lithuania), 200 nM of each primer (see Section 4.1), ~50 ng of matrix DNA (p577A) and water up to 25 µl. The mutagenesis procedure consisted of two stages. First, two overlapping PCR amplicons were produced. One was made by using PheP1_Sal_F and desired mutation reverse primer (e.g., PheP3_I106A), and the other-PheP1_Nhe_R and desired mutation forward primer (e.g., PheP3_I106A_R). For the saturation mutagenesis, a set of primers labeled 'SM' was used instead. For this PCR step, initial denaturation was 98 °C for 30 s followed by 30 cycles of 98 °C for 10 s, 55 °C for 15 s, 72 °C for 30 s and a final extension at 72 °C for 7 min. Next, these amplicons were merged by PCR to a single DNA fragment containing preferable modification. In this step initial denaturation was 98 °C for 30 s followed by 30 cycles of 98 °C for 10 s, 45–55 °C gradient for 15 s, 72 °C for 60 s and a final extension at 72 °C for 7 min. As the primers, PheP1 Sal F and PheP3 Nhe R were designed to amplify the region in pmlD gene flanked by SalI and NheI restriction endonucleases, thus combined PCR product was ready for cloning. The PCR amplicon was hydrolyzed with SalI and NheI (Thermo Fischer Scientific, Vilnius, Lithuania), and ligated to the properly digested plasmid pET_pmlABCDEF. Standard methods and techniques were employed for DNA manipulations (plasmid transformation, screening, isolation).

4.4. Chromogenic Screening Assay on Agar Plates with Indole

Mutant libraries were created by isolating total plasmid DNA from colonies of $E.\ coli\ DH5\alpha$ transformed with the ligation mixture prepared as described in Section 4.3. Then, $E.\ coli\ BL21\ (DE3)$ cells transformed with mutant library were plated on Luria-Bertani (LB) agar containing 0.5 mM indole and 0.5 mM isopropyl β -D-1-thiogalactopyranoside (IPTG). Bacteria were grown overnight at 30 °C. Bacterial colonies which possessed coloration different from the wild type counterpart were picked for DNA sequencing (Macrogen, Amsterdam, Netherlands). Composition of LB media was as follows: in g/L—tryptone (Formedium, UK) 10.0, yeast extract (Merck, Germany) 5.0, NaCl (Fluka, Buchs, Switzerland) 5.0 + agar (Formedium, Hunstanton, UK) 15.0 for LB agar plates. The medium was adjusted to pH 7.2 and autoclaved at 1 atm for 30 min.

$4.5.\ Conditions\ for\ biomass\ growth\ and\ protein\ biosynthesis$

E. coli BL21 (DE3) cells carrying PML monooxygenase variants were cultivated at 30 °C on a rotary shaker at 180 rpm in 250 mL flat-bottomed flasks containing 50 mL LB supplemented with kanamycin (40 µg mL $^{-1}$). The broth was additionally supplemented with glucose (to a final concentration of 1.0%), to prevent premature recombinant protein expression. The incubation continued until OD $_{600}$ reached 0.5–0.8. Then the culture was supplemented with IPTG to a final concentration of 0.5 mM, and placed at 20 °C on a rotary shaker at 180 rpm overnight.

4.6. Whole Cell Bioconversions using PML Mutants

After induction, cells were separated from the medium by centrifugation ($4000 \times g$ for 5 min). Then the biomass was washed twice with 10 mM potassium phosphate buffer (pH 7.0) and transferred (200–300 mg of wet weight) to 100 mL flat-bottomed flasks containing 20 mL of the same buffer and 1.0 mM of the appropriate substrate. The reaction was carried out at 30 °C on a rotary shaker at 180 rpm. After 8 h of incubation, the reaction mixture was supplemented with glucose (5 mmol), and the bioconversion was continued overnight for a total of 24 h. Compounds used in bioconversions are listed in our previous study [11].

Catalysts 2019, 9, 356 11 of 14

4.7. Calculation of Bioconversion Parameters

Conversion is expressed as $((I_a - F_a)/I_a) \times 100\%$, where $I_a =$ initial amount of a substrate before the conversion, and $F_a =$ final amount of a substrate after conversion. The substrate amount was determined by integrating the absorbance area (254 nm for most compounds) of a particular peak in high-performance liquid chromatography (HPLC) chromatogram. If no substrate was left, the conversion is defined as complete (>99%).

4.8. Isolation of the bioconversion products

The reaction mixture was separated from biomass by centrifugation (4000× g for 30 min). The volume of the supernatant was reduced under vacuum to a volume of 10–15 mL, and it was transferred into a separation funnel. Then the aqueous phase was washed >3–4 times with the equivalent volume of organic solvent, typically chloroform. However, in order to increase extraction efficiency ethyl acetate was used for more hydrophilic N-oxides (quinoxaline-1,4-dioxide), while toluene was applied for more hydrophobic ones (2,3,5-trimethylpyrazine-1,4-dioxide) instead. The organic phases were combined and dried with anhydrous Na₂SO₄. The resulting solution was evaporated under reduced pressure to give a final product. All isolation stages were monitored by thin layer chromatography (TLC). The purity of the final product was verified by high-performance liquid chromatography-mass spectrometry (HPLC-MS), and the chemical structure was NMR spectroscopy.

4.9. HPLC-MS Analysis

The cells were separated from the reaction mixture by centrifugation. The resulting supernatant was mixed with an equal part of acetonitrile, centrifuged and analyzed. HPLC-MS analysis was performed with high-performance liquid chromatography system (Shimadzu, Japan) and a mass spectrometer (LCMS-2020, Shimadzu, Kyoto, Japan) equipped with an electrospray ionization (ESI) source. The chromatographic separation was conducted using a YMC Pack Pro C18 column, 3 x 150 mm (YMC, Kyoto, Japan) at 40 °C and a mobile phase that consisted of 0.1 % formic acid water solution (solvent A), and acetonitrile (solvent B) delivered in the 5 \rightarrow 95 % gradient elution mode. Mass scans were measured from m/z 50 up to m/z 700, at 350 °C interface temperature, 250 °C DL temperature, \pm 4,500 V interface voltage, neutral DL/Qarray, using N2 as nebulizing and drying gas. Mass spectrometry data were acquired in both the positive and negative ionization modes.

4.10. 1H and 13C NMR Data of Isolated Products

NMR spectra were recorded in DMSO-d6 and CCl_3D on an Ascend 400: 1H NMR – 400 MHz, ^{13}C NMR—100 MHz (Bruker, Billerica, MA, USA). Chemical shifts (δ) are reported in ppm relative to the solvent resonance signal as an internal standard. The multiplicities are stated as follows: s = singlet, d = doublet, dd = doublet of doublets, t = triplet, m = multipliet.

2,6-Dimethylpyrazine-1,4-dioxide was isolated as a white solid. ¹H NMR (400 MHz, DMSO-d6): δ = 2.26 (s, 6H, CH3), 8.50 (s, 2H, CH). ¹³C NMR (100 MHz, DMSO-d6): δ = 14.3, 135.3, 144.4.

2,3,5,-Trimethylpyrazine-1-oxide was isolated as a brown liquid. 1 H NMR (400 MHz, DMSO-d6): δ = 2,30-2,48 (m, 9H, CH3), 8.31 (s, 1H, CH). 13 C NMR (100 MHz, DMSO-d6): δ = 21.0, 22.4, 22.5, 143.3, 125.4, 12

Quinoxaline-1,4-dioxide was isolated as an orange solid. 1 H NMR (400 MHz, DMSO-d6): δ = 7.95–8.05 (m, 2H, CH), 8.43–8.52 (m, 2H, CH), 8.54 (s, 2H, CH). 13 C NMR (100 MHz, CCl₃D): δ = 120.6, 130.4, 132.2, 138.6.

Quinazoline-1-oxide was isolated as white solid. 1 H NMR (400 MHz, DMSO-d6): δ = 7.89–7.95 (dd, J = 7.9, 7.2 Hz, 1H, CH), 8.07–8.14 (dd, J = 8.1, 7.8 Hz, 1H, CH), 8.30 (d, J = 8.2 Hz, 1H, CH), 8.47 (d, J = 8.7, 1H, CH), 9.14 (s, 1H, CH), 9.31 (s, 1H, CH). 13 C NMR (100 MHz, DMSO-d6): δ = 118.3, 128.6, 130.7, 135.4, 143.4, 147.4.

Catalysts 2019, 9, 356 12 of 14

4.11. PML Protein 3D Modelling

The 3D model of PML was generated with I-TASSER server [33], Chimera 1.13.1 was used for presentation [34].

Supplementary Materials: The following are available online at http://www.mdpi.com/2073-4344/9/4/356/s1: ¹H NMR and ¹³C NMR spectra of synthesized compounds.

Author Contributions: Investigation, data analysis, draft preparation, V.P.; data analysis, writing—review and editing, J.V.; investigation, writing—review and editing, D.V.; writing—review and editing, supervision, N.Č. writing—review and editing, supervision, N.Č.

Funding: This work was supported by the European Social Fund according to the activity 'Improvement of researchers' qualification by implementing world-class R&D projects' of Measure No. 09.3.3-LMT-K-712 (grant No. DOTSUT-34(09.3.3-LMT-K712-01-0058/LSS-600000-58)). This research was performed in cooperation with the INMARE consortium.

Acknowledgments: V.P., J.V. and N.Č. gratefully acknowledge the support of the European Social Fund.

Conflicts of Interest: The authors declare no conflict of interest.

References

- Badenhorst, C.P.S.; Bornscheuer, U.T. Getting momentum: From biocatalysis to advanced synthetic biology. Trends Biochem. Sci. 2018, 43, 180–198. [CrossRef] [PubMed]
- 2. Hughes, G.; Lewis, J.C. Introduction: Biocatalysis in Industry. Chem. Rev. 2018, 118, 1-3. [CrossRef]
- Turner, N.J.; Kumar, R. Editorial overview: Biocatalysis and biotransformation: The golden age of biocatalysis. Curr. Opin. Chem. Biol. 2018, 43, A1–A3. [CrossRef]
- Holtmann, D.; Fraaije, M.W.; Arends, I.W.; Opperman, D.J.; Hollmann, F. The taming of oxygen: Biocatalytic oxyfunctionalisations. Chem. Commun. 2014, 87, 13180–13200. [CrossRef]
- King-Smith, E.; Zwick, C.R., 3rd; Renata, H. Applications of oxygenases in the chemoenzymatic total synthesis of complex natural products. *Biochemistry* 2018, 57, 403–412. [CrossRef]
- Prier, C.K.; Kosjek, B. Recent preparative applications of redox enzymes. Curr. Opin. Chem. Biol. 2018, 49, 105–112. [CrossRef] [PubMed]
- Coleman, N.V.; Bui, N.B.; Holmes, A.J. Soluble di-iron monooxygenase gene diversity in soils, sediments and thane enrichments. Environ. Microbiol. 2006, 8, 1228–1239. [CrossRef]
- Leahy, J.G.; Batchelor, P.J.; Morcomb, S.M. Evolution of the soluble diiron monooxygenases. FEMS Microbiol. Rev. 2003, 27, 449–479. [CrossRef]
- Holmes, A.J. The diversity of doluble di-iron monooxygenases with bioremediation applications. In Advances in Applied Bioremediation; Singh, A., Kuhad, R., Ward, O., Eds.; Springer: Berlin, Germany, 2009; Volume 17.
- Notomista, E.; Scognamiglio, R.; Troncone, L.; Donadio, G.; Pezzella, A.; Di Donato, A.; Izzo, V. Tuning the specificity of the recombinant multicomponent toluene o-xylene monooxygenase from Pseudomonas sp. Strain OXI for the biosynthesis of tyrosol from 2-phenylethanol. Appl. Environ. Microbiol. 2011, 77, 5428–5437. [CrossRef] [PubMed]
- Petkevičius, V.; Vaitekūnas, J.; Tauraitė, D.; Stankevičiūtė, J.; Šarlauskas, J.; Čenas, N.; Meškys, R. A biocatalytic synthesis of heteroaromatic N-oxides by whole cells of Escherichia coli expressing the multicomponent, soluble di-iron monooxygenase (SDIMO) PmlABCDEF. Adv. Synth. Catal. 2019, 361. [CrossRef]
- Clayden, J.; Greeves, N.; Warren, S.G. Aromatic heterocycles 1: Reactions. In Organic Chemistry, 2nd ed.; Oxford University Press: New York, NY, USA, 2012; pp. 730–731.
- Mfuh, A.M.; Larionov, O.V. Heterocyclic N-oxides—An emerging class of therapeutic agents. Curr. Med. Chem. 2015, 22, 819–857. [CrossRef]
- Nichol, T.; Murrell, J.C.; Smith, T.J. Controlling the activities of the diiron centre in bacterial monooxygenases: Lessons from mutagenesis and biodiversity. Eur. J. Inorg. Chem. 2015, 2015, 3419–3431. [CrossRef]
- Notomista, E.; Cafaro, V.; Bozza, G.; Di Donato, A. Molecular determinants of the regioselectivity of toluene/o-xylene monooxygenase from *Pseudomonas* sp. Strain OX1. *Appl. Environ. Microbiol.* 2009, 75, 823–836. [CrossRef]

Catalysts 2019, 9, 356 13 of 14

 Chan Kwo Chion, C.K.; Askew, S.E.; Leak, D.J. Cloning, expression, and site-directed mutagenesis of the propene monooxygenase genes from Mycobacterium sp. Strain M156. Appl. Environ. Microbiol. 2005, 71, 1909–1914. [CrossRef]

- Sönmez, B.; Yanık-Yıldırım, K.C.; Wood, T.K.; Vardar-Schara, G. The role of substrate binding pocket residues
 phenylalanine 176 and phenylalanine 196 on *Pseudomonas* sp. OX1 toluene o-xylene monooxygenase activity
 and regiospecificity. *Biotechnol. Bioeng.* 2014, 111, 1506–1512. [CrossRef]
- Fishman, A.; Tao, Y.; Rui, L.; Wood, T.K. Controlling the regiospecific oxidation of aromatics via active site engineering of toluene para-monooxygenase of Ralstonia pickettii PKO1. J. Biol. Chem. 2005, 280, 506–514. [CrossRef]
- Vardar, G.; Wood, T.K. Protein engineering of toluene-o-xylene monooxygenase from Pseudomonas stutzeri
 OX1 for synthesizing 4-methylresorcinol, methylhydroquinone, and pyrogallol. Appl. Environ. Microbiol.
 2004, 70, 3253–3262. [CrossRef]
- Pikus, J.D.; Studts, J.M.; McClay, K.; Steffan, R.J.; Fox, B.G. Changes in the regiospecificity of aromatic hydroxylation produced by active site engineering in the diiron enzyme toluene 4-monooxygenase. *Biochemistry* 1997, 36, 9283–9289. [CrossRef]
- Halsey, K.H.; Sayavedra-Soto, L.A.; Bottomley, P.J.; Arp, D.J. Site-directed amino acid substitutions in the hydroxylase alpha subunit of butane monooxygenase from Pseudomonas butanovora: Implications for substrates knocking at the gate. J. Bacteriol. 2006, 188, 4962–4969. [CrossRef]
- Borodina, E.; Nichol, T.; Dumont, M.G.; Smith, T.J.; Murrell, J.C. Mutagenesis of the "leucine gate" to explore
 the basis of catalytic versatility in soluble methane monooxygenase. Appl. Environ. Microbiol. 2007, 73,
 6460–6467. [CrossRef]
- Rui, L.; Kwon, Y.M.; Fishman, A.; Reardon, K.F.; Wood, T.K. Saturation mutagenesis of toluene ortho-monoxygenase of Burkholderia cepacia G4 for Enhanced 1-naphthol synthesis and chloroform degradation. Appl. Environ. Microbiol. 2004, 70, 3246–3252. [CrossRef]
- Canada, K.A.; Iwashita, S.; Shim, H.; Wood, T.K. Directed evolution of toluene ortho-monooxygenase for enhanced 1-naphthol synthesis and chlorinated ethane degradation. J. Bacteriol. 2002, 184, 344

 [CrossRef]
- Petkevičius, V.; Vaitekūnas, J.; Stankevičiūtė, J.; Gasparavičiūtė, R.; Meškys, R. Catabolism of 2-hydroxypyridine by Burkholderia sp. Strain MAK1: A 2-hydroxypyridine 5-monooxygenase encoded by hpdABCDE catalyzes the first step of biodegradation. Appl. Environ. Microbiol. 2018, 84, e00387-18. [CrossRef]
- Steffan, R.J.; McClay, K.R. Preparation of Enantio-Specific Epoxides; Shaw Environmental & Infrastructure, Inc.: Washington, DC, USA, 2000.
- Tao, Y.; Fishman, A.; Bentley, W.E.; Wood, T.K. Altering toluene 4-monooxygenase by active-site engineering for the synthesis of 3-methoxycatechol, methoxyhydroquinone, and methylhydroquinone. J. Bacteriol. 2004, 186, 4705–4713. [CrossRef]
- Carlin, D.A.; Bertolani, S.J.; Siegel, J.B. Biocatalytic conversion of ethylene to ethylene oxide using an engineered toluene monooxygenase. Chem. Commun. 2015, 51, 2283–2285. [CrossRef]
- Mitchell, K.H.; Studts, J.M.; Fox, B.G. Combined participation of hydroxylase active site residues and effector protein binding in a para to ortho modulation of toluene 4-monooxygenase regiospecificity. Biochemistry 2002, 41, 3176–3388. [CrossRef]
- McClay, K.; Boss, C.; Keresztes, I.; Steffan, R.J. Mutations of toluene-4-monooxygenase that alter regiospecificity of indole oxidation and lead to production of novel indigoid pigments. Appl. Environ. Microbiol. 2005, 71, 5476–5483. [CrossRef]
- Rui, L.; Reardon, K.F.; Wood, T.K. Protein engineering of toluene ortho-monooxygenase of Burkholderia cepacia
 G4 for regiospecific hydroxylation of indole to form various indigoid compounds. Appl. Microbiol. Biotechnol.
 2005, 66, 422–429. [CrossRef]
- Stankevičiūtė, J.; Vaitekūnas, J.; Petkevičius, V.; Gasparavičiūtė, R.; Tauraitė, D.; Meškys, R. Oxyfunctionalization of pyridine derivatives using whole cells of *Burkholderia* sp. MAK1. Sci. Rep. 2016, 6, 39129. [CrossRef]

Catalysts 2019, 9, 356 14 of 14

33. Zhang, Y. I-TASSER server for protein 3D structure prediction. BMC Bioinform. 2008, 9, 40. [CrossRef]

 Pettersen, E.F.; Goddard, T.D.; Huang, C.C.; Couch, G.S.; Greenblatt, D.M.; Meng, E.C.; Ferrin, T.E. UCSF Chimera—A visualization system for exploratory research and analysis. J. Comput. Chem. 2004, 25, 1605–1612. [CrossRef]



© 2019 by the authors. Licensee MDPI, Basel, Switzerland. This article is an open access article distributed under the terms and conditions of the Creative Commons Attribution (CC BY) license (http://creativecommons.org/licenses/by/4.0/).

ACKNOWLEDGMENT

I am very grateful to my supervisor and a wonderful mentor Prof. Dr. Rolandas Meškys for his in-depth knowledge and expertise, helpful advice, spot-on insights and invaluable guidance through this remarkable scientific journey.

The tremendous gratitude goes to Justas, Jonita, Renata, Simona, Agota, Jevgenija and others lab colleagues that truly were 'a friend in need is a friend indeed'. I am fortunate to be associated with them.

I am also indebted to Habil. Dr. Narimantas Čėnas and Dr. Laura Kalinienė who both have devoted hours of reading and editing my publications drafts.

To all members of the big family of Department of Molecular Microbiology and Biotechnology for genuine support – thank you!

Nobody has been more important to me than the members of my family. I acknowledge a deep gratitude to my parents and sister for their love and support. Most importantly, I would like to thank Juratė – you are always there for me.

NOTES

Vilniaus universiteto leidykla Universiteto g. 1, LT-01513 Vilnius El. p. info@leidykla.vu.lt, www.leidykla.vu.lt Tiražas 15 egz.